Implications of Silurian granite genesis to the tectonic history of the Nashoba terrane, Eastern Massachusetts

Author: Daniel Dabrowski

Boston College

The Graduate School of Arts and Sciences

Department of Earth and Environmental Sciences

IMPLICATIONS OF SILURIAN GRANITE GENESIS TO THE TECTONIC HISTORY OF THE NASHOBA TERRANE, EASTERN MASSACHUSETTS

a thesis

by

DANIEL DABROWSKI

submitted in partial fulfillment of the requirements

for the degree of

Master of Science

May, 2014

Implications of Silurian granite genesis to the tectonic history of the Nashoba terrane, Eastern Massachusetts

Daniel Dabrowski
Advisor: J. Christopher Hepburn

ABSTRACT

The Nashoba terrane is a highly metamorphosed and sheared Paleozoic tectonic block in eastern Massachusetts. The metamorphic rocks that compose the terrane are intruded by a series of diorites, tonalites, and granites. The Andover Granite is a complex multiphase granitic suite found in the northern part of the Nashoba terrane and is composed of both foliated and unfoliated granites as well as a granodiorite phase. The Sgr Group of granites is a series of unfoliated granites exposed along the Nashoba-Avalon terrane boundary.

New crystallization ages for the foliated Andover Granite and the Sudbury Granite, southernmost body of the Sgr Group of granites, are presented. CA-TIMS U-Pb geochronology on zircons collected from these granites yielded 419.43 ± 0.52 Ma and 419.65 ± 0.51 Ma crystallization ages for the foliated Andover Granite and a 420.49 ± 0.52 Ma crystallization age for the Sudbury Granite. Geochemical and petrographic analysis of these granites indicate that the foliated Andover Granite is a high-K calc-alkaline, peralmuminous, S-type, biotite + muscovite granite and the Sudbury granite is high-K calc-alkaline, metaluminous to slightly peraluminous, I-type, biotite granite.

These two granites are interpreted to have formed from the anatexis of either Nashoba terrane metasedimentary rocks and/or its underlying basement just prior to the

Acadian orogeny. It is proposed that when Silurian diorite/tonalite magmas intruded into the Nashoba terrane, the influx of magmatic heat was sufficient to trigger crustal melting and promote granite genesis. This petrogenetic scenario fits well with regional tectonic models showing the Silurio-Devonian convergence of Avalonia towards Ganderia (which formed the eastern side of composite Laurentia at the time) in the northern Appalachians.

Prior to the collision of Avalonia to composite Laurentia, mafic and intermediate composition arc magmas intruded the eastern Ganderian margin. The large amount of heat that accompanied these intrusions is believed to have contributed to Acadian metamorphism and influenced the formation of granitic plutons along the margin. It is therefore proposed that the plutonic record of the Nashoba terrane shows that by the Late Silurian – Early Devonian, Avalonia was still outboard of Laurentia in the vicinity of southern New England.

Table of Contents

Figures

Tables

Acknowledgments

I would like to thank my parents for their support during this project. I would also like to thank my adviser Professor J. Christopher Hepburn for his advice on my project, assistance in editing this thesis, and geological wisdom over the past few years. Many thanks to Professor Yvette Kuiper for her help getting me started at Boston College, her advice on my project, and assistance in editing this thesis. My gratitude goes to Dr. Robert Buchwaldt for his advice as well as his assistance with the zircon geochronological analysis used in this project. I would like to thank Dr. Nilanjan Chatterjee, Pete Dawson, and Professor J. Michael Rhodes for their assistance and training. I would also like to thank the Electron Microprobe Facility and the Radiogenic Isotope Laboratory at MIT and the Ronald B. Gilmore X-Ray Fluorescence Laboratory at UMASS.

I am grateful for the help Kristin Sorota provided, in both training me in mineral separation procedures and our numerous Appalachian geology conversations. Thank you Hosanna Lillydahl-Schroeder for the various tectonics and structural geology conversations we have shared. Also, many thanks to my fellow graduate students at Boston College for our various geological conversations.

Partial funding for this project was provided by Geological Society of America Graduate Student Grant #9118428.

Chapter 1: Introduction

The Appalachian Mountains represent a complete Wilson super continent cycle starting with the formation of the continents Laurentia and Gondwana, during the Late Proterozoic breakup of Rodinia, and ending with the construction of Pangea during the Permian (Hatcher, 2010). In the intervening ~500 m.y., lithotectonic blocks episodically accreted to the eastern Laurentian margin. Initially, these accretionary events involved blocks that originated from or near to Laurentia (i.e. peri-Laurentian) (Karabinos et al., 1998; van Staal et al., 2007; 2009; Hatcher, 2010), while later events involved peri-Gondwanan terranes (Dunning et al., 1990; van Staal et al., 2009; 2011a; Hatcher, 2010). In the northern Appalachians, these terranes form the peri-Laurentian, Iapetus, and peri-Gondwanan realms (Figure 1.1) with the peri-Gondwanan realm being composed of the Ganderian, Avalonian, and Meguman terranes (O'Brien et al., 1983; O'Brien et al., 1996; Hibbard et al., 2007a; Hibbard et al., 2007b; van Staal et al., 1996; 2009; 2011b; Waldron et al., 2009; Hatcher, 2010).

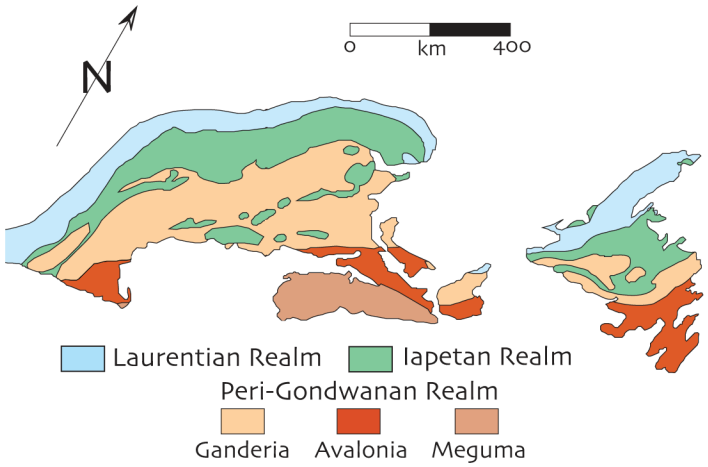

Figure 1.1 – Tectonic map showing the geology of the northern Appalachian orogen. Modified from Hibbard & Waldron (2009).

1.1 Eastern Massachusetts

The Nashoba terrane currently forms the eastern margin of Ganderia in southeastern New England. It is composed of multiply deformed and metamorphosed (to upper amphibolite facies) amphibolites, gneisses, and schists. These metamorphic rocks are intruded by Silurian to Carboniferous, calc-alkaline, intermediate to felsic composition plutons (Hill et al., 1984; Zartman & Naylor, 1984; Wones & Goldsmith, 1991; Hepburn et al., 1995; Acaster & Bickford, 1999). Geochemical, geochronological, and isotopic data from the metasedimentary rocks suggests the terrane originated as an arc/back-arc complex (Goldsmith, 1991a; Hepburn et al., 1995; Kay et al., 2011; Kay, 2012) along the Ganderian margin in the Late Proterozoic to Early Paleozoic (Loan, 2011; Loan et al., 2011).

The Merrimack and Avalon terranes join the Nashoba terrane in forming the bedrock of eastern Massachusetts (Figure 1.2). The Merrimack terrane, which lies adjacent to the Nashoba terrane to the west, is a thick sequence of calc-silicate rocks, schists, and quartzites with a metamorphic gradient increasing from the greenschist facies in the east to the amphibolite facies in the west (Goldsmith, 1991b; Markwort, 2007; Wintsch et al., 2007). The metasedimentary rocks of the Merrimack terrane are intruded by Silurian to Early Devonian plutons, which are more abundant towards the eastern border of the terrane (Zen et al., 1983; Wones & Goldsmith, 1991). Recent detrital zircon U-Pb geochronological data suggests the Merrimack terrane originated in the Silurian and Early Devonian as a depositional basin into which detritus from both Laurentia and Ganderia was deposited (Sorota et al., 2011, Sorota, 2013).

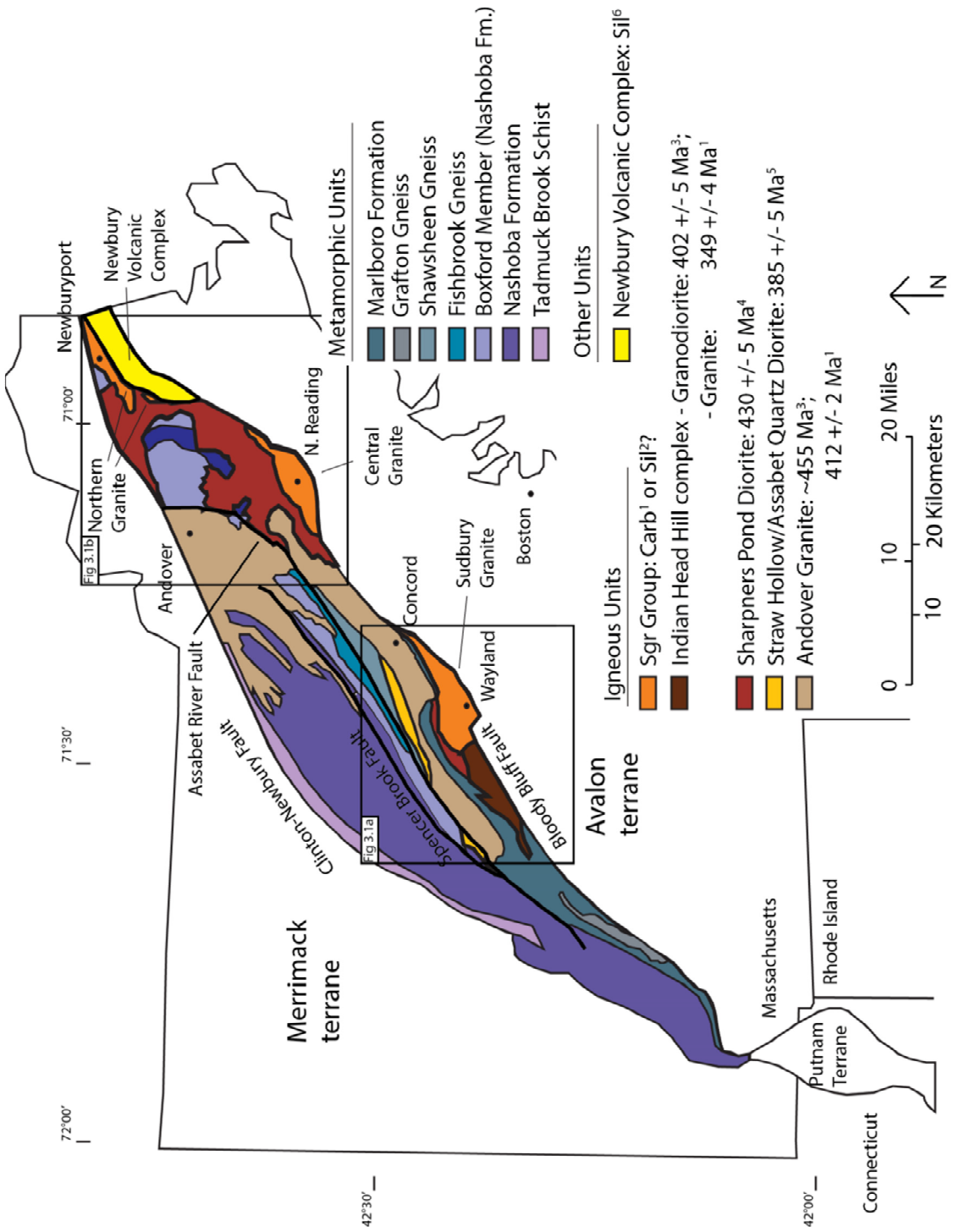

Figure 1.2 – Geologic Map of the Nashoba terrane. Modified from Goldsmith (1991a) and Wones and Goldsmith (1991). Inset boxes correspond to the sample location maps found in Chapter 3. Superscript references for ages are as follows: [1]Hepburn and others (1995), [2]Loftenius (1988) and Wones and Goldsmith (1991), [3]Hill and others (1984), [4]Zartman and Naylor (1984), [5]Acaster and Bickford (1999), [6]Shride (1976a).

The Avalon terrane, which lies adjacent to the Nashoba terrane to the east, is widely believed to be an exposure of the Avalonia micro-continent in Massachusetts (Skehan & Rast, 1983; Williams & Hatcher, 1983; Rast & Skehan, 1993; Hepburn et al., 1995). Also known as the Milford-Dedham zone (Goldsmith, 1991c), the Avalon terrane is composed of weakly metamorphosed Neoproterozoic granitoids and volcanic rocks that are overlain by Cambrian to Ordovician platform sediments (Cameron & Naylor, 1976; Williams & Hatcher, 1983; Hepburn et al., 1993; Thompson et al., 2003). These rocks were then intruded by bimodal alkaline plutons in the Late Ordovician, Early Silurian, and mid- to Late Devonian (Wones & Goldsmith, 1991).

1.2 Tectonic Background of Eastern Massachusetts

The construction of the geology now seen in eastern Massachusetts began at the end of the Taconic orogeny when the Popelogan-Victoria Arc accreted to the eastern Laurentian margin (van Staal et al., 2009; Hatcher, 2010; van Staal et al., 2011b). The Popelogan-Victoria Arc was a volcanic arc along the western Ganderian margin that rifted away from Ganderia during the Early to Middle Ordovician (van Staal et al., 2009; 2011a) forming the leading, or active, margin of Ganderia. The remainder of the micro-continent then became the passive margin of Ganderia.

Building eastern Massachusetts involved two orogenic events, the Salinic orogeny and the Acadian orogeny, which involved the peri-Gondwanan micro-continents Ganderia and Avalonia, respectively (van Staal et al., 2009; Hatcher, 2010). The Salinic orogeny is defined by the Silurian collision of the passive margin of Ganderia, on which

the Nashoba terrane sits, to the eastern margin of Laurentia (van Staal et al., 2009; Hatcher, 2010). Directly following the Salinic orogeny was the Acadian orogeny, defined by the Late Silurian – Early Devonian collision of Avalonia to the expanding eastern margin of Laurentia (van Staal et al., 2009; Hatcher, 2010).

1.3 Geologic Problem

The Andover Granite is a complex multiphase granitic suite exposed in the northern part of the Nashoba terrane (Figure 1.2). The foliated phase of the Andover Granite was believed to be the oldest phase of the suite based on a ~455 Ma Rb-Sr whole rock isochron age (Hanford, 1965; Zartman & Naylor, 1984; Hill et al., 1984). This Rb-Sr isochron age suggests that the terrane was subject to active tectonism and granite formation during the Ordovician. However, this interpretation is in conflict with current tectonic models that suggest that active tectonism and associated magmatism did not occur for at least another ~20+ m.y. (van Staal et al., 2009; Kay et al., 2011; Loan et al., 2011). These models suggest that during the Ordovician, active tectonism involved peri-Laurentian elements during the Taconic orogeny. The passive Ganderian margin (on which the terrane resides) was isolated from other continental elements by the Tetagouche-Exploits back-arc basin and Rheic Ocean to the west and east, respectively (van Staal et al., 1998; 2009; 2011b; Loan, 2011). It is a currently held belief that the passive Ganderian margin, and thus the Nashoba terrane, was subject to active tectonism and granite formation in the Late Silurian during the Acadian orogeny, not the Ordovician as these Rb-Sr ages suggest (Dunning et al., 1990; van Staal et al., 2009;

2011b; Stroud et al., 2009). Therefore, either this age on the foliated Andover Granite is incorrect or the model needs revision.

The Sudbury Granite is a small, pink, biotite granite found in Wayland, Massachusetts and the adjacent areas (Figure 1.2). This granite joins other biotite granites in North Reading and Newburyport, Massachusetts to form the 'Sgr' Group of granites of Zen and others (1983) along the eastern boundary of the Nashoba terrane. The origin of the Sgr Group is not well understood. Field and geochemical data from the Sgr Group and the Middle Silurian Sharpners Pond Diorite suggests that both plutons could have origins in a similar magmatic event (Loftenius, 1988; Wones & Goldsmith, 1991). However, the Sudbury Granite has been recently shown to be isotopically similar to the Carboniferous granite of the Indian Head Hill complex (Kay, 2012), also suggesting a possible relationship. Given the close proximity of the Sgr Group to the Nashoba-Avalon terrane boundary, understanding the origins of the Sgr Group is important to understanding the middle to late Paleozoic interaction of Ganderia and Avalonia in southeastern New England.

1.4 Project Objectives

The objectives of this project were as follows:

- Andover Granite
    - Determine a revised crystallization age of the foliated Andover Granite to better constrain the age of intrusion of the Andover Suite into the Nashoba terrane.
- Sgr Group
    - Investigate the nature of the relationship, if any, between the Sudbury Granite and the other two Sgr granites of Zen and others (1983).
    - Classify the Sgr Group of granites and determine their petrogenesis.
    - Determine the crystallization age of the Sudbury Granite to constrain the timing of the intrusion of this granite into the Nashoba terrane.
    - Investigate the nature of the relationship, if any, between the Sudbury Granite and the Nashoba-Avalon terrane boundary to determine if the granite crosscuts it, and therefore constrains, the age of Bloody Bluff fault.

Granites are excellent recorders of tectonic processes. Thus understanding the origins of these granites can refine our understanding of the tectonic processes that affected the Nashoba terrane. Due to the proximity of these granites to the Nashoba-Avalon terrane boundary, their origins could be directly related to the accretion of Avalonia in eastern Massachusetts and, when combined with other igneous rocks along the Ganderian margin, could refine our understanding of the collision of Avalonia with Laurentia, and thus the Acadian orogeny, in the southeastern New England.

Chapter 2: Nashoba terrane

The Nashoba terrane forms the bedrock of eastern Massachusetts between the Avalon terrane to the east and the Merrimack terrane to the west (Figure 1.2). The Bloody Bluff fault zone and the Clinton-Newbury fault zone form the eastern and western boundaries of the terrane, respectively. These zones are westward dipping composite fault zones consisting of both thrust and normal faults (Goldsmith, 1991b). Other faults have been observed at a regional scale within the terrane, however only two of them are large enough to be mapped regionally: the Assabet River fault and the Spencer Brook fault (Figure 1.2) (Bell & Alvord, 1976; Zen et al., 1983; Goldsmith, 1991b; Hepburn et al., 1995).

2.1 Metamorphic Units

The Nashoba terrane is composed of five metamorphic units (Figure 2.1). The Marlboro Formation is a collection of thinly layered amphibolites and biotite schists and gneisses (Zen et al., 1983) derived from interlayered volcanic, volcanioclastic, and sedimentary rocks (Goldsmith, 1991a; Hepburn et al., 1995; Hepburn & Bailey, 1999). The Shawsheen Gneiss is composed of biotite quartzofeldspathic paragneiss and sillimanite paragneiss and schist with minor occurrences of amphibolite (Zen et al., 1983; Hepburn & Bailey, 1999). The protolith for the Shawsheen Gneiss is interpreted to be a submarine wacke related to subaqueous deposition of volcanic ejecta (Bell & Alvord, 1976). The Fish Brook Gneiss is a white-to-tan biotite orthogniess with a distinctive

"swirl-form" biotite foliation (Goldsmith, 1991a) that is believed to be a metamorphosed silicic volcanogenic deposit (Goldsmith, 1991a; Hepburn & Bailey, 1999).

The Nashoba Formation is the largest metamorphic unit in the Nashoba terrane (Figure 1.2), occupying a majority of the mapped area of the terrane. Given its size, Bell and Alvord (1976) subdivided the Nashoba Formation into ten members, of which only the Boxford Member is large enough to be mapped regionally (OZnb; Zen et al., 1983) (Figure 1.2). As a whole, the formation is described as a "partly sulfidic sillimanite schist and gneiss, with amphibolite and calc-silicate gneiss and marble" (Zen et al., 1983) and its protolith is interpreted to be volcanogenic sediments interlayered with marine sediments and volcanics (Goldsmith, 1991a). The Tadmuck Brook Schist is composed of rusty-weathering andalusitic phyllite and sulfidic sillimanite schist believed to be metamorphosed weathered shales and thin quartzites (Bell & Alvord, 1976; Zen et al., 1983; Jerden, 1997).

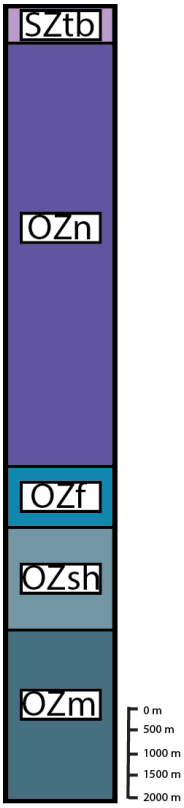

Figure 2.1 – Schematic stratigraphic column of the metamorphic rocks in the Nashoba terrane. OZm- Marlboro Formation, OZsh – Shawsheen Gneiss, OZf – Fish brook Gneiss, OZn – Nashoba Formation, SZtb – Tadmuck Brook Schist. Unit labels follow Zen and others (1983). Modified from Bell and Alvord (1976) and Goldsmith (1991a).

2.1.1 Geochronology of the Metamorphic Units

The metamorphic rocks of the Nashoba terrane are believed to be pre-Late Cambrian to Middle Silurian based on the youngest detrital zircons present in the rocks, the timing of metamorphism, and the crystallization ages of crosscutting igneous rocks

(Zartman & Naylor, 1984; Stroud et al., 2009; Loan, 2011). The youngest detrital zircons retrieved from the metasedimentary units of the Nashoba terrane vary between 463 Ma and 470 Ma for the Tadmuck Brook Schist and the Marlboro Formation, respectively, (U-Pb zircon LA-ICP-MS, Loan, 2011). U-Pb monazite ages between 435 Ma and 400 Ma constrain the oldest metamorphic events in the terrane (Stroud et al., 2009). The oldest unfoliated and unmetamorphosed pluton in the terrane is the Sharpners Pond Diorite dated at 430 ± 5 Ma (U-Pb zircon TIMS; Zartman & Naylor, 1984). Other igneous bodies that constrain the age of the metamorphic rocks in the terrane include the Grafton Gneiss (Figure 1.2) and the Fish Brook Gneiss. The Grafton Gneiss, a small body of granitic gneiss that crosscuts the Marlboro Formation (Zen et al., 1983), has an age of 515 ± 6 Ma (U-Pb zircon SHRIMP; Walsh et al., 2011). The Fish Brook Gneiss, found in the center of the terrane (Zen et al., 1983), has an igneous age of 499 +6/-3 Ma (U-Pb zircon ID-TIMS; Hepburn et al., 1995).

2.1.2 Metamorphism

The metamorphism of the Nashoba terrane is well constrained (Castle, 1964; Skehan & Abu-Moustafa, 1976; Abu-Moustafa & Skehan, 1976; Hepburn & Munn, 1984; Munn, 1987; Bober, 1989; Goldsmith, 1991b; Jerden, 1997; Stroud et al., 2009; Reynolds et al., 2010). It is described as low pressure – high temperature metamorphism, believed to be the result of crustal thickening and high heat influx from intruding mafic to intermediate composition melts (Munn, 1987; Hepburn et al., 1995; Goldsmith, 1991a; Wones & Goldsmith, 1991; Stroud et al., 2009). At least three metamorphic events are

observed in the terrane: ~423 Ma, ~390 Ma, and ~375 Ma (Stroud et al., 2009). Peak metamorphic conditions extend into the upper amphibolite facies for the Silurian and Devonian metamorphism (Stroud et al., 2009; Buchanan et al., 2014). The Middle Devonian metamorphism is thought to be coeval with migmatite formation in the terrane, suggesting slightly higher P/T conditions than the Silurian metamorphism (Hepburn et al., 1995; Stroud et al., 2009).

2.2 Igneous Units

The Silurian-Devonian plutons of the Nashoba terrane are abundantly exposed in the northern part of the terrane and to a lesser degree along the Bloody Bluff fault (Figure 1.2). These rocks are calc-alkaline diorites, tonalites, and granites and are interpreted to have formed in a continental volcanic arc tectonic setting (Collins, 1987; Loftenius, 1988; Hill et al., 1984; Wones & Goldsmith, 1991; Hepburn et al., 1995; Kay, 2012). The Sharpners Pond Diorite is a large, unfoliated, intermediate composition, plutonic suite composed of hornblende and biotite hornblende quartz diorite/tonalite, hornblende gabbro, and biotite granite (Castle, 1964; Loftenius, 1988). The suite is observed to intrude the Marlboro Formation, the Nashoba Formation, and the Fish Brook Gneiss (Zen et al., 1983; Wones & Goldsmith, 1991). The Assabet River Quartz Diorite and the Straw Hollow Quartz Diorite are unfoliated to slightly foliated hornblende quartz diorites observed intruding the Nashoba Formation (Zen et al., 1983; Wones & Goldsmith, 1991). The Indian Head Hill complex intrudes the Marlboro Formation and is composed of both

a hornblende biotite tonalite and a younger biotite granite (Zen et al., 1983; Hepburn et al., 1995).

Multiple authors have constrained the emplacement of these generally intermediate composition plutonic rocks to between the Middle Silurian and Early Carboniferous (Figure 1.2). The Sharpners Pond Diorite has a U-Pb zircon age of 430 ± 5 Ma (ID-TIMS; Zartman & Naylor, 1984). The Straw Hollow Quartz Diorite formed 385 ± 5 Ma (U-Pb zircon ID-TIMS; Acaster & Bickford, 1999). The tonalite of the Indian Head Hill complex has an age of 402 ± 5 Ma (Hill et al., 1984) based on Rb-Sr whole rock geochronology, while the biotite granite is 349 ± 4 Ma based on titanite and zircon U-Pb ID-TIMS geochronology (Hepburn et al., 1995).

2.2.1 Andover Granite

The Andover Granite is a multiphase granitic suite composed of biotite, muscovite, and two mica (biotite-muscovite) granites, as well as a granodiorite phase. Locally, these granites can be garnet bearing and/or pegmatitic (Castle, 1964; Collins, 1987). The suite intrudes the Nashoba Formation (Castle, 1964; Zen et al., 1983) and its age is constrained to the Middle Ordovician to Early Devonian (Zartman & Naylor, 1984; Hill et al., 1984; Hepburn et al., 1995). Texturally, the granite phases vary between unfoliated and foliated, and in some cases almost gneissose, (Castle, 1964) with the foliations generally parallel to the regional foliation in the Nashoba terrane (Hepburn et al., 1995). Geochemically, the suite has an aluminous to peraluminous composition with trace element characteristics consistent with igneous rocks that formed in a continental

volcanic arc tectonic setting (Collins, 1987; Kay, 2012). Sm-Nd isotope data analyzed from the suite supports the continental volcanic arc affinity for the suite (Kay, 2012). Additionally, the Sm-Nd data suggests that the source region of the suite is composed of a mixture of both geochemically primitive and evolved material (Kay, 2012).

2.2.2 Sudbury Granite

The Sudbury Granite is the southernmost body of the Sgr Group of granites and is exposed along the Nashoba-Avalon terrane boundary (Zen et al., 1983; Figure 1.2). It is an unfoliated, pink, medium-grained, potassium feldspar rich, biotite granite located in and around Wayland, Massachusetts (Figure 1.2). The name 'Sudbury Granite' is adopted from Kohut (1999) and is proposed for the name of this granite to distinguish it from the central and northern granites of the Sgr Group, which are currently unnamed. The Sudbury Granite can be separated into three facies (Langford, 2007). The type locality, in Wayland, Massachusetts, defines the normal Sudbury Granite facies and is composed of unfoliated, medium-grained, potassium feldspar rich, biotite granite. The dark Sudbury Granite facies represents material north of the type locality and consists of a darker, more biotite rich variety of the Sudbury Granite. The mixed Sudbury Granite facies identifies granite found at the northern part of the mapped area of the pluton and is composed of a mixture of both the normal and dark facies.

2.3 Previous work

2.3.1 Andover Granite

2.3.1.1 Petrography

The first mention of a granite in the vicinity of Andover, Massachusetts was made by Hitchcock (1833) during the construction of the 1833 state geologic map of Massachusetts. This was followed by C. H. Clapp in 1910 when the name Andover Granite was given to muscovite granite outcrops in and around the town of Andover, Massachusetts (Castle, 1964). Emerson (1917) conducted the first mapping investigation of the granite during the compilation of the 1917 state geologic map of Massachusetts. The first study focused on the Andover Granite specifically was completed by Clapp (1921) with a general description of the pluton. Hansen (1956) performed a more detailed field and petrographic study of the granite, specifically in the Hudson and Maynard quadrangles. Castle (1964) achieved a thorough field and petrographic investigation of the Andover Granite. In this study, Castle (1964) subdivided the granite into six separate but transitional facies: a muscovite granite-gneiss, a biotite granite-gneiss, a fine-grained granite-gneiss, an undifferentiated granite-gneiss, a binary granite, and a pegmatitic granite. Later, Castle and Theodore (1972) undertook a detailed investigation of the Andover Granite pegmatites in the northeastern part of the pluton.

2.3.1.2 Geochemistry

Collins (1987) performed the first thorough geochemical investigation of the Andover Granite. The results from this investigation were multifold. First, the Andover Granite can be subdivided into: muscovite, biotite, and two mica (muscovite-biotite) granites, as well as a granodiorite. Additionally, the granite phases can be further subdivided into foliated and unfoliated granites. These subdivisions differ from Castle (1964), specifically with the inclusion of a granodiorite phase and removal of the pegmatitic granite facies. Collins (1987) observed that Andover Granite pegmatite could be found locally throughout the suite, rather than restricted to any specific phase. Secondly, these phases, while part of the same suite, are geochemically dissimilar. This, and the then available isotope data, suggested that the source region for the suite was heterogeneous. Thirdly, the suite as a whole is mildly to strongly peraluminous. Trace element patterns of the suite are similar to that seen in continental volcanic arcs, suggesting that the Andover Granite formed either as the result of arc magmatism or from the partial melting of arc rocks, or both. Recently analyzed Sm-Nd isotope data from the suite supports the interpretation of the involvement of continental arc material in the petrogenesis of the suite and also suggests the inclusion of older crustal material (Kay, 2012).

2.3.1.3 Geochronology

Handford (1965) completed the first geochronological investigation of the Andover Granite by performing Rb-Sr geochronology on whole rock samples from the

northeastern part of the pluton. This investigation resulted in the suite falling on a 450 ± 22 Ma isochron, indicating the suite crystallized sometime between the Early Ordovician and Early Silurian. Later, Zartman and Naylor (1984) performed additional Rb-Sr whole rock analyses, but they interpreted their results cautiously. Using all of the samples retrieved from the pluton, Zartman and Naylor (1984) obtained an isochron age of 408 ± 22 Ma. However, by only analyzing just the granite samples and removing samples containing aplitic and pegmatitic material this age becomes 446 ± 32 Ma. They concluded that the pegmatite samples must have undergone Rb-Sr isotopic resetting at some point after the formation of the Andover Granite, but suggest that at least part of the pluton is as old as Late Ordovician. Subsequent to Zartman and Naylor (1984), Hill and others (1984) made four additional Rb-Sr analyses and combined their results with the data from Handford (1965) and Zartman and Naylor (1984). Hill and others (1984) determined that the Andover Granite falls on two Rb-Sr isochrons: ca. 455 Ma and ca. 415 Ma (Figure 2.2). More recently, Hepburn and others (1995) dated material from an unfoliated muscovite granite from the Andover Granite suite via U-Pb monazite ID-TIMS geochronology and obtained a concordant 412 ± 2 Ma age. Hepburn and others (1995) interpreted this age as representing the upper age constraint on the intrusion for the Andover Granite suite.

2.3.2 Sgr Group

Shride (1971) described and mapped a pink biotite granite in Byfield, Massachusetts, near the town of Newburyport. Shride (1976a) also observed and

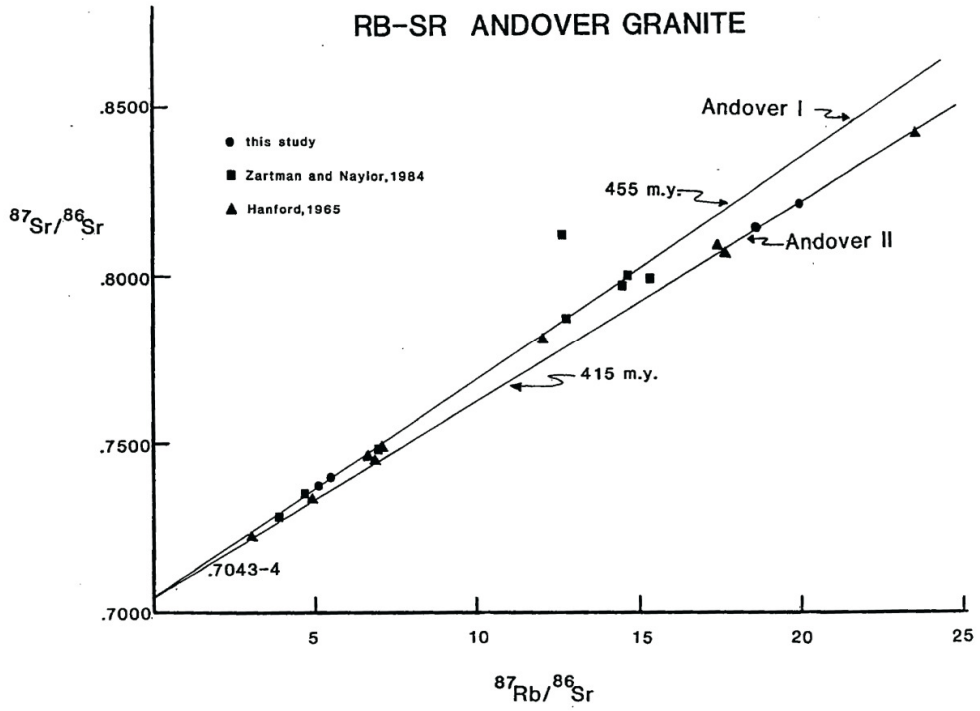

Figure 2.2 – Rb-Sr whole rock isochrons for the Andover Granite suite. Andover I is described as a mildly peraluminous biotite-muscovite-garnet granite. Andover II is described as a strongly peraluminous muscovite-garnet granite. Figure taken from Hill and others (1984).

described a pink biotite granite intruding the Sharpners Pond Diorite in the area of Reading, Massachusetts. The three granitic bodies of the Sgr Group in the towns of Wayland, North Reading, and Newburyport, Massachusetts were first identified during reconnaissance mapping for the Massachusetts bedrock map of Zen and others (1983) (Wones & Goldsmith, 1991). Loftenius (1988) observed a pink biotite granite intruding the Sharpners Pond Diorite and described a pink biotite granite in the area of North Reading, Massachusetts, possibly similar to the granite Shride (1976a) observed. Furthermore, Loftenius (1988) determined that this biotite granite has a calc-alkaline geochemistry with characteristics similar to rocks found in continental volcanic arcs.

Kohut (1999) mapped in the Weston-Lexington area west of Boston, Massachusetts, including part of the Nashoba terrane. During this investigation, Kohut (1999) identified and described the pink biotite granite of Zen and others (1983) in Wayland, Massachusetts and renamed it 'Sudbury Granite'. Langford (2007) mapped the Concord quadrangle of Massachusetts and observed that the Sudbury Granite can be subdivided into a normal, dark, and mixed facies based on biotite content. Recently, Sm-Nd isotopic analysis on the pluton suggests the involvement of continental volcanic arc material in the formation of the Sudbury Granite (Kay, 2012).

Chapter 3: Data

3.1 Methods

To solve the geologic problems presented in Section 1.3, three techniques were applied to samples collected from the foliated Andover Granite and the Sgr Group of granites: thin section petrography, whole rock X-Ray Fluorescence (XRF) geochemistry, and high precision U-Pb Chemical Abrasion – Thermal Ionization Mass Spectrometry (CA-TIMS) geochronology. Sample locations can be found in Appendix A and in Figures 3.1a and 3.1b. Two samples were collected from geographically opposite sides of the foliated Andover Granite (approximately 40 km apart), as defined by Collins (1987), and prepared for petrographic, geochemical, and geochronological analysis (Figures 3.1a and 3.1b). Additional geochemical or petrographic analyses from the foliated Andover Granite were deemed unnecessary as the investigation by Collins (1987) of the Andover Granite was quite thorough. The geochemical dataset from Collins (1987) was included in this investigation (See Appendix C). Sixteen samples were collected from the Sgr Group for petrographic analysis (Figures 3.1a and 3.1b). Of these sixteen, seven were prepared for geochemical analysis, and one sample from the Sudbury Granite was prepared for geochronological analysis. Additionally, three samples were collected from locations around the Sudbury Granite and prepared for petrographic analysis to assist in the field investigation (Figures 3.1a and 3.1b).

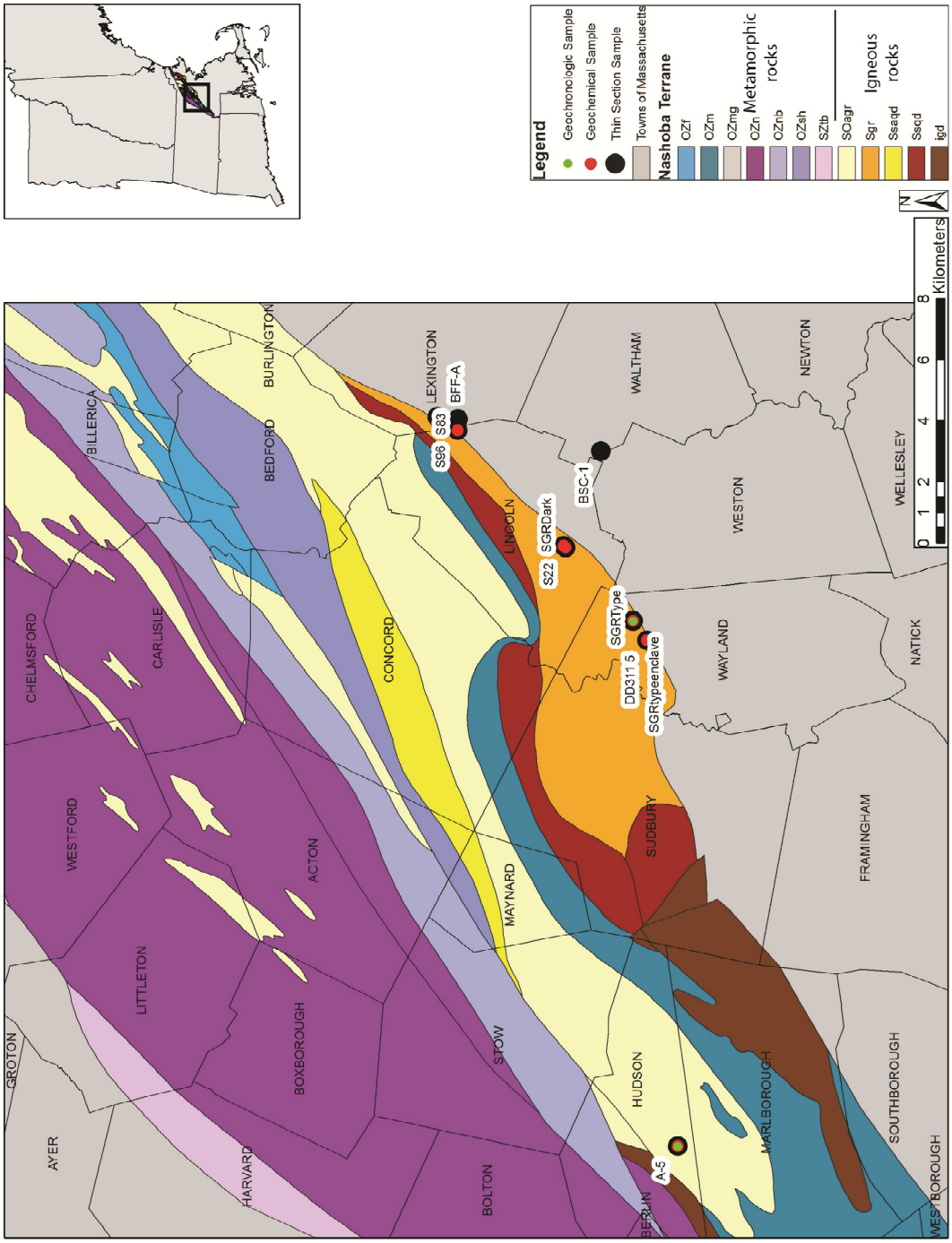

Figure 3.1a – Geologic map showing the locations of the samples collected from the southern part of the Nashoba terrane. This map includes samples collected from the Sudbury Granite, the Bloody Bluff type locality, east of the Bloody Bluff fault, and the foliated Andover Granite. Bedrock map labels after Zen and others (1983).

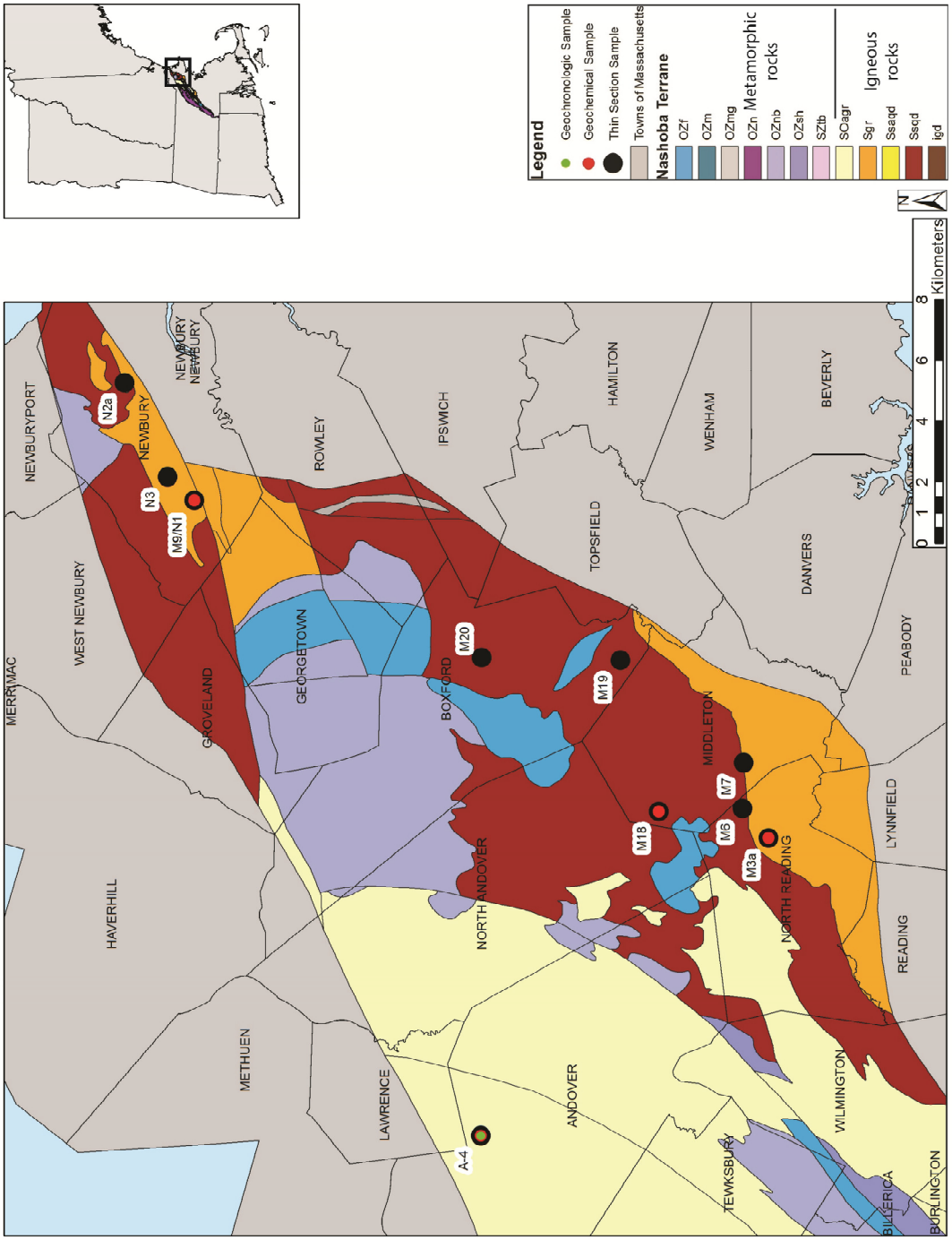

Figure 3.1b – Geologic map showing the locations of the samples collected from the northern part of the Nashoba terrane. This map includes samples collected from the central and northern Sgr granites and the foliated Andover Granite. Bedrock map labels after Zen and others (1983).

3.1.1 Geochemistry

In preparation for whole rock XRF geochemical analysis, samples were crushed and powdered in the Boston College Rock Preparation Laboratory. Samples were first broken into fist sized pieces via a sledgehammer. These pieces were then hand washed and dried to remove any dirt, moss, or other contaminants. Any altered material or weathered surface present was removed with a rock hammer or diamond studded rock saw and set aside. Samples were inspected to check for contamination from the rock saw. If present, this contaminated material was removed and discarded. The altered and weathered material was used as a "pre-grind". The pre-grind was processed through each preparation step prior to the sample. This was done to minimize contamination by insuring that if any contamination did occur it would be limited to material from the same sample.

A Bico International Inc. Jaw Crusher was used to reduce the sample from fist sized pieces to approximately half-inch sized pieces. After the machine was thoroughly cleaned, the pre-grind material was fed into the crusher and the resulting pieces were collected and set aside. This was then followed by the sample. For both the pre-grind and the sample, the crushed material was randomly split by cone quartering until a fraction of material approximately 80-100g, or 40 mL, in size was isolated. This fraction was processed in a shatterbox, a machine that uses an alumina puck and container to pulverize material into a fine powder. Like the crusher, once the shatterbox chamber was thoroughly cleaned, the pre-grind material was run first and then followed by the sample. After the shatterbox, the pre-grind and sample was processed by a tungsten carbide ball mill. Like the shatterbox, once the ball mill chamber was fully cleaned, the pre-grind

material was run first and then followed by the sample. The ball mill reduced the sample from the fine powder produced by the shatterbox to approximately 400 mesh size, sufficient for XRF analysis.

XRF analysis was done at the Ronald B. Gilmore X-Ray Fluorescence Laboratory, Department of Geosciences, University of Massachusetts, Amherst, Massachusetts. At the lab, each sample was heated to 1000 °C to oxide iron to Fe^{3+} and to remove volatiles. The mass of the sample was measured both before and after heating to determine volatile content. A portion of the sample was mixed with a flux, melted, and fused into a glass disc using a graphite die. This glass disc was then used for major element analysis. A portion of the sample was mixed with a binding agent and pressed into a pellet for trace element analysis. Major element abundances were determined using a Siemens MRS-400 multi-channel, simultaneous X-ray spectrometer. Trace element concentrations were measured using a Philips PW2300 sequential spectrometer. The USGS G-2 granite standard was used as an internal laboratory standard (See Table B.1 in Appendix B for laboratory standard data). The measured G-2 standard composition was within the error range of the accepted G-2 standard composition (Table B.1) except for MgO, Rb, and Ce which were 2%, 2%, and 9%, respectively, off the accepted G-2 standard values for those elements. A full description of the technique used can be found in Rhodes and Vollinger (2004) and Rhodes and Vollinger (2005).

3.1.2 Geochronology

To prepare for CA-TIMS geochronology, samples were processed in the Boston College Rock Preparation Laboratory. Due to the minute size of the zircons present within these rocks, sources of contamination can be too small to be seen with the naked eye. To avoid contamination, the apparatus to be used at each step in the process was thoroughly cleaned both before and after processing. This was accomplished by going over the entire apparatus with wire scrub brushes, taking particular care to areas that the sample would come in contact with, and then hand washing the apparatus with ethyl alcohol and paper towel. This process was repeated until the paper towel came back clean after wiping down the apparatus.

Any intensely weathered or altered material present in the sample was first removed with a rock hammer or diamond studded rock saw and discarded. The samples were then hand washed and dried to remove any dirt, moss, or other contaminants. At this point the samples were considered clean. This meant that samples were handled with clean and/or gloved hands, stored in clean and previously unused containers, and any surface they were to be in contact with was thoroughly cleaned and covered with a clean and previously unused sheet of paper.

Samples collected for geochronological analysis were first broken into fist sized pieces using a sledgehammer. A Bico International Inc. Jaw Crusher was then used to reduce the sample from fist sized pieces to approximately half-inch sized pieces. The sample was then processed by a Bico International Inc. Disc Mill Pulverizer. The

pulverizer was calibrated to reduce the grain size of the sample from half-inch sized pieces down to a fine-to-medium grained sand.

After grinding, the sample was divided by grain size on a Ro-Tap automatic sieving machine. Sieve sizes of 500 μm and 255 μm were used resulting in three size fractions: > 500 μm, 500 μm < x > 255 μm, and < 255 μm. If majority of the sample fell into the > 500 μm size fraction, that material was reprocessed by the disc mill pulverizer and sieved again. Each size fraction was then placed in clean and previously unused containers and properly labeled. The < 255 μm size fraction was then processed on an Outotec® Wilfley concentrating table. In the case of the Sudbury Granite sample, the < 255 μm fraction was determined to have an insufficient amount of material to continue processing. The 500 μm < x > 255 μm size fraction was reprocessed by the disc mill pulverizer, sieved, and then joined the < 255 μm size fraction to be processed on the Outotec® Wilfley concentrating table.

The Outotec® Wilfley concentrating table uses a gravity separation method involving water to separate mineral grains by mass. This results in the heaviest minerals, e.g. zircon, being the last grains to fall off the table. Small sample containers were placed along the edge of the table to collect the minerals. The lighter mineral fractions were dried in an oven and then combined into a single sample container, properly labeled, and stored. The heavy mineral fraction was collected in a clean and previously unused sample container. Once the entire sample was processed on the Outotec® Wilfley concentrating table, the heavy mineral fraction was sprayed with ethyl alcohol, filtered, and immediately dried under a heat lamp to remove the water present and prevent any

oxidation. Once dried, a hand-held rare-earth magnet was used to remove all the metal filings introduced into the sample as the result of normal use of the disc mill pulverizer.

When all the metal filings were removed, the sample was processed by a Frantz® Isodyamic separator, an apparatus that uses a magnetic field to separate magnetic and paramagnetic minerals from non-magnetic minerals (e.g. zircons). The sample was introduced to the magnetic field via an angled channel. The channel was set-up with a 20° forward slope and a 10° side slope and gently vibrated to provide a consistent delivery of material into the magnetic field. The separation was performed at the 0.4 Amps setting. After the separation, the magnetic separates were placed in a clean, previously unused, and properly labeled sample container, then set aside. The non-magnetic separate was then processed using the methylene iodide density separation technique.

Methylene iodide (MI) is a heavy liquid with a density of 3.3 g/cm^3. When minerals are introduced to the MI, the denser minerals (e.g. zircon with a density of 4.6 g/cm^3) will sink, while the lighter minerals (e.g. quartz with a density of 2.63 g/cm^3 and the feldspars with densities between 2.55 g/cm^3 and 2.76 g/cm^3) will float. The amount of MI used was determined by the total volume of the sample and poured into a separation funnel. The sample was poured on top of the MI and the funnel was swirled to ensure all the grains were in suspension. Once in suspension the sample was allowed to separate. When all the grains settled, the heavy separates were drained out of the funnel into a filter and set aside. The remaining material was then collected into a separate filter. Both filters were rinsed with acetone to remove any MI remaining in the pore space within the sample and dried under a heat lamp. Once dry, the light mineral separate was put into a clean, previously unused, and properly labeled sample container and set aside. When the

heavy mineral separate fully dried, it was processed on the Frantz® Isodyamic separator two more times at the 0.8 Amps and 1.2 Amps settings to ensure that the zircons present in the sample were separated out from the undesirable minerals.

The non-magnetic separate from the 1.2 Amp separation was then placed in an ethyl alcohol suspension in a petri dish and examined under a microscope. Using color, relief, and morphology as optical criteria (Corfu et al., 2003) over 150 zircons were handpicked and placed into an ethyl alcohol suspension in another petri dish. From these handpicked grains, 30 of the 'cleanest' zircons (based on color and morphology) were selected for grain mounting. Only a handful of grains were selected because the CA-TIMS technique only requires a few grains for an age determination. The selected zircons were mounted in a 25 mm diameter epoxy grain mount. This grain mount was then polished on a Struers Labo-Pol 5 grain mount polisher until the cores of the zircons were exposed.

After polishing, the grain mounts were carbon coated and placed in a scanning electron microscope for cathodoluminescence (CL) imaging at the Electron Microprobe Facility, Earth, Atmospheric, and Planetary Sciences Department, Massachusetts Institute of Technology, Cambridge, Massachusetts. In CL imagery, zircons can display an oscillatory zoning texture. This texture is indicative of an igneous origin (Corfu et al., 2003; Hoskin & Schaltegger, 2003) and indicates that the U-Pb ages determined from these grains reflect the crystallization ages of their host rocks. Thus, zircons exhibiting the strongest oscillatory zoning were chosen for geochronological analysis to ensure the highest quality data.

The CA-TIMS technique utilizes a pre-TIMS chemical treatment during which zones within the zircon crystal suffering from Pb loss are subjected to thermal annealing and acid leaching. The zircons were then subject to complete dissolution and subsequent column chemistry to isolate the U and Pb present in the grain, as part of the typical TIMS analysis. The chemical abrasion pretreatment allows grains analyzed by CA-TIMS to yield much more concordant ages than typical TIMS analysis (Mattinson, 2005).

Data reduction, age calculation, and the generation of concordia plots were carried out using the method of McLean and others (2011) and the statistical reduction and plotting program REDUX (Bowring et al., 2011). U-Pb errors on analyses in this study are reported as: ±X/Y/Z, where X is the internal error in absence of all systematic errors, Y includes the tracer calibration error, and Z includes both tracer calibration and the decay constant errors of Jaffey and others (1971). For simplicity, the larger Z error was used when discussing the U-Pb ages in this study. Since it includes both the tracer calibration and the decay constant errors, the Z error is accepted as an external error. The TIMS analysis was performed on a VG Sector 54 thermal ionization mass spectrometer at the Radiogenic Isotope Laboratory, Earth, Atmospheric, and Planetary Sciences Department, Massachusetts Institute of Technology, Cambridge, Massachusetts. A complete description of the CA-TIMS technique can be found in Mattinson (2005) and Rameszani and others (2007).

3.2 Andover Granite

The samples collected from the foliated Andover Granite are foliated, fine-to-medium grained, biotite + muscovite, garnet-bearing, leucogranites (Figure 3.2), consistent with the definition for the foliated Andover Granite by Collins (1987). These samples are composed of up to 8 % biotite, 11 % muscovite, and 1 % almandine garnet (Table 3.1). Modal analysis of these two samples indicates a monzogranite rock type (Figure 3.3). In thin section, pressure solution and myrmekitic textures are present as well as minor alteration of plagioclase to sericite and biotite to chlorite (Figure 3.4). Geochemically (Table 3.2), these samples are silica rich (> 75 wt. % SiO_2) with between 7 wt. % and 9 wt. % alkaline elements (Na_2O and K_2O) (Figure 3.5) and less than ~2 wt. % ferromagnesian elements (Fe_2O_3, MnO, and MgO). Trace element concentrations of Nb, Rb, and Y, elements of particular interest in granite investigations (Pearce et al., 1984), are 20.0 ppm, 271.3 ppm, and 35.5 ppm, respectively, for sample A-4 and 17.0 ppm, 196.7 ppm, and 31.0 ppm, respectively, for sample A-5 (Table 3.2).

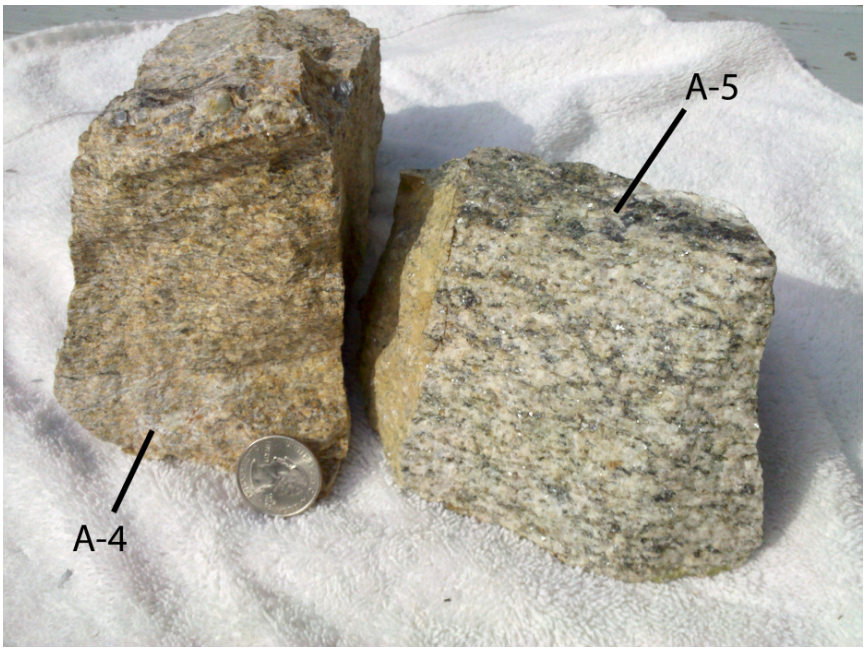

Figure 3.2 – Hand samples of the foliated Andover Granite samples. Sample labels are as indicated. Quarter for scale.

Mineralogy of the Andover Granite in Modal %		
Sample	**A-4**	**A-5**
Quartz	35	37
Potassium Feldspar	27	26
Plagioclase	22	20
Biotite	8	5
Muscovite	8	11
Garnet	-	1
Grain Size	Fine (0.1 mm - 0.2 mm)	Med to Fine (0.25 mm - 1.0
Alteration Products	Sericite	Chlorite, Sericite
Classification	Monzogranite	Monzogranite

Table 3.1 – Modal mineralogy of the two analyzed samples from the foliated Andover Granite. The lack of albite twinning in the plagioclase crystals of both samples hindered An_x determination.

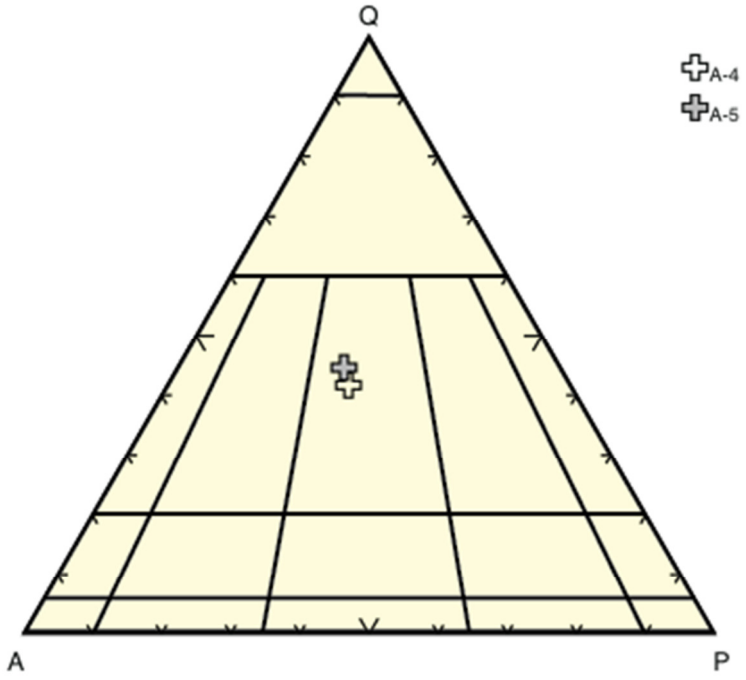

Figure 3.3 – IUGS ternary of the two analyzed samples from the foliated Andover Granite. The samples fall within the monzogranite field. See Table 3.1 for mineralogy. Q-Quartz, A-Alkaline Feldspar, P-Plagioclase Feldspar.

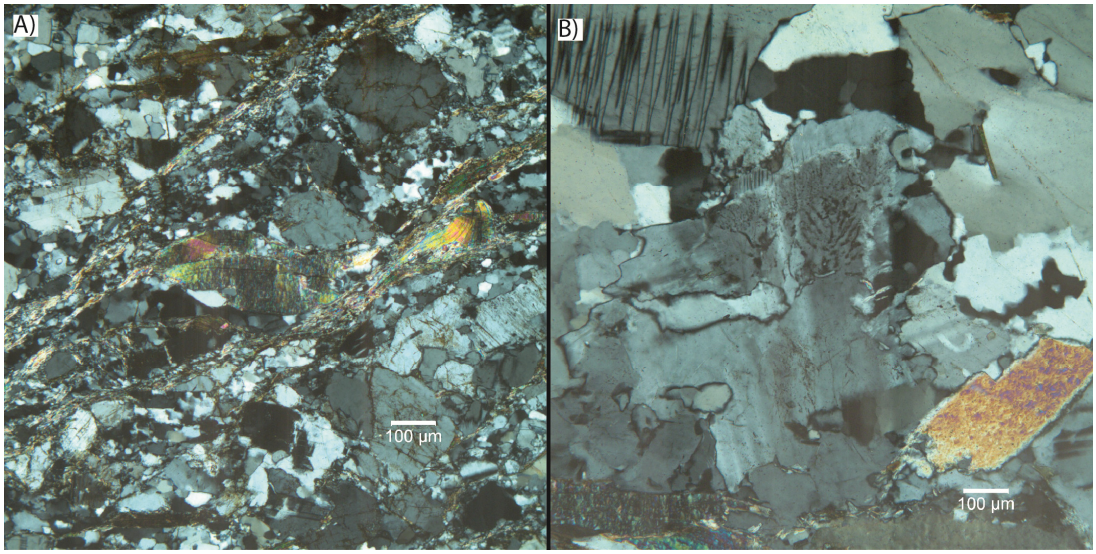

Figure 3.4 – Photomicrographs with crossed polars of thin sections taken from the foliated Andover Granite samples. Scale bar is 100 microns. A) Sample A-4: Note the pressure solution textures. B) Sample A-5: Note the myrmekitic texture.

Major Elements for the Andover Granite in wt. %		
	A-4	A-5
SiO_2	75.81	75.45
TiO_2	0.10	0.04
Al_2O_3	13.89	14.20
Fe_2O_3*	1.12	1.63
MnO	0.06	0.04
MgO	0.22	0.17
CaO	0.57	0.49
Na_2O	3.75	3.17
K_2O	4.56	5.07
P_2O_5	0.07	0.08
Total	100.15	100.34
LOI	0.84	0.71

Trace Elements for the Andover Granite in ppm		
	A-4	A-5
Ba	213	19
Rb	271.3	196.7
Sr	43	16
Y	35.5	31.0
Zr	80	56
Nb	20.0	17.0
Zn	35	29
Ga	17	16
Ni	3	2
V	4	1
La	17	4
Ce	43	15
Cr	3	4
Th	16	4
U	10	3
Pb	30	42

Table 3.2 – Major and trace element geochemistry of the analyzed foliated Andover Granite samples. LOI – Loss On Ignition, volatile content. See Table B.1 for laboratory standard data. Note: Fe_2O_3* is TOTAL Fe and totals have not been recalculated using the LOI value.

3.2.1 Geochronology

U-Pb geochronological data from the foliated Andover Granite is presented in Table 3.3. Zircons retrieved from the foliated Andover Granite are brownish with both rounded and dipyramidal morphologies (Figure 3.6A-B). In CL imagery, these zircons display oscillatory zoning varying from nonexistent to strong. Due to the deformation present in these samples, zircons exhibiting the strongest oscillatory zoning were chosen for CA-TIMS analysis (Figure 3.6C-F) to ensure that the resulting age reflects the crystallization age of the host rock. Ages from zircons that lack oscillatory zoning could reflect the timing of metamorphism and as such were not selected. The analyzed zircons yielded concordant weighted mean $^{206}Pb/^{238}U$ ages (Figure 3.7) of 419.43 ± 0.52 Ma (Sample A-4) and 419.65 ± 0.51 Ma (Sample A-5).

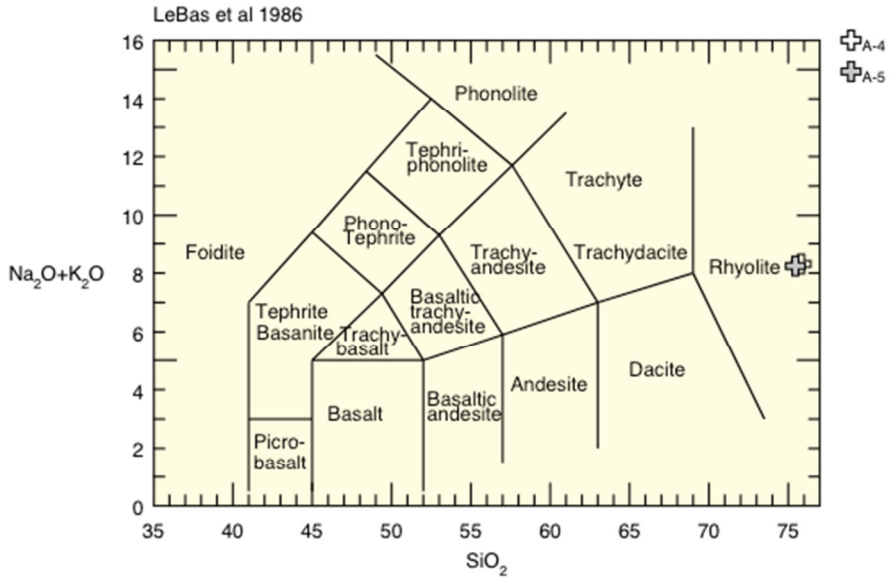

Figure 3.5 – Alkali vs Silica rock type plot. The two analyzed foliated Andover Granite samples fall within the rhyolite compositional field. Fields from LeBas and others (1986).

U-Pb Geochronological data for the Andover Granite														
		A-4								A-5				
Grain Composition	Zircon	CL7	CL16	CL16a	CL16b	CL24a	CL41	CL42		CL11	CL12	CL13	CL29
	Th/U [a]	0.41	0.27	0.42	0.36	0.04	0.18	0.95		0.22	0.17	0.22	0.12
	Pb* (pg) [b]	0.38	0.38	0.39	0.55	0.43	0.20	0.39		0.17	0.57	0.18	0.48
	Pb*/Pbc [d]	79.52	14.95	22.43	25.95	105.67	34.56	34.16		34.12	42.50	52.30	17.61
Isotopic Ratios	$^{206}Pb/^{204}Pb$ [e]	4895	971	1390	1633	7196	2273	1847		2224	2802	3397	1190
	$^{206}Pb/^{238}U$ [f,g]	0.067236	0.068072	0.068050	0.068025	0.067502	0.067255	0.067199		0.067237	0.067291	0.067265	0.067241
	±2σ %	0.05	0.14	0.15	0.08	0.06	0.26	0.10		0.10	0.07	0.07	0.11
	$^{207}Pb/^{235}U$ [f]	0.512693	0.519969	0.519822	0.518700	0.515052	0.511895	0.511243		0.512426	0.512229	0.511930	0.514081
	±2σ %	0.20	1.02	0.63	0.53	0.16	0.67	0.49		0.50	0.32	0.36	0.79
	$^{207}Pb/^{206}Pb$ [f,g]	0.055329	0.055425	0.055427	0.055327	0.055364	0.055226	0.055202		0.055274	0.055233	0.055198	0.055475
	±2σ %	0.18	0.99	0.60	0.51	0.13	0.66	0.46		0.44	0.30	0.33	0.77
Dates [Ma]	$^{206}Pb/^{238}U$ [g,h]	**419.48**	**424.53**	**424.39**	**424.25**	**421.09**	**419.60**	**419.26**		**419.49**	**419.82**	**419.66**	**419.51**
	±2σ (abs.)	0.22	0.59	0.62	0.34	0.25	1.06	0.39		0.41	0.28	0.28	0.44
	$^{207}Pb/^{235}U$ [h]	**420.26**	**425.13**	**425.03**	**424.28**	**421.84**	**419.72**	**419.28**		**420.08**	**419.95**	**419.75**	**421.19**
	±2σ (abs.)	0.70	3.53	2.19	1.84	0.54	2.31	1.67		1.72	1.09	1.24	2.74
	$^{207}Pb/^{206}Pb$ [g,h]	**424.52**	**428.40**	**428.50**	**424.47**	**425.95**	**420.40**	**419.42**		**423.33**	**420.67**	**420.23**	**430.40**
	±2σ (abs.)	4.04	22.11	13.36	11.45	2.90	14.75	10.34		9.87	6.67	7.32	17.08
	Corr. Coef.	0.51	0.25	0.32	0.30	0.59	0.24	0.34		0.64	0.36	0.55	0.32

Table 3.3 – U-Pb geochronological data of the foliated Andover Granite samples. Blank and Oxygen composition: $^{206}Pb/^{204}Pb = 18.42 \pm 0.35$; $^{207}Pb/^{204}Pb = 15.35 \pm 0.23$; $^{208}Pb/^{204}Pb = 37.46 \pm 0.74$; $^{18}O/^{16}O = 0.00205 \pm 0.00002$.

Superscripts are as follows: a) Th contents calculated from radiogenic ^{208}Pb and the $^{207}Pb/^{206}Pb$ date of the sample, assuming concordance between U-Th and Pb systems, b) Total mass of radiogenic Pb, c) Total mass of common Pb, d) Ratio of radiogenic Pb (including ^{208}Pb) to common Pb, e) Measured ratio corrected for fractionation and spike contribution only, f) Measured ratios corrected for fractionation, tracer, blank and initial common Pb, g) Corrected for Initial Th/U disequilibrium using radiogenic ^{208}Pb and Th/U [magma] = 2.8, h) Isotopic dates calculated using the decay constants $\lambda^{238} = 1.55125E\text{-}10$, $\lambda^{235} = 9.8485E\text{-}10$ (Jaffey et al., 1971), and for the $^{238}U/^{235}U = 137.818 \pm 0.045$ (Hiess et al., 2012).

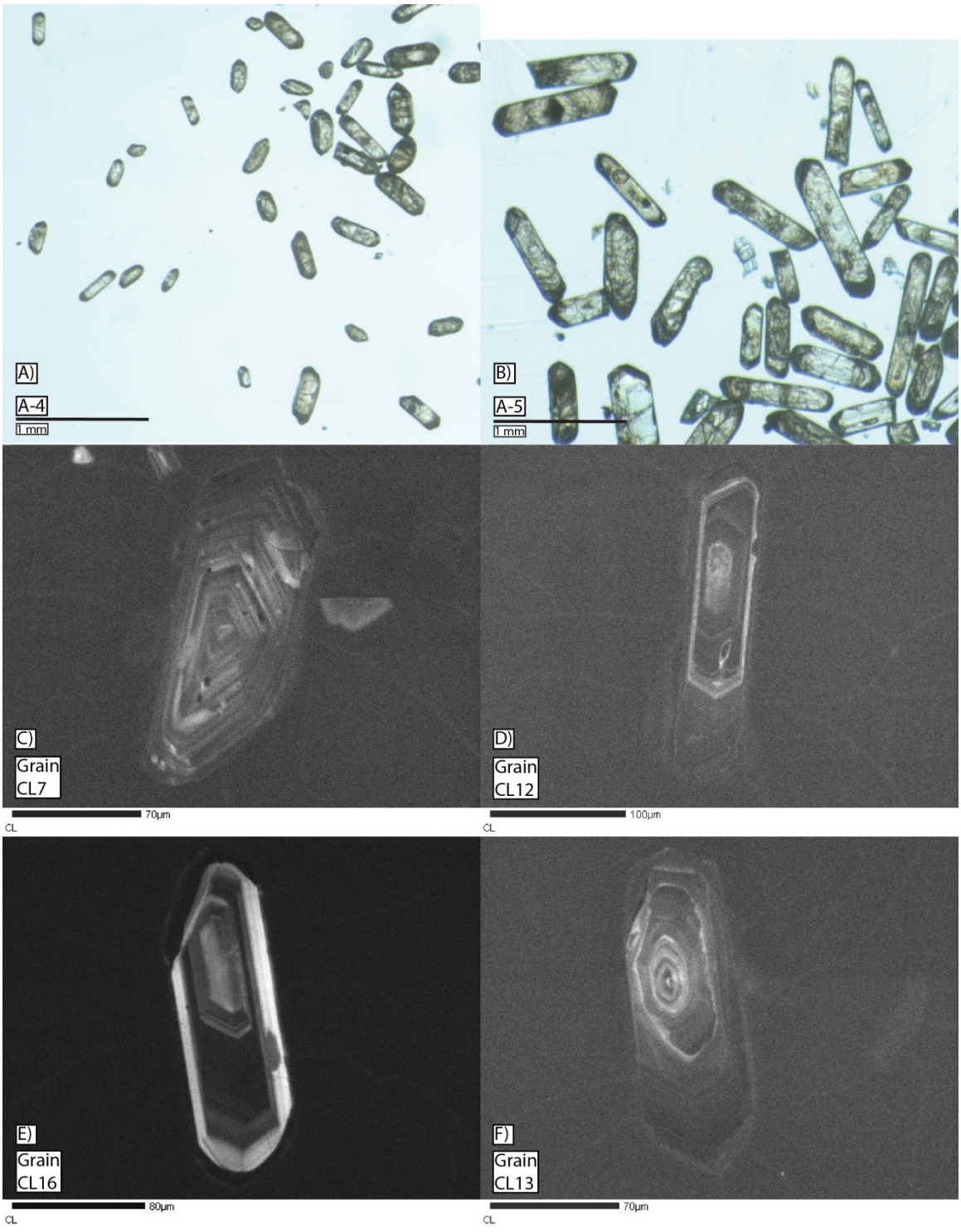

Figure 3.6 – Optical and CL images of zircons retrieved from the two foliated Andover Granite samples. A) Zircons retrieved from Sample A-4 as seen in plain light. B) Zircons retrieved from Sample A-5 as seen in plain light. C-F) CL images of zircon grains. Grain CL7 (C) and CL16 (E) were collected from Sample A-4. Grain CL12 (D) and CL13 (F) were collected from Sample A-5. Note the oscillatory zoning visible in CL images. See Table 3.3 for U-Pb isotopic data specific to these grains.

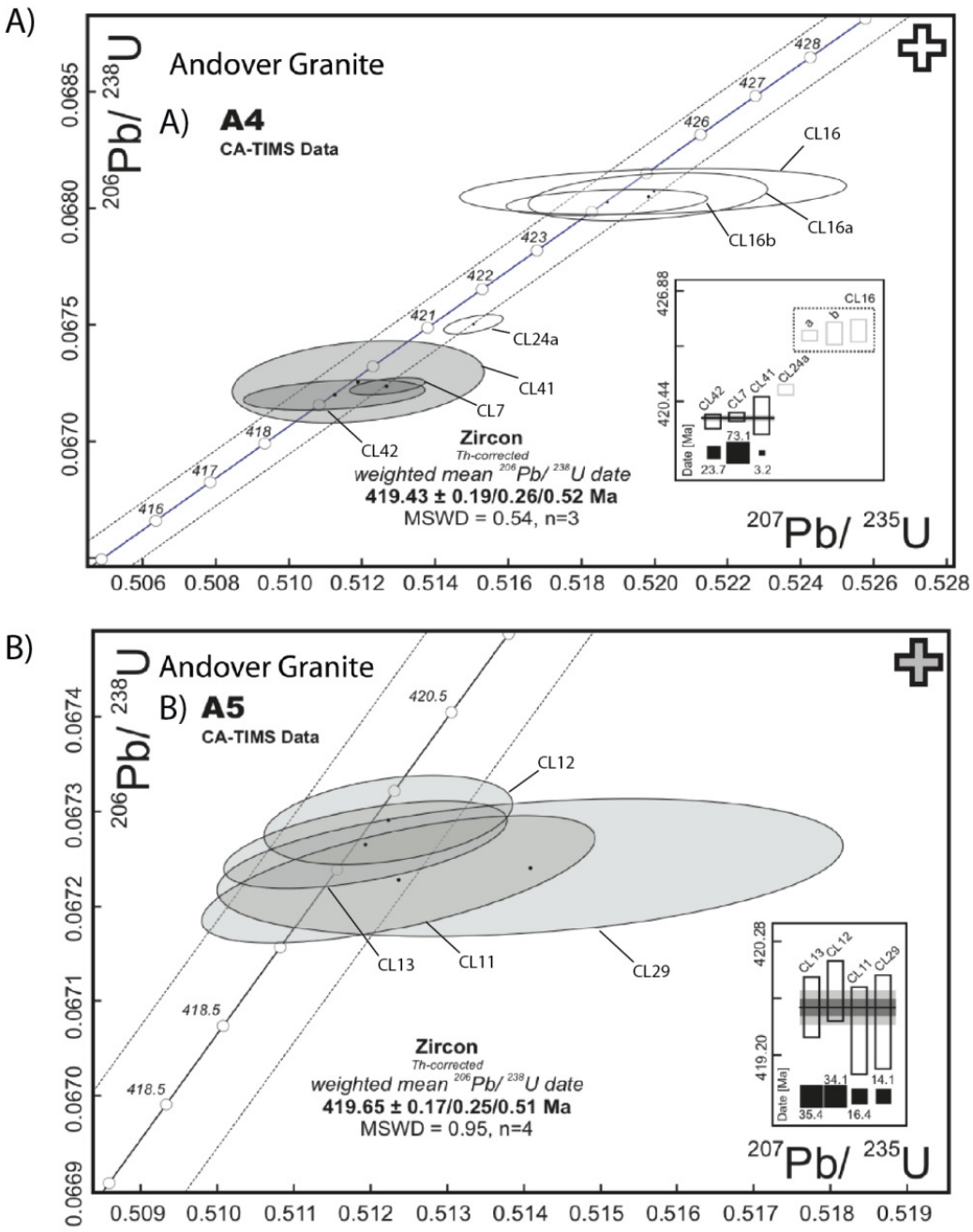

Figure 3.7 – U-Pb Concordia for the foliated Andover Granite. A) Sample A-4. B) Sample A-5. The error associated with the concordia is represented by the dotted lines flanking the concordia. Each analyzed zircon grain is represented by a data point and the surrounding ellipse reflects the accompanying error of that data point. Grains are considered concordant if the data point or error ellipse falls within the error margin of the concordia. The shaded ellipses highlight the grains that contributed to the age calculation. The inset box displays the contribution of each grain to the mean standard weight deviation for the age calculation. The size of the black box correlates with the contribution of each grain to the age calculation. Note: While grains CL24a and CL16 from Sample A-4 are concordant, they were not considered for the age calculation because prior to CA-TIMS analysis the grains broke apart during the final stages of sample preparation. Therefore, U-Pb analysis from these fragments may not be an accurate representation of the crystallization age of the grain.

3.3 Sgr Group

3.3.1 Sudbury Granite

The samples collected from the Sudbury Granite are medium-grained, pink, biotite granites (Figure 3.8) and can be separated into two groups on the basis of quartz content: a quartz rich group and a quartz poor group. During field work, a contact relationship between these two groups and the surrounding country rock was not observed. However, numerous pink aplite dikes were observed throughout the pluton and were accompanied by sharp contacts between the dike and granite. Furthermore, enclaves were observed within the granite. These enclaves are small, on the order of 10s of centimeters in length, and are composed of a higher concentration of biotite than the surrounding granite (Table 3.4).

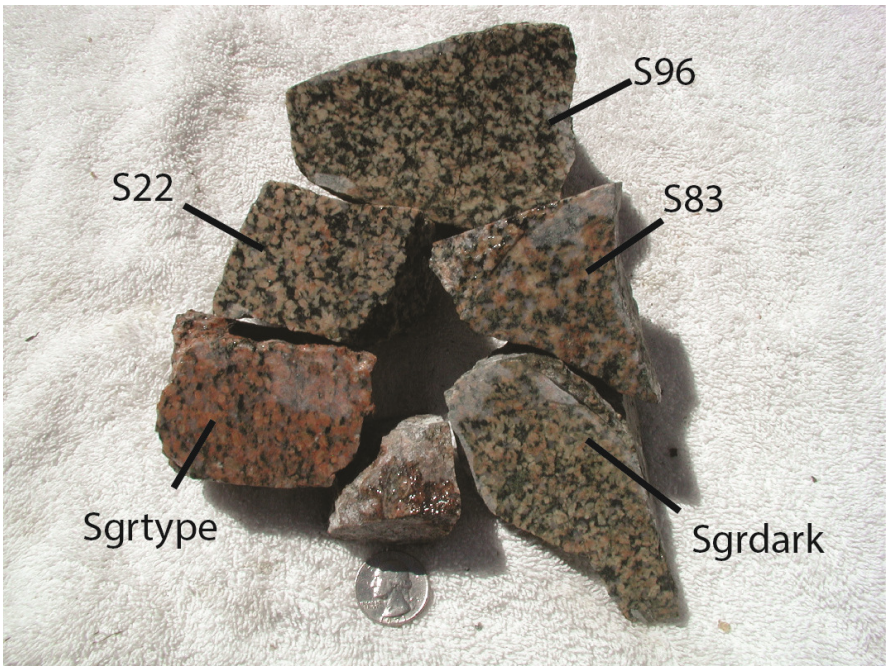

Figure 3.8 – Hand samples of the Sudbury Granite. Sample labels are as indicated. Quarter for scale.

Sgr Group Mineralogy in Modal %							
	Sudbury Granite						
Sample	SgrType	D311_5	S83	Sgrtypeenclave	SgrDark	S22	S96
Quartz	25	23	27	19	19	19	19
Potassium Feldspar	35	39	36	32	36	40	30
Plagioclase	25	28	24	22	32	29	27
An_x	26	28	-	-	-	14	30
Biotite	11	8	11	17	11	7	14
Hornblende	1	-	-	-	-	3	7
Titanite	3	2	2	10	2	2	3
Grain Size	Medium (2 mm - 5 mm)	Medium (2 mm - 5 mm)	Medium (2 mm - 5 mm)	Medium (2 mm - 5 mm)	Medium (2 mm - 5 mm)	Medium (2 mm - 5 mm)	Medium (2 mm - 5 mm)
Alteration Products	Chlorite, Sericite/Sausserite	Chlorite, Sericite/Sausserite	Chlorite, Sericite/Sausserite	Chlorite, Sericite	Chlorite, Sericite	Chlorite, Sericite	Chlorite, Sericite
Classification	Monzogranite	Monzogranite	Monzogranite	-	Monzogranite	Monzogranite	Monzogranite
Notes:	Perthite	Perthite, Pleochroic Halos	Secondary Cal/Q			Perthite, Myrmekite	

Central Granite							
Sample	M3a	M6	M7	M18	M19	M20	
Quartz	27	30	26	21	27	22	
Potassium Feldspar	50	20	46	45	20	45	
Plagioclase	20	35	22	27	35	30	
An_x	6	-	-	-	26	26	
Biotite	3	15	6	6	15	3	
Hornblende	-	-	-	-	3	-	
Titanite	-	-	-	-	-	-	
Grain Size	Fine to Med (0.5 mm - 2 mm)	Fine (0.5 mm - 1 mm)	Fine (0.5 mm - 1 mm)	Fine to Med (0.5 mm - 2 mm)	Fine to Med (0.5 mm - 2 mm)	Fine to Med (0.5 mm - 2 mm)	
Alteration Products	Chlorite, Sericite	Chlorite, Sericite	Chlorite, Sericite	Chlorite, Sericite	Chlorite, Sericite	Chlorite, Sericite	
Classification	Syenogranite	Monzogranite	Syenogranite	Monzogranite	Monzogranite	Monzogranite	
Notes:	Perthite, Myrmekite, Kspar megacryst, Pleochroic Halos	Pleochroic Halos	Pleochroic Halos	Myrmekite, Black Oxides, Kspar megacryst, Pleochroic Halos	Pleochroic Halos	Perthite, Myrmekite, Pleochroic Halos	

Table 3.4 – Modal mineralogy of the Sgr group and Bloody Bluff fault samples. The color highlighting was selected to allow for the easier identification of each zone. Green and red represents the Sudbury Granite with green selected for the quartz rich group and red for the quartz poor group. Dark blue represents the central Sgr granite. Light blue represents the northern Sgr granite. White represents samples collected on or near the Bloody Bluff fault. Note: Sgrtypeenclave is a thin section of an enclave taken from a hand sample of the Sudbury Granite. (Continued on next page).

	Northern Granite			
Sample	**M9/N1**	**N2a**	**N2a**	**N3**
Quartz	33	25	-	30
Potassium Feldspar	30	30	-	34
Plagioclase	35	30	3	27
An_x	-	-	-	-
Biotite	1	15	27	9
Hornblende	-	-	70	-
Titanite	-	-	-	-
Grain Size	Fine to Med (0.5 mm - 2 mm)	Fine (0.5 mm - 1 mm)	Fine (0.5 mm - 1 mm)	Fine (0.5 mm - 1 mm)
Alteration Products	Chlorite, Sericite	Chlorite, Sericite	Chlorite, Sericite	Chlorite, Sericite
Classification	Alk. Fld. Granite	-	-	Monzogranite
Notes:		Pleochroic Halos		Pleochroic Halos

	Bloody Bluff Fault		
Sample	**BBFType**	**BBF-A**	**BSC-1**
Quartz	27	-	25
Potassium Feldspar	29	-	45
Plagioclase	21	-	29
An_x	-	-	-
Biotite	6	-	1
Hornblende	-	-	-
Titanite	2	-	-
Grain Size	Medium (2 mm - 5 mm)	Medium (2 mm - 5 mm)	Fine to Med (0.5 mm - 2 mm)
Alteration Products	Chlorite, Sericite	Chlorite, Sericite	Sericite
Classification	Fault Breccia	Fault Breccia	Syenogranite
Notes:	Secondary Cal + Ank	Secondary Cal + Ank	Pleochroic Halos

Table 3.4 (Cont.) – Modal mineralogy of the Sgr Group and Bloody Bluff fault samples.

3.3.1.1 Sudbury Granite - Quartz Rich Group

The quartz rich group is composed of 23 % - 27 % quartz, 35 % - 39 % potassium feldspar, and 24 % - 28 % plagioclase feldspar (Oligoclase; An_x: 26 - 28) with between 8 % and 11 % biotite, 2 % - 3 % titanite, and up to 1 % hornblende (Table 3.4). Modal analysis of the quartz rich group indicates monzogranite rock types (Figure 3.9). Perthite is present in thin section, as are pleochroic halos surrounding zircon grains found in the biotite crystals. Weathering is pervasive, with plagioclase and biotite being heavily altered to sericite ± sausserite and chlorite, respectively. This group is silica rich (> 70 wt. % SiO_2) with a high abundance of K_2O (> 3.63 wt. %) (Figure 3.10). Trace element concentrations of Nb, Rb, and Y fall between 14.1 ppm and 16.3 ppm, 104.2 ppm and 125.9 ppm, and 15.0 ppm and 18.5 ppm, respectively (Table 3.5).

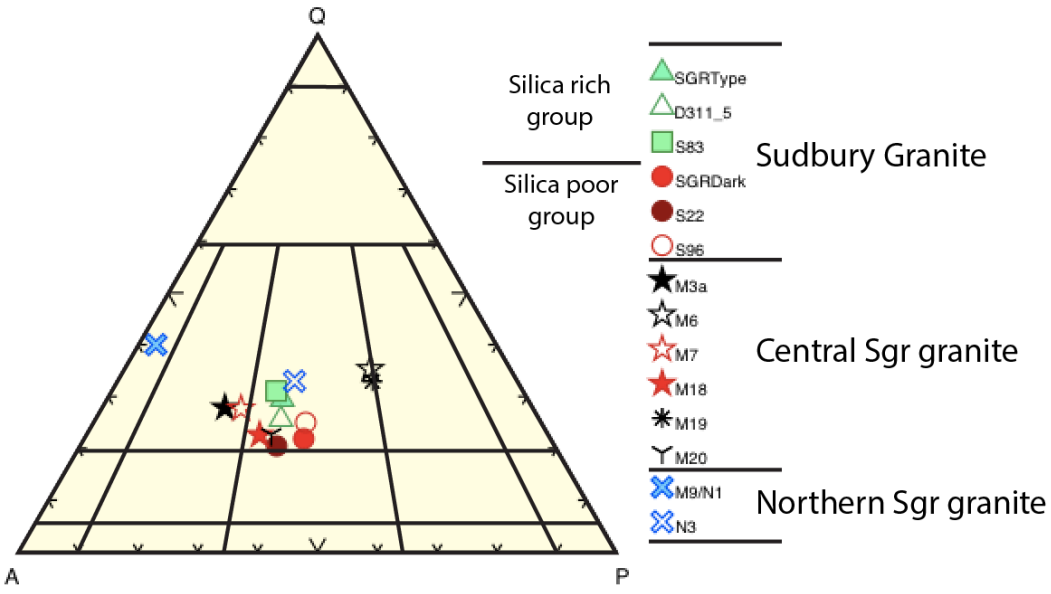

Figure 3.9 – IUGS ternary of the Sgr Group. The Sudbury Granite samples fall within the monzogranite field. The central Sgr Granite ranges from syenogranite to monzogranite. The northern Sgr granite falls within the alkali feldspar granite and monzogranite fields. See Table 3.4 for mineralogy. Q-Quartz, A-Alkaline Feldspar, P-Plagioclase Feldspar.

Major Elements for Sgr Group in wt. %								
	Sudbury Granite					Central Granite		Northern Granite
	Sgrtype	D3II_5	Sgrdark	S22	S96	M3a	M18	M9/N1
SiO_2	71.92	71.26	63.07	64.24	63.37	73.59	74.75	72.95
TiO_2	0.37	0.40	0.84	0.80	0.82	0.28	0.23	0.35
Al_2O_3	14.46	14.64	17.11	16.51	16.61	14.34	14.33	14.72
Fe_2O_3*	2.61	3.10	5.72	5.24	5.31	2.18	1.96	2.96
MnO	0.07	0.08	0.13	0.14	0.13	0.05	0.05	0.08
MgO	1.28	1.29	2.73	2.74	2.57	0.62	0.52	0.81
CaO	1.85	2.31	4.07	3.84	4.40	1.43	0.54	2.39
Na_2O	3.45	3.76	3.89	3.87	4.00	3.55	3.57	4.58
K_2O	4.31	3.63	2.27	2.24	2.49	4.25	4.82	1.43
P_2O_5	0.12	0.13	0.30	0.29	0.27	0.09	0.08	0.11
Total	100.44	100.60	100.13	99.91	99.97	100.38	100.85	100.38
LOI	1.23	1.80	2.30	2.19	1.33	1.20	1.14	1.27

Trace Elements for Sgr Group in ppm								
	Sudbury Granite					Central Granite		Northern Granite
	Sgrtype	D3II_5	Sgrdark	S22	S96	M3a	M18	M9/N1
Ba	562	433	708	906	533	787	497	205
Rb	104.2	125.9	74.8	71.6	107.8	111.3	169.0	83.9
Sr	357	287	587	754	538	195	75	229
Y	18.5	15.0	34.9	38.6	26.3	18.4	30.9	14.2
Zr	133	151	278	289	267	190	194	199
Nb	14.1	16.3	19.0	18.3	17.0	11.1	16.9	14.8
Zn	46	50	89	113	105	59	37	42
Ga	14	15	17	18	18	14	16	17
Ni	9	10	22	21	21	4	4	3
V	38	43	90	91	93	20	14	25
La	35	44	45	41	44	29	36	18
Ce	63	77	98	93	89	58	88	39
Cr	15	15	35	34	36	6	5	6
Th	24	24	12	9	14	13	20	6
U	2	7	1	0	2	1	3	2
Pb	22	19	11	25	19	44	27	17

Table 3.5 – Major and trace element geochemistry of the Sgr Group samples. Green and red represents the quartz rich and quartz poor groups of the Sudbury Granite, respectively. Dark blue represents the central Sgr Granite. Light blue represents the northern Sgr Granite. LOI – Loss On Ignition, volatile content. See Table B.1 for laboratory standard data. Note: Fe_2O_3* is TOTAL Fe and totals have not been recalculated using the LOI value.

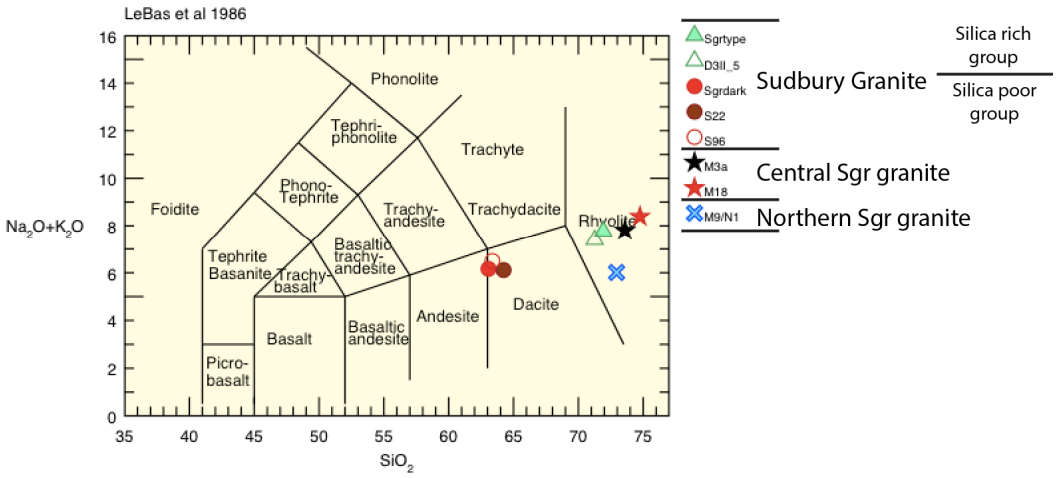

Figure 3.10 – Silica vs Alkali element bivariate plot. The quartz rich group of the Sudbury Granite and the central and northern Sgr granites fall within the rhyolite compositional field. The quartz poor group of the Sudbury Granite falls within the dacite compositional field. Fields from LeBas and others (1986).

3.3.1.2 Sudbury Granite - Quartz Poor Group

The quartz poor group is composed of 19 % quartz, 30 % - 40 % potassium feldspar, and 27 % - 32 % plagioclase feldspar (Oligoclase; An_x: 14 - 30), with 7 % - 14 % biotite, 2 % - 3 % titanite, and up to 7 % hornblende (Table 3.4). Modal analysis of the quartz poor group indicates monzogranite rock types (Figure 3.9). Like the quartz rich group, the samples of this group are heavily weathered, albeit more heavily weathered than the quartz rich group. Biotite is nearly completely altered to chlorite. Perthite is visible in thin section. Myrmekite is also present in thin section, but rare. Geochemically (Table 3.5), this group is silica poor (< 70 wt. % SiO_2) with less than 2.5 wt. % K_2O (Figure 3.10). Trace element concentrations of Nb, Rb, and Y fall between 17.0 ppm and 18.3 ppm, 71.6 ppm and 107.8 ppm, and 26.3 ppm and 38.6 ppm, respectively (Table 3.5).

3.3.1.3 Geochronology

Zircons retrieved from the Sudbury Granite are clear and exhibit a near euhedral morphology (Figure 3.11A). In CL imagery, these zircons display oscillatory zoning varying from nonexistent to strong. Zircons exhibiting the strongest oscillatory zoning were chosen for CA-TIMS analysis (Figure 3.11B) to ensure that the resulting age reflects the crystallization age of the host rock. CA-TIMS analysis of these grains yielded a concordant weighted mean $^{206}Pb/^{238}U$ age for the Sudbury Granite at 420.49 ± 0.52 Ma (Figure 3.12; Table 3.6).

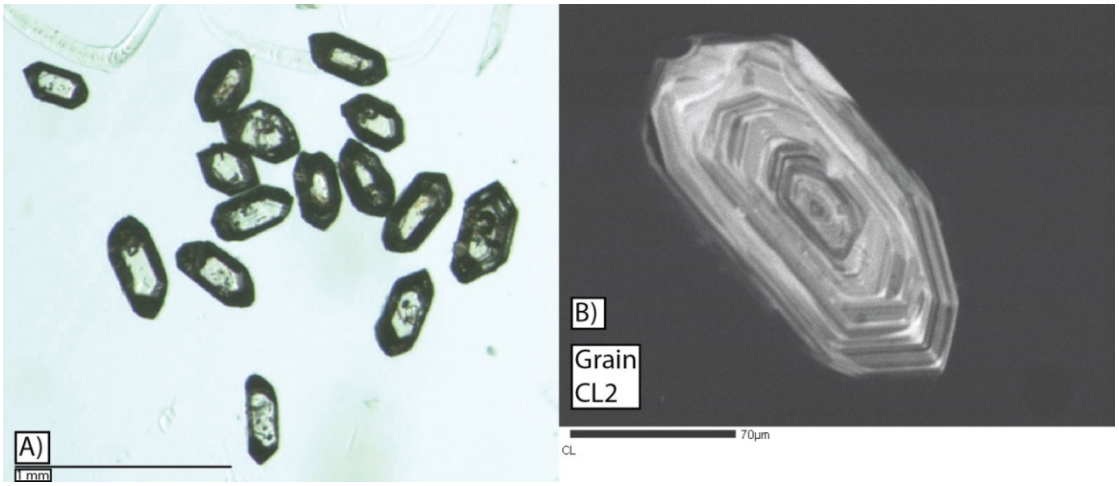

Figure 3.11 – Optical and CL images of zircons collected from the Sudbury Granite. A) Zircons retrieved from the Sudbury Granite as seen in plain light. B) CL image of Grain CL2. Note the strong oscillatory zoning. See Table 3.6 for U-Pb isotopic data for grain CL2.

U-Pb Geochronological data for the Sudbury Granite					
SudburyType					
Grain Composition	Zircon	**CL2**	**CL5**	**CL6**	**CL7**
	Th/U [(a)]	0.74	0.69	0.80	0.55
	Pb* (pg) [(b)]	0.32	0.51	1.85	0.23
	Pb*/Pbc [(d)]	174.31	132.74	19.67	141.78
Isotopic Ratios	$^{206}Pb/^{204}Pb$ [(e)]	9846	7593	1109	8390
	$^{206}Pb/^{238}U$ [(f,g)]	0.067385	0.067408	0.067442	0.067384
	±2σ %	0.12	0.07	0.11	0.08
	$^{207}Pb/^{235}U$ [(f)]	0.514196	0.514760	0.516936	0.514188
	±2σ %	0.17	0.15	0.77	0.15
	$^{207}Pb/^{206}Pb$ [(f,g)]	0.055343	0.055385	0.055591	0.055343
	±2σ %	0.11	0.12	0.74	0.11
Dates [Ma]	$^{206}Pb/^{238}U$ [(g,h)]	**420.38**	**420.52**	**420.72**	**420.38**
	±2σ (abs.)	0.51	0.28	0.46	0.33
	$^{207}Pb/^{235}U$ [(h)]	**421.27**	**421.64**	**423.10**	**421.26**
	±2σ (abs.)	0.60	0.53	2.65	0.52
	$^{207}Pb/^{206}Pb$ [(g,h)]	**426.11**	**427.78**	**436.08**	**426.10**
	±2σ (abs.)	2.40	2.69	16.57	2.58
	Corr. Coef.	0.79	0.65	0.27	0.66

Table 3.6 – U-Pb geochronological data of the Sudbury Granite.
Blank and Oxygen composition: $^{206}Pb/^{204}Pb = 18.42 \pm 0.35$; $^{207}Pb/^{204}Pb = 15.35 \pm 0.23$; $^{208}Pb/^{204}Pb = 37.46 \pm 0.74$; $^{18}O/^{16}O = 0.00205 \pm 0.00002$.
Superscripts are as follows: a) Th contents calculated from radiogenic ^{208}Pb and the $^{207}Pb/^{206}Pb$ date of the sample, assuming concordance between U-Th and Pb systems, b) Total mass of radiogenic Pb, c) Total mass of common Pb, d) Ratio of radiogenic Pb (including ^{208}Pb) to common Pb, e) Measured ratio corrected for fractionation and spike contribution only, f) Measured ratios corrected for fractionation, tracer, blank and initial common Pb, g) Corrected for Initial Th/U disequilibrium using radiogenic ^{208}Pb and Th/U [magma] = 2.8, h) Isotopic dates calculated using the decay constants $\lambda^{238} = 1.55125E\text{-}10$, $\lambda^{235} = 9.8485E\text{-}10$ (Jaffey et al., 1971), and for the $^{238}U/^{235}U = 137.818 \pm 0.045$ (Hiess et al., 2012).

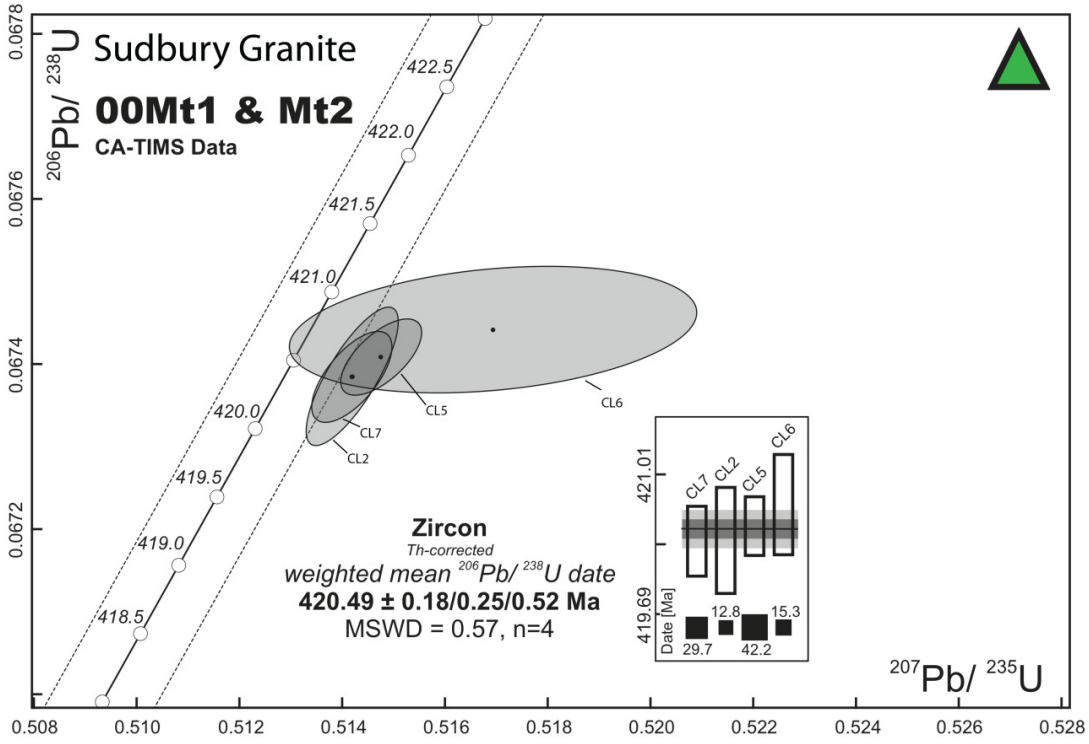

Figure 3.12 – U-Pb Concordia for Sudbury Granite. The error associated with the concordia is represented by the dotted lines flanking the concordia. Each analyzed zircon grain is represented by a data point and the surrounding ellipse reflects the accompanying error of that data point. Grains are considered concordant if the data point or error ellipse falls within the error margin of the concordia. The shaded ellipses highlight the grains that contributed to the age calculation. The inset box displays the contribution of each grain to the mean standard weight deviation for the age calculation. The size of the black box correlates with the contribution of each grain to the age calculation.

3.3.2 Central Sgr Granite

Samples collected from the central Sgr granite are fine-to-medium grained, pink or gray/white, biotite granites (Figure 3.13). These samples are composed of 21 % - 30 % quartz, 20 % - 50 % potassium feldspar, and 20 % - 35 % plagioclase feldspar with between 3 % and 15 % biotite, and up to 3 % hornblende (Table 3.4). Modal analysis of these samples indicates monzogranite to syenogranite rock types (Figure 3.9). In thin section, perthite and myrmekite textures are visible as are pleochroic halos surrounding the zircon grains found in biotite crystals. Weathering is common with moderate sericitization of the feldspars (extreme in some cases) and near complete chloritization of biotite.

The samples collected from this zone are silica rich (> 70 wt. % SiO_2) with a high abundance of K_2O (> 4.25 wt. %) (Figure 3.10). Trace element concentrations of Nb, Rb, and Y are between 11.1 ppm and 16.9 ppm, 111.3 ppm and 169.0 ppm, and 18.4 ppm and 30.9 ppm, respectively (Table 3.5). During field work, contact relationships between this zone and surrounding country rock were not observed. This is despite exposures of a biotite hornblende diorite (likely the Sharpners Pond Diorite) being observed in close proximity to the granite outcrops. Additionally, no contact relationships were observed between the varieties of granites observed in the zone. Pink aplite dikes were observed to intrude the granite and have both sharp and diffuse contacts between dike and granite.

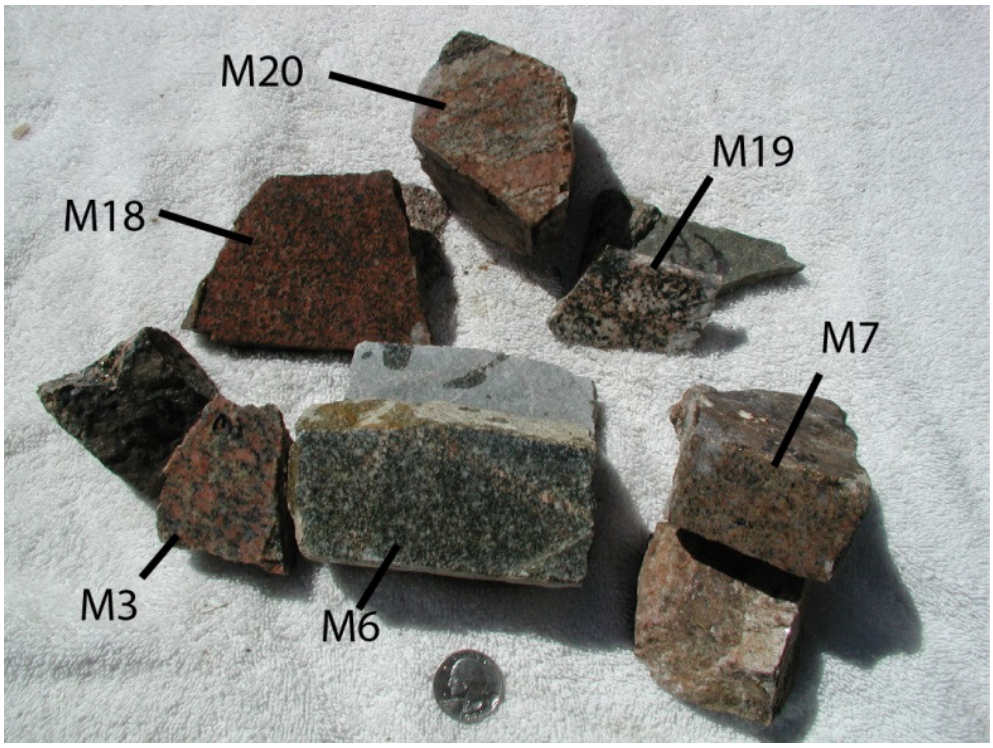

Figure 3.13 – Hand samples of the central Sgr granite. Sample labels are as indicated. Quarter for scale.

3.3.3 Northern Sgr Granite

Samples collected from the northern Sgr granite are fine-to-medium grained, white, biotite granites (Figure 3.14) composed of 25 % - 33 % quartz, 30 % - 34 % potassium feldspar, and 27 % - 25 % plagioclase feldspar with 1 % - 15 % biotite (Table 3.4). Modal analysis of these samples indicates they are monzo- to alkaline feldspar granites (Figure 3.9). Weathering is intense with heavy feldspar sericitization and biotite chloritization. Pleochroic halos are observed in thin section surrounding the zircon grains found in the biotite crystals. This zone is silica rich (72.95 wt. % SiO_2) (Table 3.5) with a high abundance of Na_2O (4.58 wt. %) (Figure 3.10). Trace element concentrations of Nb, Rb, and Y in this zone are 14.8 ppm, 83.9 ppm, and 14.2 ppm, respectively (Table 3.5). During field work, a single diffuse contact was observed between this granite and the surrounding country rock, a biotite hornblende diorite (Figure 3.15).

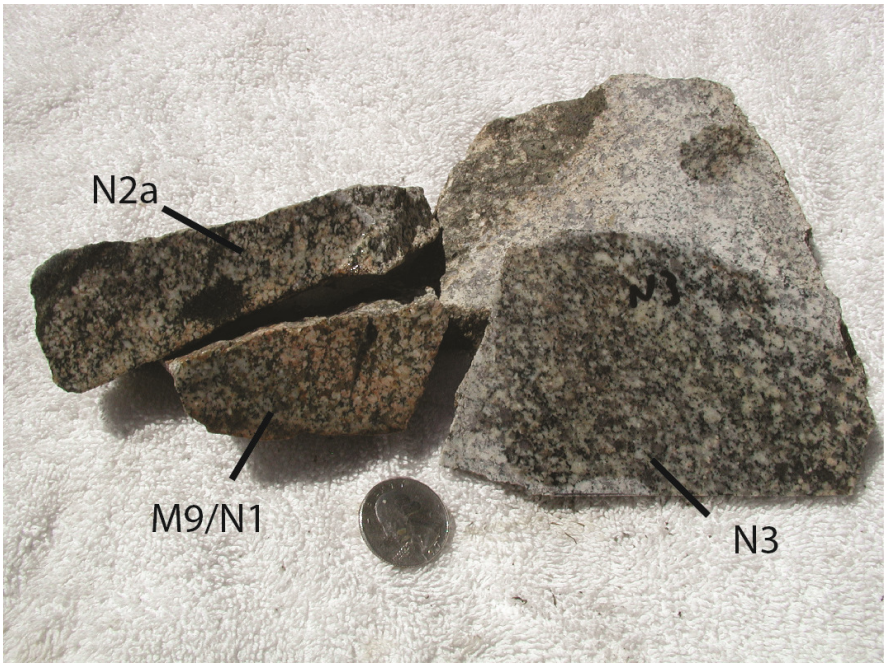

Figure 3.14 – Hand samples of the northern Sgr granite. Sample labels are as indicated. Quarter for scale.

Figure 3.15 – Hand sample taken of the contact between the northern Sgr granite and the country rock. Note the diffuse nature of the contact. Field of view is 18.5 cm wide, note the hammer for scale.

3.4 Granites in Bloody Bluff Fault Zone

The type locality of the Bloody Bluff fault is in Concord, Massachusetts at the northern border of the Sudbury Granite (Figure 1.2). Recent flora removal at this location allowed for excellent observation and description. Two thin sections (Figure 3.16) were prepared from rocks collected from this exposure (Table 3.4). As expected for a fault exposure, these rocks are brittlely deformed and secondary mineralization involving calcite and possibly ankerite was common throughout both thin sections.

One of the primary goals of the investigation of the Sudbury Granite was to determine if the granite was exposed across the Bloody Bluff fault in the Avalon terrane, thereby crosscutting the fault. Only one observation was made of a pink biotite granite east of the Bloody Bluff fault adjacent to the Sudbury Granite. This granite was found in Waltham, Massachusetts and is a fine-grained, pink, biotite granite (Figure 3.17). It is composed of 25 % quartz, 45 % potassium feldspar, 29 % plagioclase feldspar, and up to 1 % biotite. Weathering is minor, with only a little sericite present in thin section. Although the granite is undeformed in both hand sample and outcrop, some shear planes were visible in thin section.

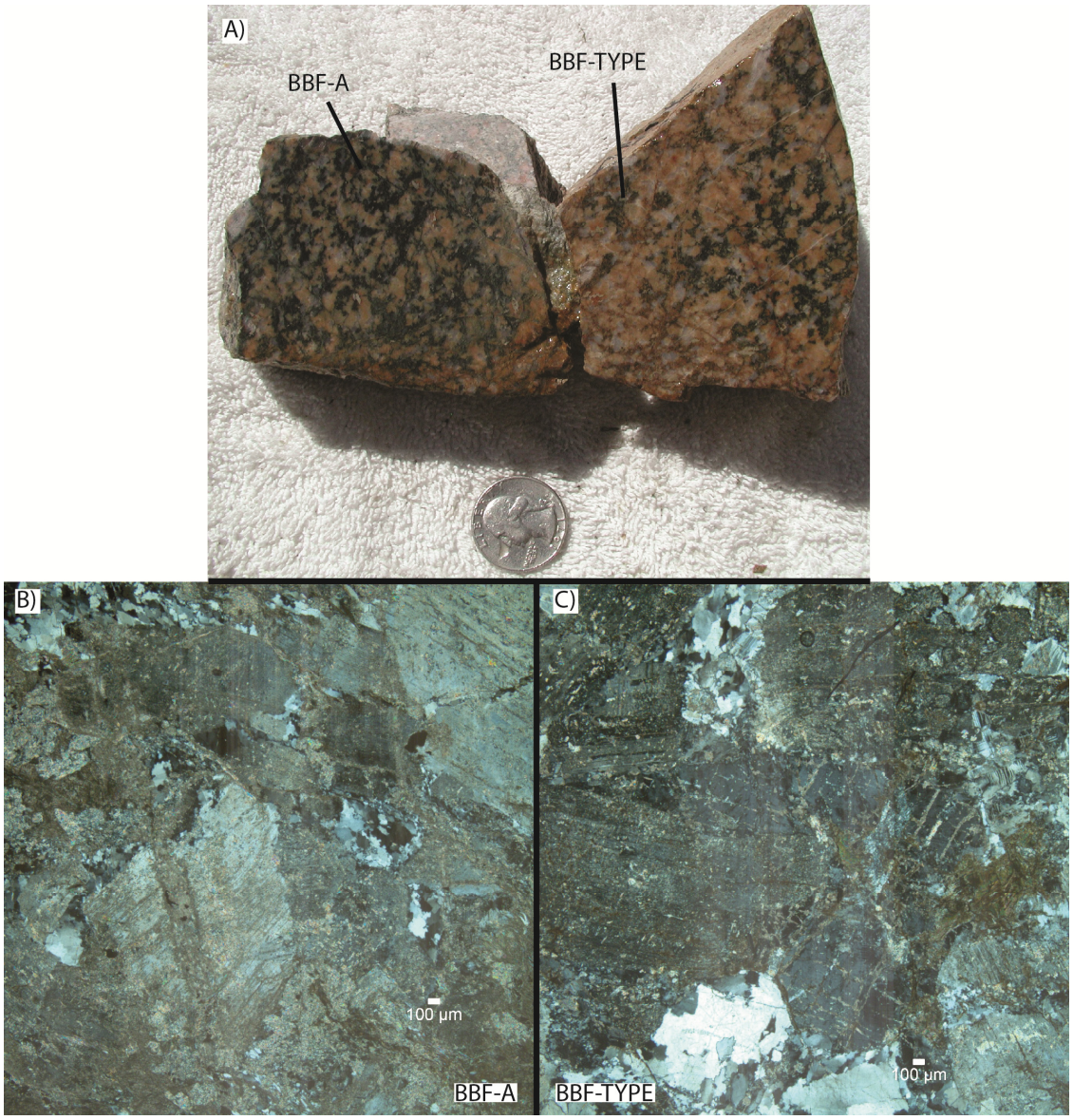

Figure 3.16 – A) Hand samples collected from the Bloody Bluff fault type locality. Quarter for scale. B-C) Photomicrographs with crossed polars of Bloody Bluff fault samples BFF-A (B) and BFF-Type (C). Scale bar is 100 microns. Note the extensive secondary mineralization.

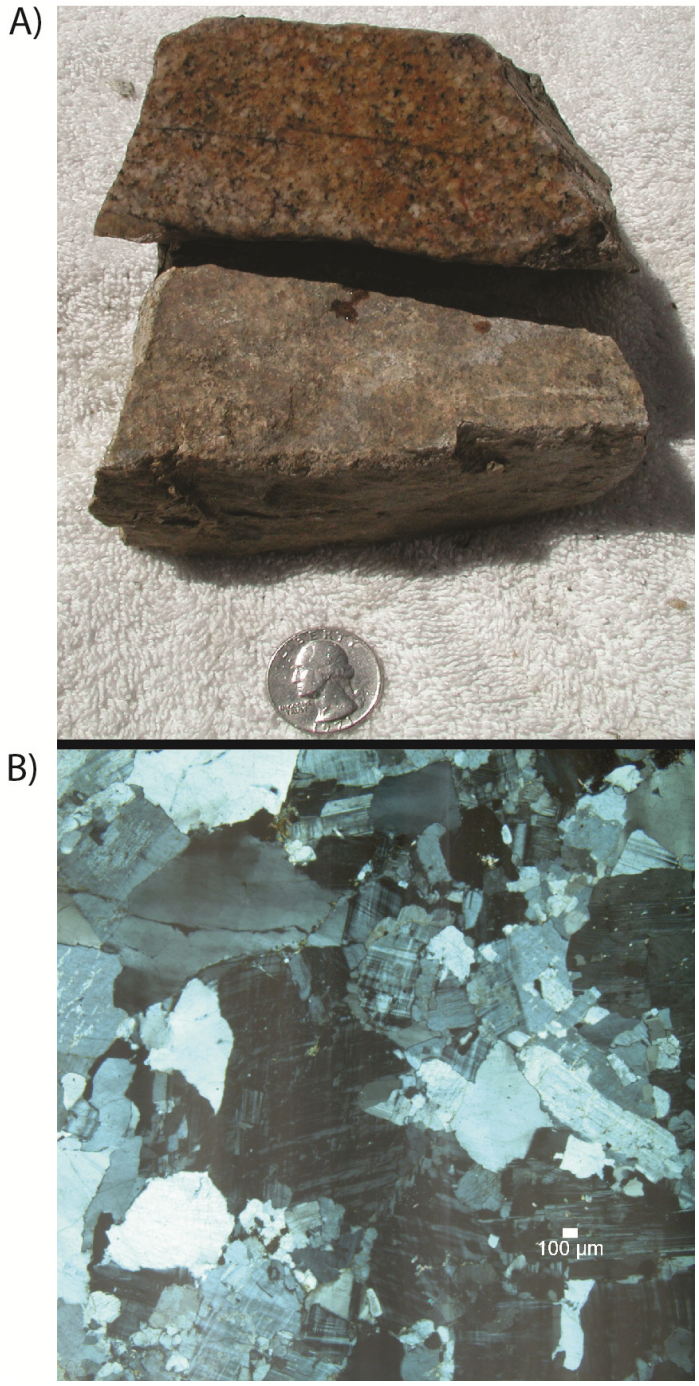

Figure 3.17 – Hand sample (A) and photomicrograph with crossed polars (B) of sample BSC-1, the biotite granite east of the Bloody Bluff fault in the vicinity of the Sudbury Granite. Quarter for scale. Scale bar is 100 microns.

Chapter 4: Discussion

4.1 Andover Granite

4.1.1 Classification

Combining the work of Castle (1964) and Collins (1987) with the newly analyzed samples from this study, the Andover Granite suite can be characterized as a sillimanite, garnet, biotite, muscovite leucogranite with a high-K calc-alkaline (Figure 4.1) and slightly peraluminous to peraluminous (Figure 4.2) composition. These characteristics are consistent with S-type granites of the S-I-A-M granite classification scheme (Chappell & White, 1974; Collins, 1987; Winter, 2001). S-type granites are believed to form in active orogenic systems from the anatexis of aluminous metasediments (Chappell & White, 1974; Winter, 2001).

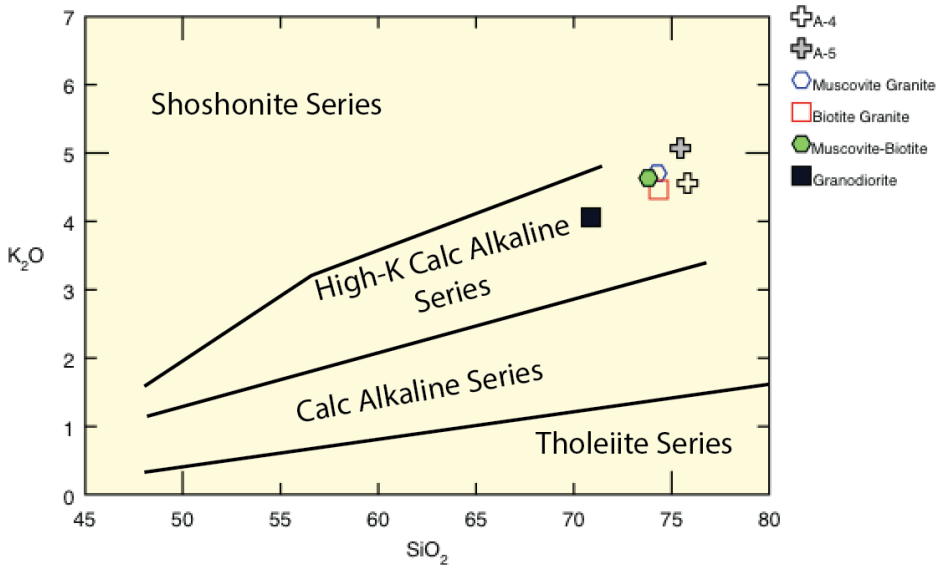

Figure 4.1 – Magma series plot of the Andover Granite, including the newly analyzed foliated granite samples. The Muscovite, Biotite, Muscovite-Biotite, and Granodiorite points represent an average composition of that phase from Collins (1987) (See Appendix C).

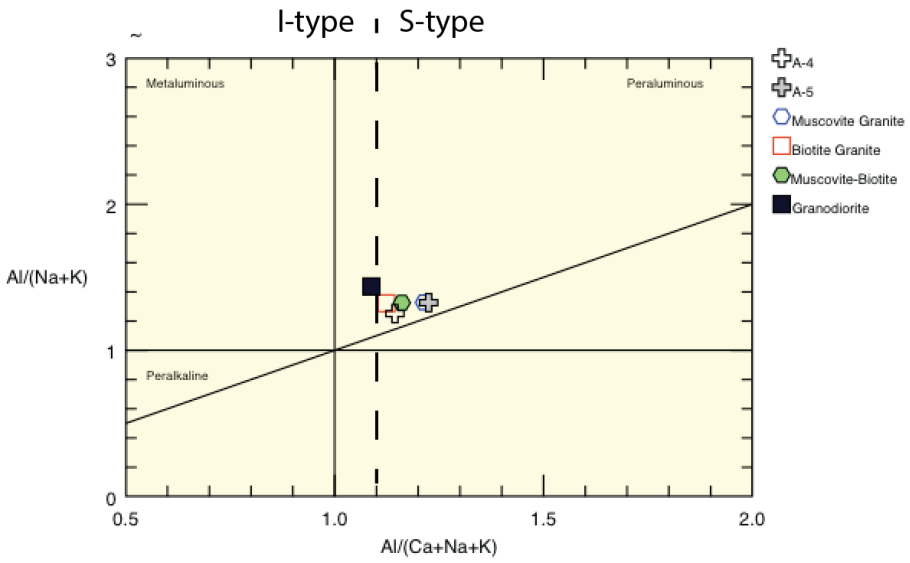

Figure 4.2 – Alumina Index plot of the Andover Granite, including the newly analyzed foliated granite samples. Most of the suite has an alumina index > 1.1, consistent with S-type granites. The dashed line demarcates the boundary between I-type and S-type granites (Alumina Index of 1.1) (Chappell & White, 1974). The Muscovite, Biotite, Muscovite-Biotite, and Granodiorite points represent an average composition of that phase from Collins (1987) (See Appendix C).

4.1.2 Tectonic Setting

Harris and others (1986) observed that granites of known tectonic settings share common geochemical characteristics. They concluded that granitoid intrusions resulting from orogenesis fall into one of four groups on the basis of geochemistry. According to Harris and others (1986), pre-collisional calc-alkaline arc intrusions are characterized by selective enrichments in Large Ion Lithophile (LIL) elements, syn-collisional peraluminous intrusions are identified by high Rb/Zr and Ta/Nb and low K/Rb ratios, late or post-collisional calc-alkaline intrusions are distinguished by high Ta/Hf and Ta/Zr ratios, and post-collisional alkaline intrusions display high LIL and High Field Strength (HFS) elemental concentrations. The Rb/Zr ratios of the Andover Granite phases are 3.18 for the Muscovite Granite, 1.59 for the Biotite Granite, 2.32 for the Muscovite-Biotite

Granite, and 0.60 for the Granodiorite (See Appendix C for geochemical data), consistent with the syn-collisional peraluminous intrusions of the model. The high Na_2O/CaO, MgO/MnO, and low Na_2O/K_2O ratios of the Andover Granite, an alumina index between 1.09 and 1.21, and the presence of modal biotite, garnet, muscovite, and sillimanite within the suite are also characteristics consistent with granites that formed in a continental collision tectonic setting, according to the tectonic setting discrimination schemes of Maniar and Piccoli (1989), Barbarin (1990), and Barbarin (1999).

The calc-alkaline composition of the Andover Granite is a common characteristic of igneous rocks that formed in active volcanic arcs (Wilson, 1989; Winter, 2001). The depletion of Nb and Ti and enrichment of Pb seen in the multielement spider diagrams of the suite (Figure 4.3) are also characteristics akin to volcanic arc rocks (Wilson, 1989; Winter, 2001). Pearce and others (1984), like Harris and others (1986), observed that granites of similar tectonic settings have similar geochemical characteristics. Using observations based on Rb, Y, and Nb concentrations, Pearce and others (1984) segregated granitoids into Volcanic Arc Granites (VAG), Ocean Ridge Granites (ORG), Syn-Collisional Granites (Syn-COLG), or Within Plate Granites (WPG). Due to the high concentration of Rb and moderate concentration of Nb and Y in the Andover Granite, the suite falls within the VAG field (Figure 4.4) suggesting the pluton formed in a volcanic arc tectonic setting.

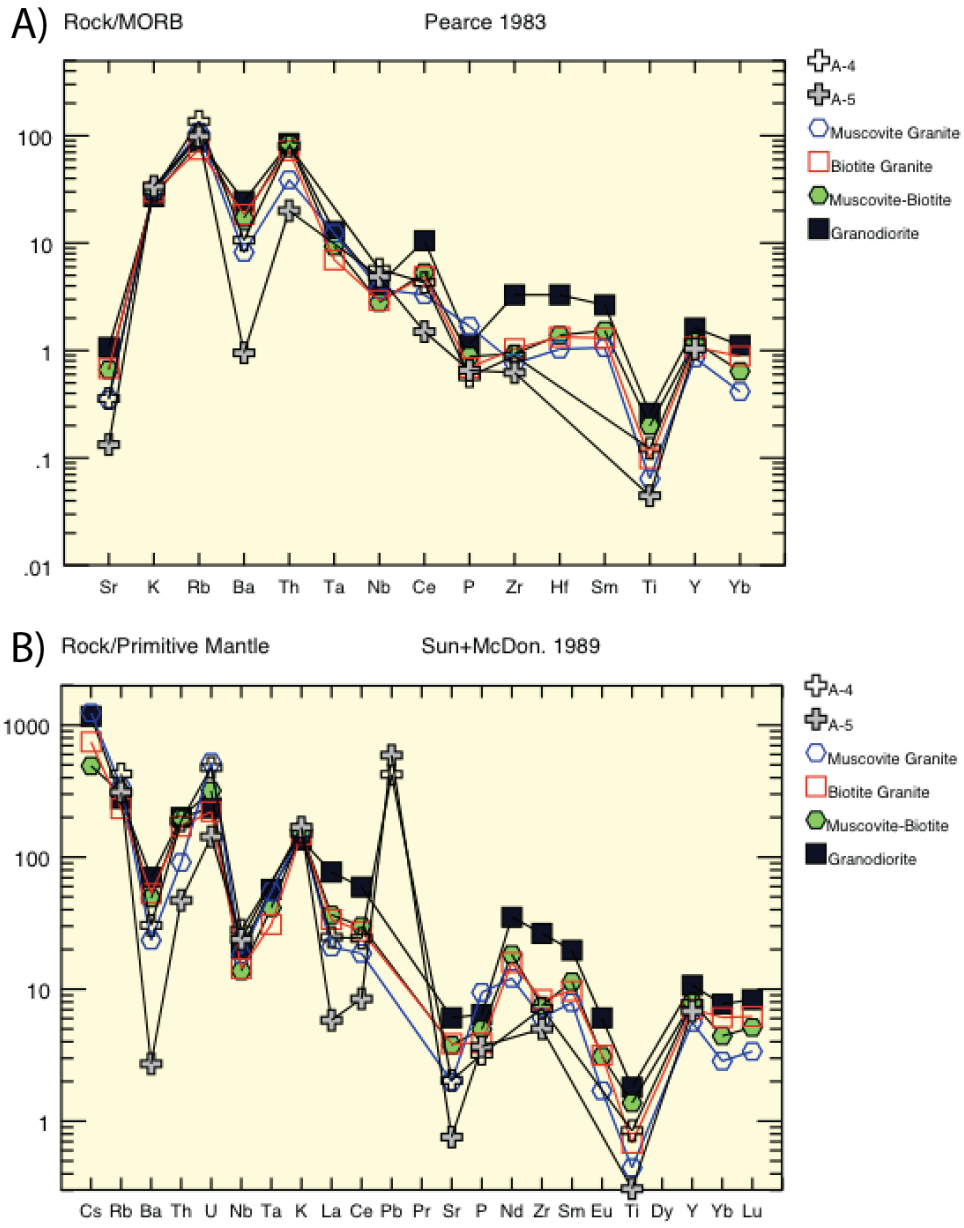

Figure 4.3 – Multielement spider diagrams of the Andover Granite suite including the newly analyzed foliated granite samples. A) Normalized to average Mid-Ocean Ridge Basalt (MORB) compositions (Pearce, 1983). B) Normalized to an average Primitive Mantle composition (Sun & McDonough, 1989). The Muscovite, Biotite, Muscovite-Biotite, and Granodiorite points represent an average composition of that phase from Collins (1987) (See Appendix C).

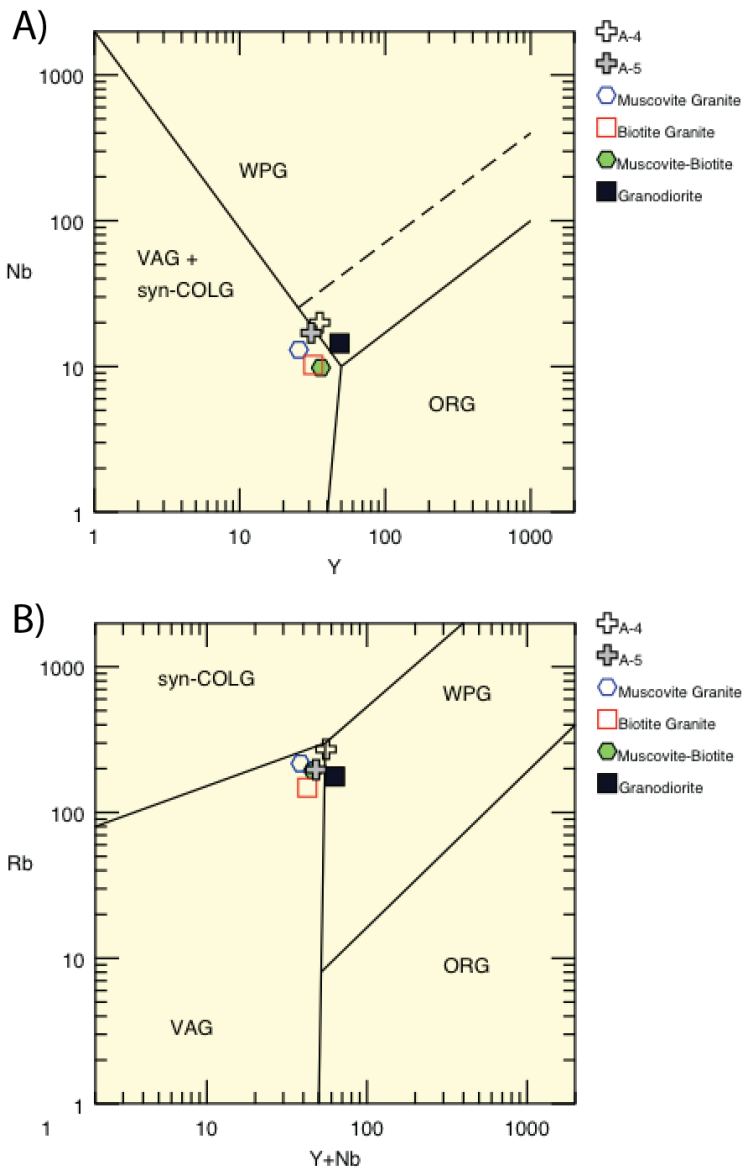

Figure 4.4 – The Y vs Nb (A) and Y+Nb vs Rb (B) tectonic discrimination diagrams for the Andover Granite, including the newly analyzed foliated granite samples. The Muscovite, Biotite, Muscovite-Biotite, and Granodiorite points represent an average composition of that phase from Collins (1987) (See Appendix C). The dotted line in (A) represents the upper boundary for ORG from anomalous ridges and does not apply in this case. Note that while Rb is considered a mobile element, the placement of granites into the VAG vs WPG fields in both (A) and (B) are controlled primarily by immobile elements Nb and Y. Figure from Pearce and others (1984).

The contrasting collisional vs. volcanic arc results of tectonic setting discrimination for the Andover Granite suggests that the suite formed in one of two tectonic settings: a continental collision tectonic setting or a volcanic arc tectonic setting. While the geochemistry of the newly analyzed samples of the foliated Andover Granite indicates an orogenic origin (Figure 4.5), it is likely that the suite inherited at least some of its geochemical characteristics from its source region, a common occurrence with granitic rocks (Winter, 2001). This would result in a granite forming either from the anatexis of crustal rocks in a volcanic arc tectonic setting or the melting of volcanic arc rocks inside the collision zone of two continental blocks. The close proximity of the Andover Granite to the calc-alkaline Sharpners Pond Diorite (interpreted to have formed in a continental volcanic arc; Loftenius, 1988), makes the former scenario more likely.

4.1.3 Geochronology

The ~455 Ma Rb-Sr isochron age (Hill et al., 1984) on the foliated Andover Granite is now believed to not reflect the true crystallization age of the pluton. Zartman and Naylor (1984) commented that the Rb-Sr data analyzed from the Andover Granite suite should be interpreted cautiously as they believe that the pluton likely underwent Rb-Sr isotopic resetting at some point after the crystallization of the pluton. Any resetting of the Rb-Sr system in the foliated Andover Granite would likely result in an age that is erroneously too young. This lends support the idea that this Rb-Sr age does not reflect the true crystallization age of the foliated Andover Granite.

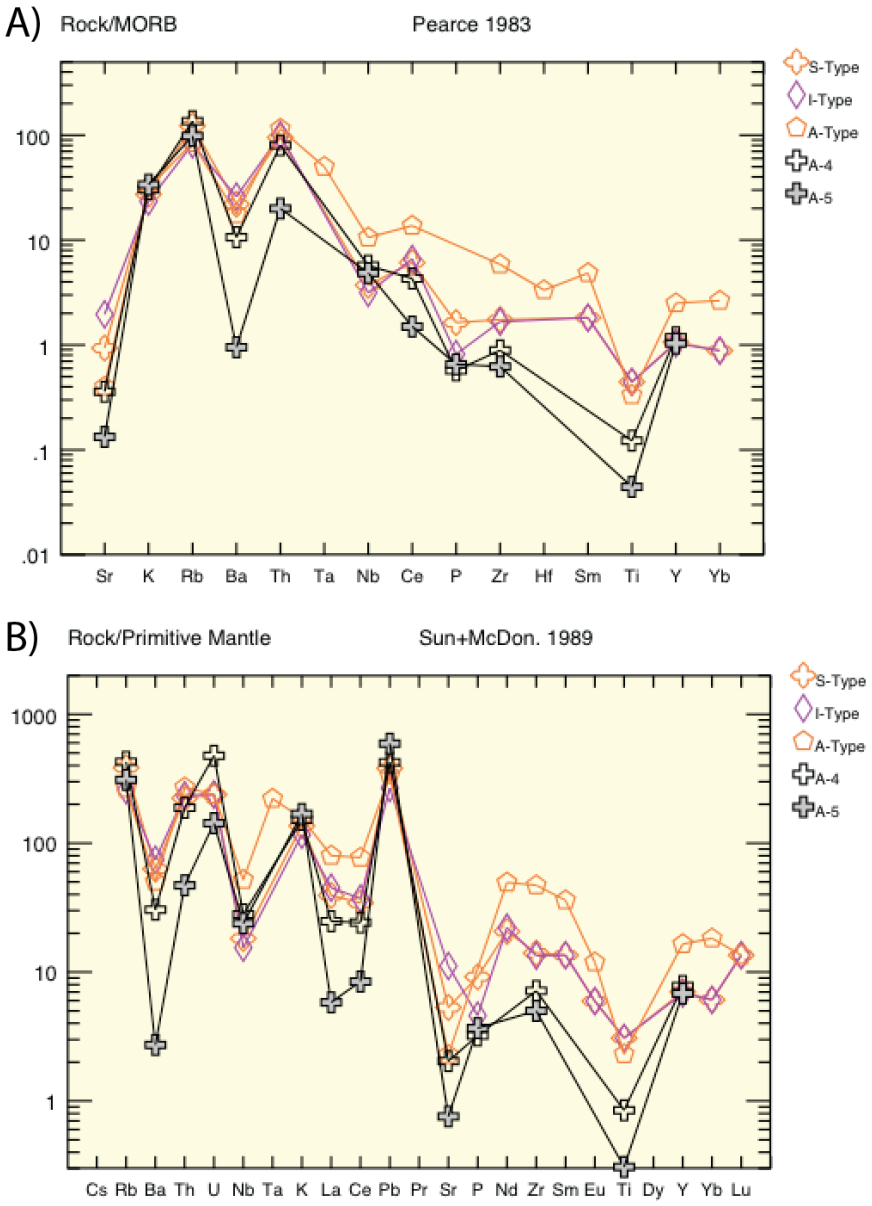

Figure 4.5 – Multielement spider diagrams of the newly analyzed foliated Andover Granite samples plotted with representatives of S-, I-, and A-type granites. A) Normalized to average Mid-Ocean Ridge Basalt (MORB) compositions (Pearce, 1983). B) Normalized to an average Primitive Mantle composition (Sun & McDonough, 1989). S-, I-, and A-type granite values taken from Winter (2001). Note how the foliated Andover Granite samples roughly parallel the S- and I- type granites, suggesting an orogenic origin.

New CA-TIMS U-Pb geochronological data shows that the two foliated Andover Granite samples crystallized at 419.43 ± 0.52 Ma (Sample A-4) and 419.65 ± 0.51 Ma (Sample A-5) (weighted mean $^{206}Pb/^{238}U$ ages; Table 3.3). These ages fall on the Silurian-Devonian boundary (Walker et al., 2012). Being within error of each other and sampled from geographically opposite ends of the foliated granite phase, these ages suggest the foliated Andover Granite was emplaced coevally throughout the suite. These data constrain the emplacement of the foliated Andover Granite to latest Silurian time by revising the earlier Rb-Sr isochron ages determined by Hill and others (1984) and Zartman and Naylor (1984). Furthermore, when combined with the 412 ± 2 Ma age from Hepburn and others (1995), these new ages constrain the emplacement of the entire Andover Granite suite to between ~419 Ma and ~412 Ma.

4.2 Sgr Group

4.2.1 Geographic Variation

4.2.1.1 Petrography

In hand sample the three bodies of the Sgr Group are texturally dissimilar (Figure 4.6). The Sudbury Granite is coarser grained than the other two Sgr bodies. The northern Sgr granite is dissimilar to the Sudbury Granite, being both finer grained and a different color. The central Sgr granite is not texturally consistent within itself, being composed of a variety of different granites (Figure 4.6). This contrasts with the Sudbury Granite and the northern Sgr granite, both of which are internally consistent. Also, the granites found in the central Sgr granite are texturally dissimilar to the Sudbury Granite and the northern

Figure 4.6 – Hand samples from all three Sgr granite bodies. Note the differences in texture. Quarter for scale.

Sgr granite, varying in both color and grain size. However, a few of the granites found in the central Sgr granite do show some similarities to the northern Sgr granite (Figure 4.6).

The textural dissimilarity between the granites also extends into observed mineralogy (Table 3.4). Mean mineral abundances show a variation of up to 7 % quartz, 7 % potassium feldspar, 3 % plagioclase feldspar, and 3 % biotite between the three bodies. The differences are stronger with accessory minerals. Hornblende is present in the Sudbury Granite and minor in the central Sgr granite, but absent in the northern Sgr granite. Titanite is absent in the central and northern Sgr granites, being only present in the Sudbury Granite and common among the quartz poor group of the Sudbury Granite.

4.2.1.2 Geochemistry

Interestingly, the three granites of the Sgr Group are not significantly geochemically dissimilar (Figures 4.7 and 4.8). In fact, in Figure 4.7 the three granites consistently fall on a line in major element bivariate plots, except for the northern Sgr granite with regards to K_2O and Na_2O, suggesting a possible petrologic relationship. However, this would be difficult to test without observing the contact relationships between each granite and the country rock (See Section 4.2.3). Furthermore, the three granites being genetically related is an unlikely possibility given the geographic separation between the three bodies, ~25 km between the Sudbury Granite and central Sgr granite and ~20 km between the central and northern Sgr granites (Figure 1.2). Trace element concentrations reflect the major element abundances, in that all three Sgr

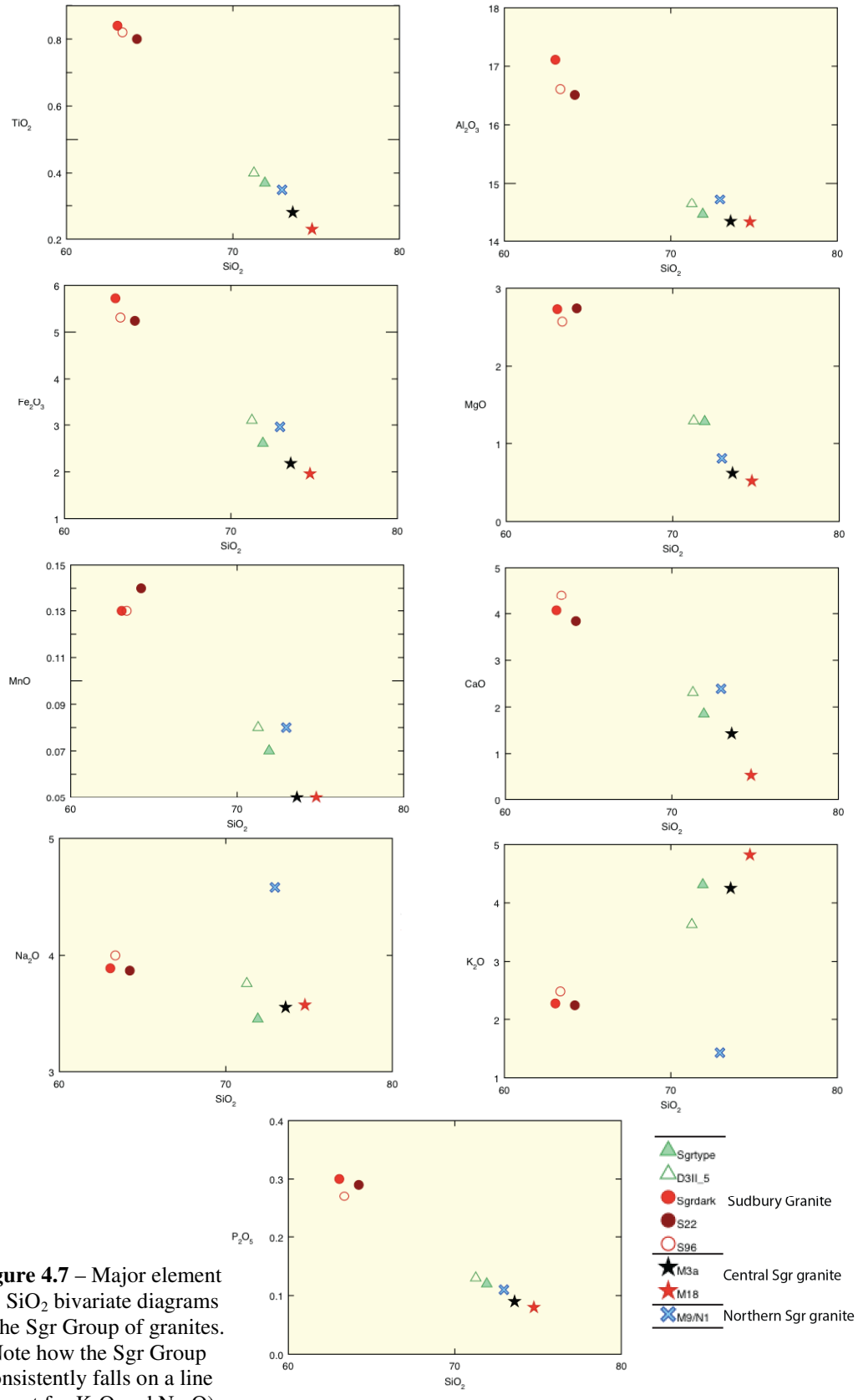

Figure 4.7 – Major element vs. SiO_2 bivariate diagrams of the Sgr Group of granites. Note how the Sgr Group consistently falls on a line (except for K_2O and Na_2O).

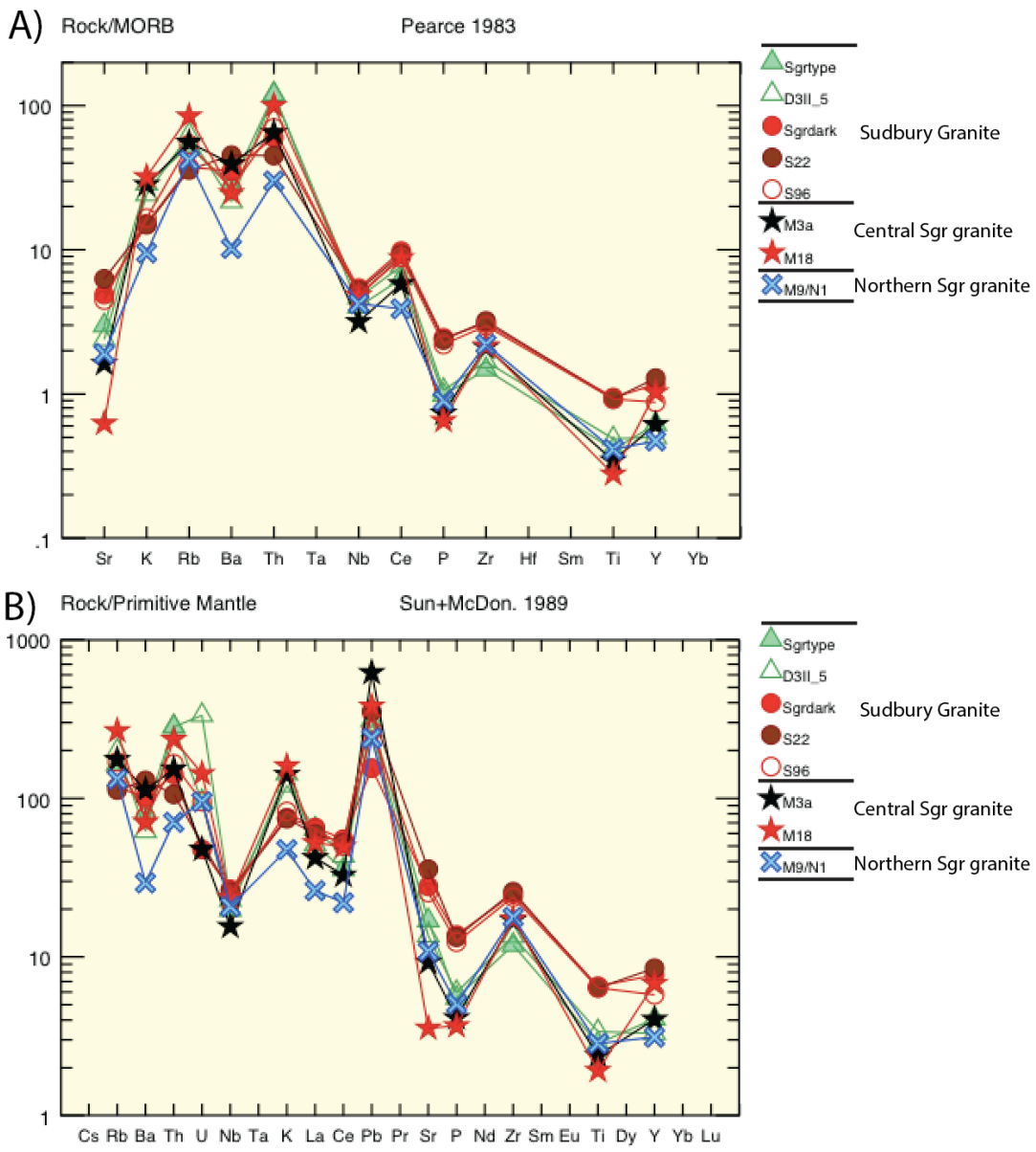

Figure 4.8 – Multielement spider diagrams of the Sgr Group of granites. A) Normalized to average Mid-Ocean Ridge Basalt (MORB) compositions (Pearce, 1983). B) Normalized to an average Primitive Mantle composition (Sun & McDonough, 1989).

granites cluster together (Figure 4.8). Indeed there is some variation between the granites, but the differences are only minor. Similar to the major elements, the northern Sgr granite stands apart from the other two granites, specifically with respect to Ba, Ce, K, La, and Th.

4.2.1.3 Interpretation

The textural differences between the three Sgr bodies suggest that each body is composed of a different granite. However, the minor geochemical variation between the granites of the three zones could suggest that each granite formed from similar petrogenetic processes affecting a source region of similar composition. Given the small size of the Nashoba terrane, this could be a possibility. The most likely source rocks for the Sgr Group are the Marlboro Formation and the Nashoba Formation (or other crustal rocks that are not exposed at the surface) due to their close proximity to the Sgr group. The Marlboro Formation and the Nashoba Formation extend almost the full length of the terrane. This would allow for some spatial consistency in a potential granite source region and could explain the textural similarities observed between some of the central Sgr granite samples and the northern Sgr granite. Given the geographic distance between each body (~25 km between the Sudbury Granite and central Sgr granite and ~20 km between the central and northern Sgr granites, See Figure 1.2) any similarities seen between the granites would likely result from a similar source rock rather than any magma interaction or comingling processes.

4.2.2 The Sudbury Granite – The southern Sgr granite

The samples collected from the Sudbury Granite were separated into two groups on the basis of quartz content: quartz rich and quartz poor. These two groups also differ in biotite, hornblende, and titanite contents (Table 3.5) as well as in various major element abundances (Table 3.6 and Figure 4.8). The quartz rich samples were collected from locations within the normal Sudbury Granite facies and the quartz poor samples were collected from locations within the dark Sudbury Granite facies. The strong geochemical variation between these two groups with both major (Figure 4.7) and trace elements (Figure 4.8) suggests that the difference between the normal and dark Sudbury Granite facies extends beyond a simple difference in biotite content.

4.2.3 Contact Relationships

Due to thick glacial cover, contact relationships between the country rock and the central Sgr granite or Sudbury Granite were not observed. Additionally, no contact relationships were observed between the three facies of the Sudbury Granite. However, a single contact was observed between the northern Sgr granite and a biotite hornblende diorite, likely the Sharpners Pond Diorite. The diffuse texture of the contact (Figure 3.11) suggests that both bodies were warm during magma interaction, but does not indicate an order of intrusion. The contact does suggest, however, that the two plutons are coeval.

Loftenius (1988) observed the Sharpners Pond Diorite forming magmatic pillows in a biotite granite in the areas of Middleton and Newburyport, Massachusetts. This biotite granite, and the biotite granite observed within the Sharpners Pond Diorite pluton,

is composed of approximately 30 % quartz, 30 % plagioclase feldspar, 30 % potassium feldspar, and between 2 % and 10 % biotite (Loftenius, 1988), modal abundances that are very similar to the central and northern Sgr granites (Table 3.4). This could suggest that granites associated with these magmatic pillows might be one of the granites present in the central and northern Sgr granites (an interpretation also suggested by Loftenius (1988)).

If this is true, then the presence of the pillows would suggest that the granite and diorite are coeval. This would indicate that the central and northern Sgr granites are Silurian aged, based on the 430 ± 5 Ma age of the Sharpners Pond Diorite (U-Pb zircon ID-TIMS; Zartman & Naylor, 1984). Furthermore, if the central and northern Sgr granites and the Sharpners Pond Diorite are coeval, this opens the possibility that one or more of the granites found in the Sgr Group may not locally derived and might have ascended into the crust with the Sharpners Pond Diorite. This would allow for the basement underlying the Nashoba terrane (if present) to be a possible Sgr Group source region. Certainly, the Nd isotope data from the Sudbury Granite does suggest that either the Nashoba terrane or an underlying basement is a possible source region (Kay, 2012). If so, then it could help explain the textural differences between the Sgr Group granites.

4.2.4 The Bloody Bluff Fault

While the rocks exposed at the Bloody Bluff fault type locality in Concord, Massachusetts (Figure 1.2) are brittlely deformed, in hand sample these rocks are medium-grained biotite granites. Best estimates of modal mineralogy for the outcrop

(Table 3.5) shows that granites at this locality have a similar mineralogy to the mixed facies of the Sudbury Granite. Additionally, these rocks in hand sample are texturally identical to the rocks of the mixed facies of the Sudbury Granite (Figure 4.9), except for being brittlely deformed. Therefore it is interpreted that the Bloody Bluff fault type locality in Concord, Massachusetts is composed of the mixed facies of the Sudbury Granite.

4.2.4.1 East of the Bloody Bluff Fault

One of the project objectives was to determine if the Sudbury Granite crosscuts the Nashoba-Avalon terrane boundary, the Bloody Bluff fault. The fine-grained, tan-to-pink, biotite granite represented by Sample BSC-1 (See Section 3.4) was the only observation of a pink biotite granite east of the fault adjacent to the Sudbury Granite in the Nashoba terrane. This granite was found in Waltham, Massachusetts inside the Cambridge Reservoir Suite mapped by Kohut (1999). The composition and texture of this granite differs greatly from that of the Sudbury Granite (Figure 4.10). This Waltham granite is finer grained than the Sudbury Granite and has a much less biotite present (1 % biotite for this granite compared to the ~10 % mean biotite content of the Sudbury Granite). Furthermore, the biotite in the Waltham granite is more evenly distributed, compared to the clumped biotite in the Sudbury Granite.

The Waltham granite is also believed to be much younger than the Sudbury Granite or the rest of the Sgr Group. Kohut (1999) suggests that the Waltham granite intruded late in the formation of the Cambridge Reservoir Suite, post-dating the intrusion

of the 378 ± 3 Ma aged hornblende gabbro-diorite (U-Pb zircon; Hepburn et al., 1993) that dominates the suite. This would suggest that the Waltham granite, along with the Cambridge Reservoir Suite, is too young to be derived from the same igneous processes that formed the Sudbury Granite or the rest of the Sgr Group. The differences in mineral content, texture, and likely age thus support the interpretation that the Waltham granite is not an exposure of the Sudbury Granite. Therefore, it is interpreted that the Sudbury Granite does not crosscut the fault and is restricted to the Nashoba terrane.

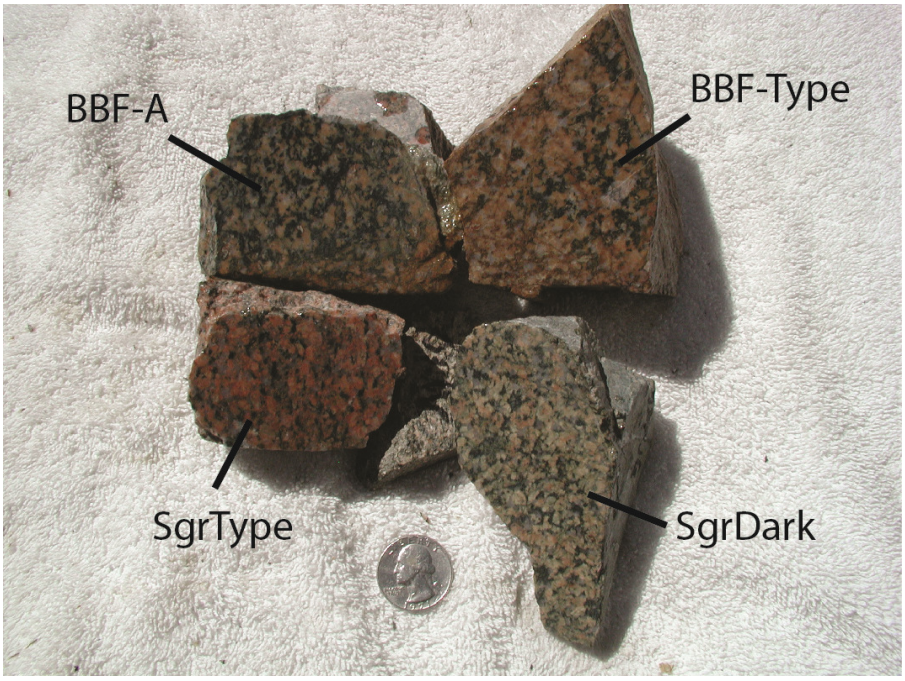

Figure 4.9 – Hand samples of granites from the Bloody Bluff fault and the Sudbury Granite. Note the similarities in texture. Quarter for scale.

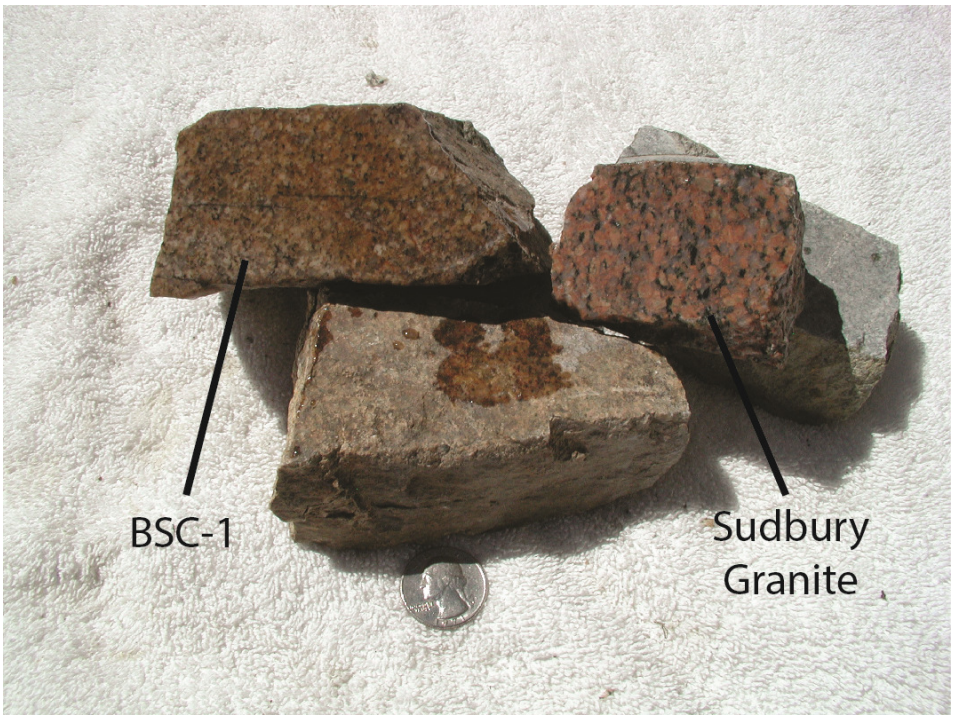

Figure 4.10 – Hand samples of the granite found in Waltham, Mass (Sample BSC-1) and the Sudbury Granite. Note the differences in texture; it is clear that these are two different granites. Quarter for scale.

4.2.4 Classification

The Sudbury Granite, as well as the other Sgr granites, are fine-to-medium grained, biotite ± titanite ± hornblende granites with high-K calc-alkaline to calc-alkaline (Figure 4.11) and slightly metaluminous to slightly peraluminous compositions (Alumina Index 0.9 < x > 1.2, Figure 4.12). These characteristics are consistent with I-type granites of the S-I-A-M granite classification (Chappell & White, 1974; Roberts & Clemens, 1993; Winter, 2001). I-type granites are believed to have formed inside active orogenic systems, specifically volcanic arcs, resulting from either the fractionation of arc magmas or country rock contamination of intermediate composition magmas (Chappell & White, 1974; Winter, 2001).

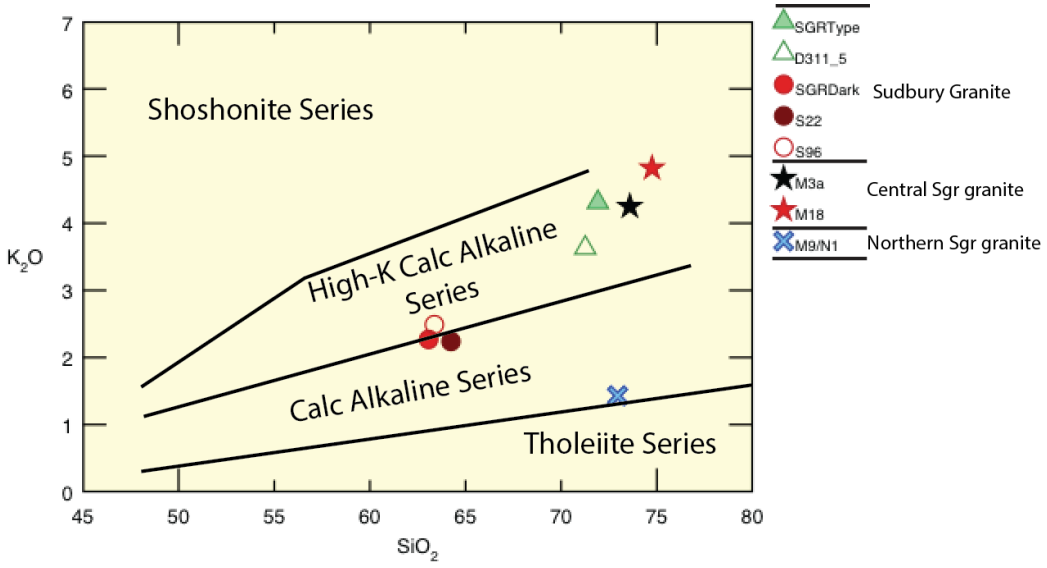

Figure 4.11 – Magma series plot of the Sgr Group.

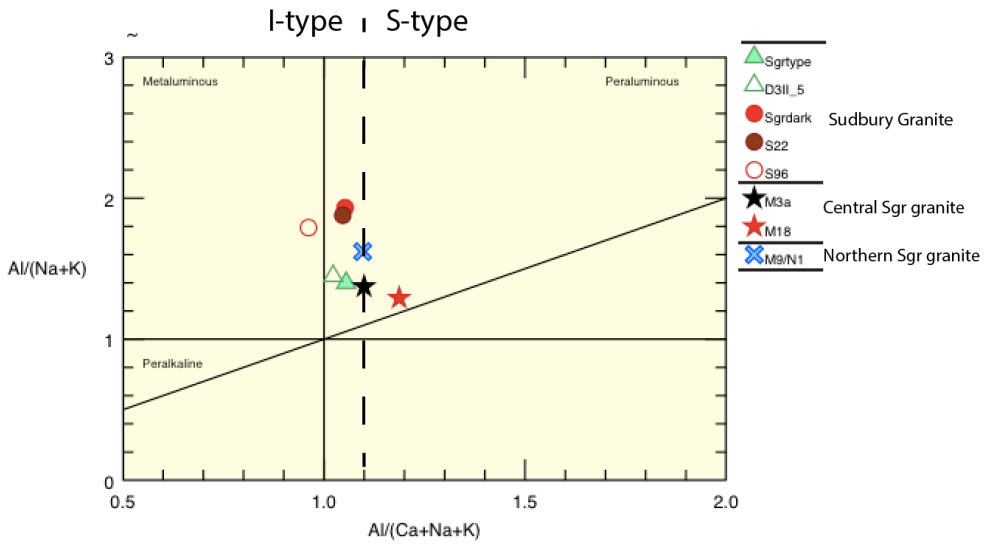

Figure 4.12 – Alumina Index plot for the Sgr Group of granites. Except Sample M18 from the central Sgr granite, the Sgr Group falls within the I-type field. The dashed line demarcates the boundary between I-type and S-type granites (Alumina Index of 1.1) (Chappell & White, 1974).

4.2.5 Tectonic Setting

A calc-alkaline composition is a common characteristic of rocks that formed in volcanic arcs (Wilson, 1989; Winter, 2001). The depletion of Nb and Ti and enrichment of Pb seen in the multielement spider diagrams of the granites (Figure 4.8) are also characteristics common to volcanic arc rocks (Wilson, 1989; Winter, 2001). The positive LIL / HFS element ratio (Figure 4.8A) suggests a continental volcanic arc rather than an oceanic volcanic arc, as the interaction of arc magmas with continental crust during ascent and emplacement commonly leads to the enrichment in the more mobile trace elements (Winter, 2001). Specific to the Sgr Group, these characteristics are consistent with the classification of pre-collisional calc-alkaline intrusions of Harris and others (1986).

In Y vs. Nb and Y+Nb vs. Rb trace element bivariate plots, the Sgr Group, except for the dark facies of the Sudbury Granite, falls in the VAG field (Figure 4.13). The dark Sudbury Granite facies clusters near, or just over, the line separating the VAG field from the WPG field. Other tectonic setting discrimination schemes also suggest the Sgr Group formed in a continental volcanic arc tectonic setting based on their low to moderate K_2O and ferromagnesian major element abundances, low Na_2O/CaO and Na_2O/K_2O ratios, a high MgO/MnO ratio, an alumina index between 0.9 and 1.20, and biotite ± hornblende mineralogy (Maniar & Piccoli, 1989; Barbarin, 1990; Barbarin, 1999).

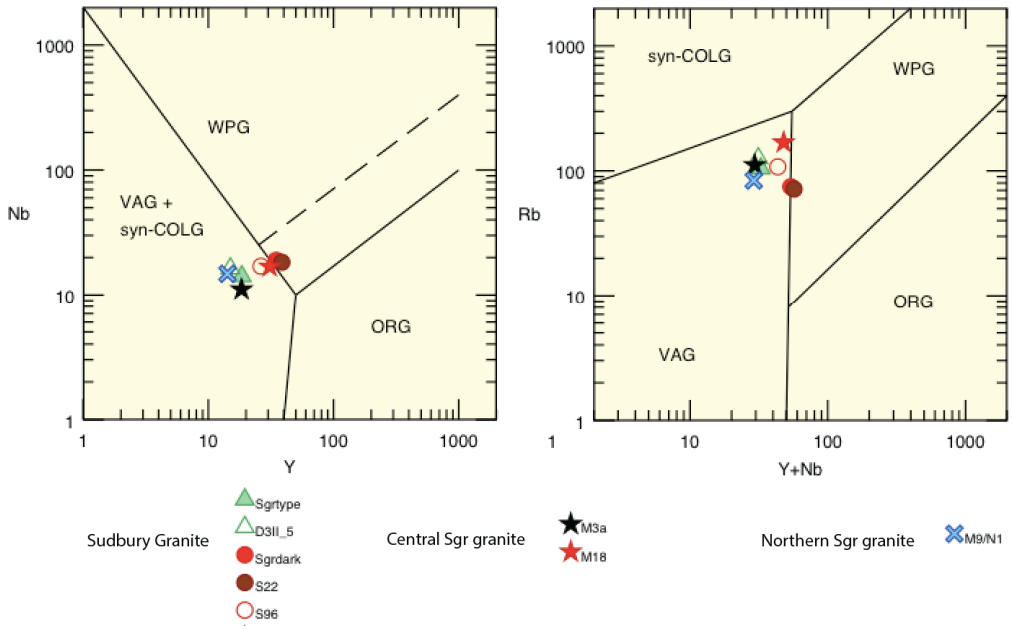

Figure 4.13 – The Y vs Nb (A) and Y+Nb vs Rb (B) tectonic discrimination diagram for the Sgr Group of granites. The dotted line represents the upper boundary for ORG from anomalous ridges and does not apply in this case. Note that while Rb is considered a mobile element, the placement of granites on this figure is controlled primarily by immobile Nb and Y. Figure from Pearce and others (1984).

4.2.6 Geochronology

New CA-TIMS U-Pb geochronological data shows the Sudbury Granite crystallized at 420.49 ± 0.52 Ma (weighted mean $^{206}Pb/^{238}U$ age; Table 3.6), during latest Silurian time (Walker et al., 2012). This Silurian age suggests that the Sudbury Granite is coeval with the Silurian orogenesis in the Nashoba terrane described by Zartman and Naylor (1984), Hepburn and others (1995), Stroud and others (2009), Loan (2011), and Kay (2012). Furthermore, the samples collected from the Bloody Bluff fault type locality in Concord, Massachusetts are interpreted to be composed of the Sudbury Granite, suggesting that the brittle deformation along the Bloody Bluff fault is no older than Late Silurian in eastern Massachusetts. Considering that it is widely believed that interaction between Avalonia and Ganderia occurred during the middle Paleozoic, this is not surprising.

Chapter 5: Petrogenesis

5.1 Petrogenesis of Arc Granites

It is understood that granites with an arc affinity commonly form from the differentiation of mafic arc magmas, the anatexis of calc-alkaline crustal arc rocks, or a combination of the two (Chappell & White, 1974; Wilson, 1989; Winter, 2001). When granites differentiate from a mafic magma, the final granite volume is believed to be only about 20 %, or less, of the volume of the initial mafic magma (Winter, 2001; Brown, 2013). So a very large parent magma body, like a batholith, would be required to produce a large granitic suite like the Andover Granite (with a mapped area of ~ 316 km^2; Zen et al., 1983) via differentiation. Given the small size of the Nashoba terrane, it is unlikely that such a batholith exists beneath the terrane.

It is more likely that the Andover Granite and the Sgr Group of granites formed via the anatexis of calc-alkaline crustal rocks. Recent work in I-type granite petrogenesis suggests that I-type granites are the result of the anatexis of aluminous igneous protoliths, rather than magmatic differentiates (Clemens et al., 2011). By partial melting aluminous calc-alkaline crustal rocks, the resulting granites could inherit both the aluminous character and the calc-alkaline geochemistry of the parent rocks, similar to the geochemistry seen in both the Andover Granite and the Sgr Group. Furthermore, recent Nd isotope data from both the Andover and Sudbury Granites suggests that a significant contribution was made from older crustal material (Kay, 2012). This would not be the case if these granites differentiated out of a younger parent magma.

5.2 Andover Granite

5.2.1 Source constraints

Recent Nd isotope data suggests that the source region for the Andover Granite is either the Nashoba terrane, its underlying basement, or both (Kay, 2012). This interpretation is supported by multiple lines of evidence. Conditions that were favorable for anatexis to occur did exist in the Nashoba terrane (metamorphisms M1 and M2 in Figure 5.1). Devonian aged migmatites observed within the Nashoba Formation (Hepburn et al., 1995), albeit younger than the Andover Granite, demonstrate that anatexis did occur during the metamorphism of the terrane (Stroud et al., 2009). The presence of muscovite and the large volumes of pegmatite in the Andover Granite suggest that the suite was likely derived from a hydrous melt (Collins, 1987). It has been shown that hydrous felsic melts typically do not travel far from their source rocks (Hyndman, 1981) and the Andover Granite is observed intruding into the metasediments of the Nashoba terrane (Zen et al., 1983). The Nashoba terrane is composed, in part, of aluminous metasediments. These rocks are typical S-type granite source rocks (Chappell & White, 1974; Clemens & Wall, 1981; Winter, 2001). The terrane is also heterogeneous, possibly explaining the diverse nature of the restitic material and xenoliths that Collins (1987) observed throughout the Andover Granite suite.

5.2.2 Emplacement constraints

The primary mechanism behind the formation of S-type granites is the dehydration of muscovite (Miller, 1981), which occurs at 650 °C (Clemens & Vielzeuf, 1987). However, this process only produces a melt fraction between 10 % and 20 % melt per modal % muscovite present in the source rock (Spear et al., 1999). It is difficult to estimate how much melt the metapelitic rocks of the Nashoba terrane would generate via muscovite dehydration because much of the muscovite present today is believed to be secondary (personal communication, J. C. Hepburn, 2014). However, these rocks are composed of approximately 10 % to 50 % muscovite (Kay, 2012) thus a melt fraction of 1 % - 10 % would be generated by this process if it occurred today. If a majority of the muscovite present in the Nashoba Formation today formed due to metamorphism, and thus was not available for melting, then a 1 % - 10 % melt fraction would be an overestimate. Given that melt fractions as high as 25 % are estimated to be required to form the Andover Granite (Collins, 1987; Kay, 2012), muscovite dehydration alone is likely insufficient to form the suite and thus another process would be necessary to produce the remaining melt.

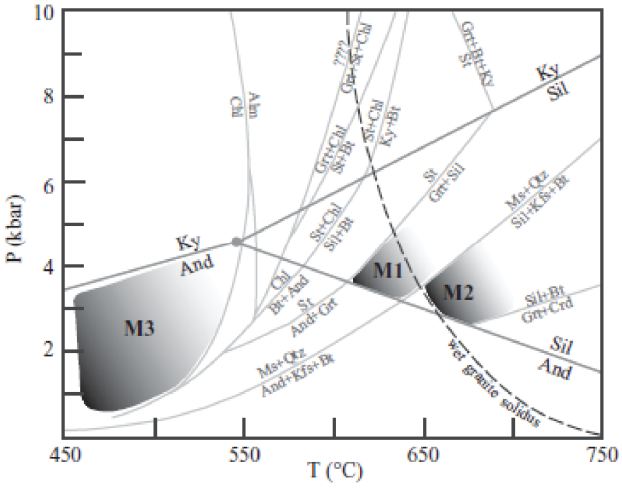

Figure 5.1 – Petrogenetic grid denoting the peak pressure and temperature conditions of the Nashoba terrane metamorphism. M1- Late Silurian metamorphism, M2 – Middle Devonian metamorphism, M3 - Late Devonian metamorphism. Note that the Silurian metamorphism and the Middle Devonian metamorphism peak pressure and temperature conditions were at or above the wet granite solidus. Figure taken from Stroud and others (2009).

The dehydration of biotite occurs at higher temperatures (750 °C and 850 °C) and can produce a melt fraction between 30 % - 70 % melt per modal % biotite present in the source rock (Clemens & Vielzeuf, 1987; Spear et al., 1999), considerably more than that of muscovite dehydration. The metapelitic rocks of the Nashoba terrane are composed of approximately 10 % to 20 % biotite (Kay, 2012), thus would yield 3 % - 14 % melt via this process. Together, both processes would be able to produce sufficient melt to form the Andover Granite, suggesting the suite formed between 750 °C and 850 °C. Indeed, Clemens and Vielzeuf (1987) commented that melts derived from metapelites that are of sufficient volume to escape their source rocks formed from both biotite and muscovite dehydration.

Experimental data indicates that for the temperatures presented above, biotite and muscovite dehydration reactions would have likely occurred at pressures between 5 kbar and 10 kbar (Clemens & Vielzeuf, 1987; Spear et al., 1999). This suggests formation depths between 17.5 km and 35 km in the middle to lower crust. Normative mineralogy of the Andover Granite suggests that the suite crystallized at pressures of approximately 5 kbar (Figure 5.2), corresponding to a depth of ~17.5 km (Collins, 1987). The pegmatite of the Andover Granite is also believed to have crystallized at a pressure of approximately 5 kbar (Castle & Theodore, 1972). Additionally, the likely presence of primary muscovite in the granite suite (Collins, 1987) also suggests an emplacement depth of at least ~17.5 km (Clemens & Wall, 1981; Miller et al., 1981).

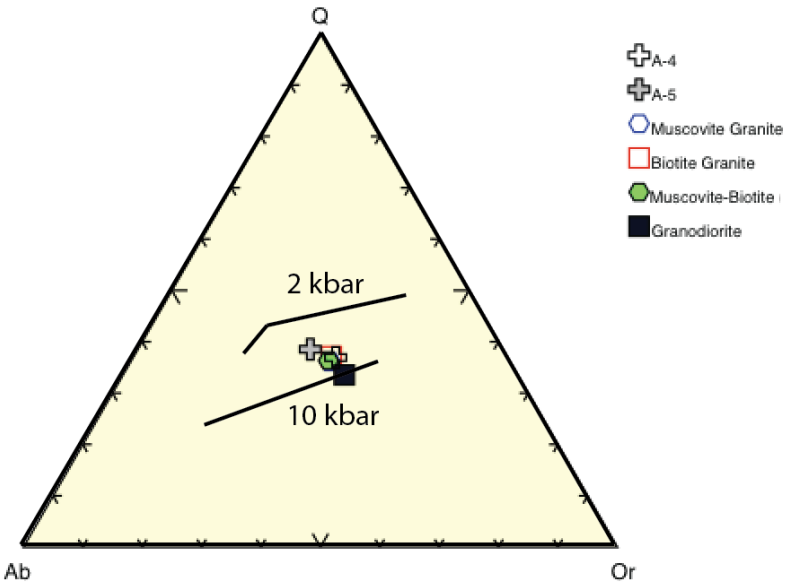

Figure 5.2 – Q-Ab-Or normative mineralogy ternary of the Andover Granite. The two lines represent emplacement pressures of 2 kbar and 10 kbar, respectively. The Muscovite, Biotite, Muscovite-Biotite, and Granodiorite points represent an average composition of that phase from Collins (1987) (See Appendix C). Modified from Collins (1987). After Winkler (1979) and Wintsch and Aleinikoff (1987).

5.3 Sgr Group

5.3.1 Source constraints

I-type granites are believed to be derived, at least partially, from metaigneous source rocks (Chappell & White, 1974; Chappell & Stephens, 1988; Roberts & Clemens, 1993; Chappell et al., 2004; Clemens et al., 2011; Chappell et al., 2012). The high-K calc-alkaline composition of the Sudbury Granite and the central Sgr granite (Figure 4.13) suggests that these metaigneous source rocks are calc-alkaline to high-K calc-alkaline meta-andesites or metamorphosed basaltic andesites (Roberts & Clemens, 1993). The calc-alkaline composition of the northern Sgr granite (Figure 4.13) suggests these metaigneous source rocks are calc-alkaline meta-andesites or metamorphosed basaltic andesites (Roberts & Clemens, 1993). Furthermore, it is believed that the Sgr Group source rocks were probably at least somewhat homogeneous based on the regular chemical variation throughout the granites and lack of restitic or xenolithic material within these rocks (Chappell & Stephens, 1988). Among the rocks of the Nashoba terrane, the Marlboro Formation and Nashoba Formation are composed of metaigneous rocks in the form of amphibolites and schists (Zen et al., 1983). These rocks are interpreted to be metamorphosed calc-alkaline to high-K calc-alkaline andesites and basaltic andesites (Kay, 2012), and as such are consistent with what Roberts and Clemens (1993) suggest for I-type granite source rocks.

5.3.2 Emplacement constraints

Biotite and hornblende are considered to be the primary hydrous minerals involved in the formation of I-type granites (Roberts & Clemens, 1993). The dehydration of these minerals can produce 30 % - 70 % melt and up to 70 % melt per modal % biotite and modal % hornblende, respectively, in the source rock (Clemens & Vielzeuf, 1987; Spear et al., 1999). The metaigneous rocks of the Marlboro Formation and Nashoba Formation are composed of up to 20 % biotite for the schists and ~60 % hornblende for the amphibolites (Kay, 2012) and thus would yield 6 % - 14 % melt via biotite dehydration and up to 42 % melt via hornblende dehydration. Both processes would produce sufficient melt individually to generate a pluton of sufficient size to escape its source region (Rosenberg & Handy, 2005; Brown, 2013). Experimental data shows that these minerals dehydrate between 750 °C and 850 °C for biotite and 850 °C and 950 °C for hornblende at pressures between 5 kbar and 10 kbar (Clemens & Vielzeuf, 1987; Spear et al., 1999; Roberts & Clemens, 1993).

Chappell and others (2004) propose that I-type granites can be distinguished as high- or low-temperature granites on the basis of Zr behavior and zircon textures. They observed that granites believed to have crystallized at lower temperatures (~650 °C to ~750 °C) had simple linear Zr geochemical trends and contained zircons with strong inheritance textures while granites believed to have crystallized at higher temperatures (~800 °C to ~900 °C) had more complex Zr geochemical trends and contained zircons that lacked inheritance textures. The lack of inheritance textures within zircons retrieved from the Sudbury Granite (Figure 3.6) and a curved Zr geochemical trend (Figure 5.3) in the Sgr Group suggest that the Sgr Group can be classified as high temperature granites.

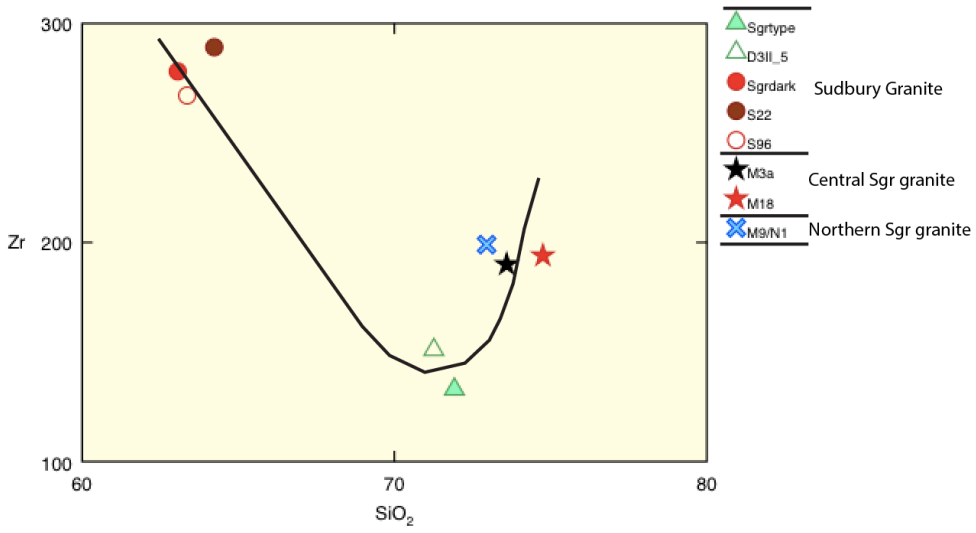

Figure 5.3 – Zr vs SiO_2 bivariate plot of the Sgr Group of granites. Note the curved best fit line estimate shown as a black line in the figure. This curved distribution of data points suggest a high crystallization temperature (Chappell et al., 2004).

5.4 Petrogenetic Model Based on Mineralogical and Geochemical Evidence

The Andover Granite formed between 419 Ma and 412 Ma and the geochronological constraints on the Sgr Group are 420 Ma (for the Sudbury Granite) and potentially ~ 430 Ma (for the central and northern Sgr granites). These ages indicate the granites are approximately coeval to the first metamorphic event in the Nashoba terrane (M1 in Figure 5.1). Based on the discussion in the preceding sections, it is clear that the granite formation temperatures proposed exceed the peak amphibolite facies metamorphic temperatures of the M1 event seen at current surface exposure levels in the terrane. Thus, additional heat beyond what was needed to metamorphose the terrane would be necessary to trigger anatexis and granite formation.

For the Andover Granite, the additional heat could be accommodated by the increased depth suggested by the mineralogy and pegmatite data (Figure 5.2) analyzed from the suite (Collins, 1987). Assuming a geothermal gradient of about 50 °C/km, an acceptable value given the low P – high T metamorphism of the Nashoba terrane (Hepburn et al., 1995), only an additional 2 km – 3 km of depth would be required to generate sufficient heat to develop a hydrous melt that could form the Andover Granite. Indeed, a 5 kbar formation pressure suggests that the suite formed just beneath the rocks observed at the surface today. As Kay (2012) concluded, the Sm-Nd isotope data from the Andover Granite suggests that a potentially significant contribution was made from crustal material older than that seen in the Nashoba terrane, i.e. a Nashoba terrane basement. Thus, it is certainly plausible that the increase in depth could provide the additional heat necessary to form the Andover Granite.

However, the same cannot be said about the Sgr Group. It has been proposed that the Sgr Group likely formed at similar pressures to the Andover Granite (~5 kbar), but at hotter temperatures (approximately 800 °C to 900 °C, compared to 750 °C and 850 °C for the Andover Granite). Increased depth alone is unlikely responsible for triggering the crustal melting needed to form the Sgr Group, thus another heat source is required.

It is believed that the primary mechanism behind the metamorphism of the Nashoba terrane, beyond crustal thickening, was the intrusion of diorite/tonalite magmas (Zartman & Naylor, 1984; Hepburn et al., 1995; Stroud et al., 2009). Since melts of intermediate composition are on the order of 1000 °C (Winter, 2001), a significant amount of heat would be introduced into the surrounding country rock during intrusion. This heat flux is believed to be the largest contributor of heat to the low pressure / high temperature amphibolite facies metamorphism seen in the terrane (Stroud et al., 2009).

A simple observation of the geological map of the Nashoba terrane shows that the Andover Granite and the Sgr Group are mapped either adjacent to, or in close proximity of, the Sharpners Pond Diorite (Figure 1.2). It is certainly plausible that local to the intruding diorite/tonalite magmas, crustal temperatures met or exceeded those proposed for the formation of the these granites. Multiple workers have suggested that the intrusion of mafic melts into the crust can provide conditions conducive for granite generation and, in some cases, even trigger granite formation (e.g. Huppert & Sparks, 1988; Brown, 2013 and references therein).

This has also been proposed for the formation of other granites in the northern Appalachians. Whalen and others (2006) concluded that the Silurian granites associated with the Salinic orogeny in Newfoundland were likely generated by the coeval intrusion of mafic magmas. Schofield and D'Lemos (2000) suggest that the mafic magma injections seen in the Gander zone of Newfoundland created higher temperature conditions locally in the source regions for the Silurian to Devonian granites that intrude the Gander zone. Furthermore, Yang and others (2008) suggest that a mafic under-plate likely triggered lower crustal I-type granite generation in the Late Silurian to Late Devonian to form the granodiorites, monzogranites, and granites found in southwestern New Brunswick. Therefore, it is proposed here that the additional heat introduced into the terrane by the intruding diorite/tonalite magmas (e.g. the Sharpners Pond Diorite) was sufficient to trigger the dehydration of hydrous minerals present in the warm metasedimentary rocks of the Nashoba terrane and/or its basement, notably biotite and hornblende, thereby initiating anatexis and granite formation.

Chapter 6: Tectonic Implications

6.1 Implications for the Evolution of the Nashoba terrane

The Silurian ages for the foliated Andover Granite and the Sudbury Granite indicate that granite crystallization is coeval with both the metamorphism of the Nashoba terrane (Stroud et al., 2009) and the intrusion of dioritic and tonalitic plutons (Zartman & Naylor, 1984). The close spatial association of the granites with the intermediate intrusions (Figure 1.2), combined with coeval ages, suggest that the heat influx from the intermediate composition magmas likely triggered anatectic melting (See Section 5.4). Therefore, the orogenic processes that affected the Nashoba terrane during the Late Silurian not only metamorphosed the terrane but also promoted granite formation.

6.2 Regional Correlations

The plutons of the Nashoba terrane have been interpreted to be related to Acadian orogenesis based on their Silurian – Devonian ages, geochemistry, and proximity to the Ganderia – Avalonia boundary in Massachusetts (Hepburn et al., 1995; Kay, 2012). As such, these plutons can be correlated to, or contrasted with, other Acadian aged igneous bodies in the northern Appalachians.

6.2.1 Newbury Volcanic Complex

The Newbury Volcanic Complex is found adjacent to the Nashoba terrane in Rowley, Massachusetts (Shride, 1976b; Zen et al., 1983; Figures 1.2 and 6.1). The complex is composed of weakly metamorphosed calc-alkaline basalts, andesites, rhyolites, and related sediments believed to be late Silurian in age based on fossil and geochronological evidence (Shride; 1976b; Loan, 2011; personal communication, J. C. Hepburn, 2014). The complex is thought to represent the surface expression of continental arc magmatism in Massachusetts just prior to the Acadian orogeny (Loan, 2011; Kay, 2012). This is supported by the interpretation that the Nashoba terrane metasediments contributed material to the formation of some of the metavolcanics found in the Newbury Volcanic Complex (Kay, 2012) and the volcanic arc setting of the similar aged plutons in the terrane.

6.2.2 Coastal Volcanic Belt

The Coastal Volcanic Belt is a Silurian-Devonian volcanic belt composed of calc-alkaline to tholeiitic, basalt to rhyolite deposits along the coastline of easternmost Maine (Piñán Llamas, 2002; Piñán Llamas & Hepburn, 2013; Figure 6.1). The belt was interpreted to include a shift in the magmatic regime of pre-Acadian to Acadian igneous rocks from arc to non-arc magmatism (Piñán Llamas & Hepburn, 2013). This geodynamic change was also observed elsewhere in the northern Appalachians (Zartman & Gallego, 1979; Hogan & Sinha, 1989; Barr, 1990; Tucker et al., 2001; Gibson & Lux, 2009; van Staal et al., 2011a) as well as during the preceding Salinic orogeny (Whalen,

1993; Whalen et al., 2006). The switch from arc to non-arc magmatism is believed to potentially be the result of asthenospheric upwelling due to the break off of the subducting slab beneath Laurentia sometime after the collision of Avalon to Laurentia (Tucker et al., 2001; Whalen et al., 2006; Piñán Llamas & Hepburn, 2013).

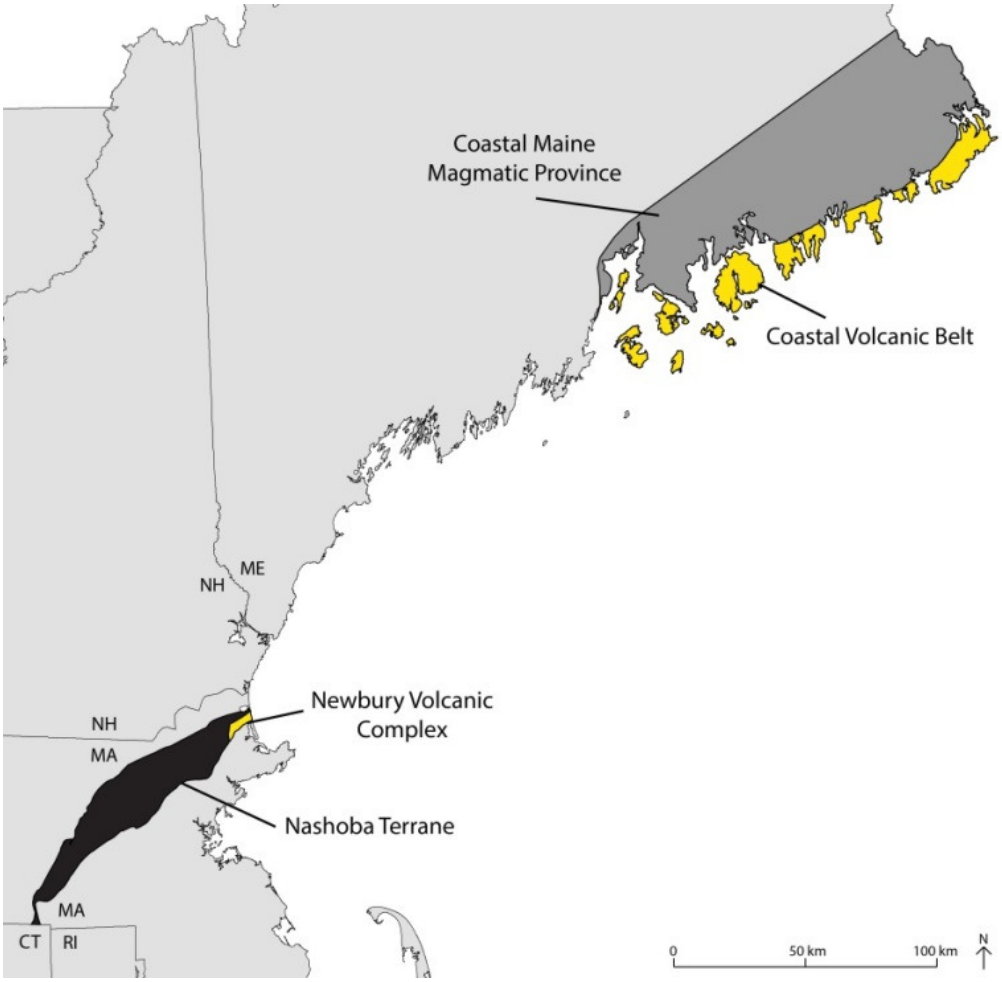

Figure 6.1 – Map showing likely regional correlations for the plutonic rocks of the Nashoba terrane in New England.

Figure 6.2 shows available Rare Earth Element (REE) data from the Nashoba terrane plutons compared with the Coastal Volcanic Belt. It is unclear to which group of the more mafic volcanic rocks the diorites of the terrane correlate, but the Nashoba terrane granites clearly correlate with the felsic arc volcanic rocks and contrast with the felsic non-arc volcanic rocks. This is unsurprising given the abundant mineralogical, geochemical, and isotopic data from the Nashoba terrane plutons that suggest the involvement of a volcanic arc in their petrogenesis (Hill et al., 1984; Collins, 1987; Loftenius, 1988; Wones & Goldsmith, 1991; Hepburn et al., 1995; Kay, 2012; Chapter 4).

6.2.3 Coastal Maine Magmatic Province

The Coastal Maine Magmatic Province is a collection of late Silurian to Early Carboniferous, alkaline, mafic to felsic plutons exposed in eastern Maine (Hogan & Sinha, 1989; Figure 6.1). The plutons within the province are interpreted to have formed within an extensional tectonic setting based on their alkaline geochemistry and mineralogy (Hogan & Sinha, 1989). This alkaline geochemistry contrasts with the calc-alkaline to high-K calk-alkaline geochemistry of the Nashoba terrane plutons as does the their volcanic arc tectonic setting interpretation (Collins, 1987; Loftenius, 1988; Kay, 2012). This suggests the Coastal Maine Magmatic Province and the Nashoba terrane formed in two different tectonic settings.

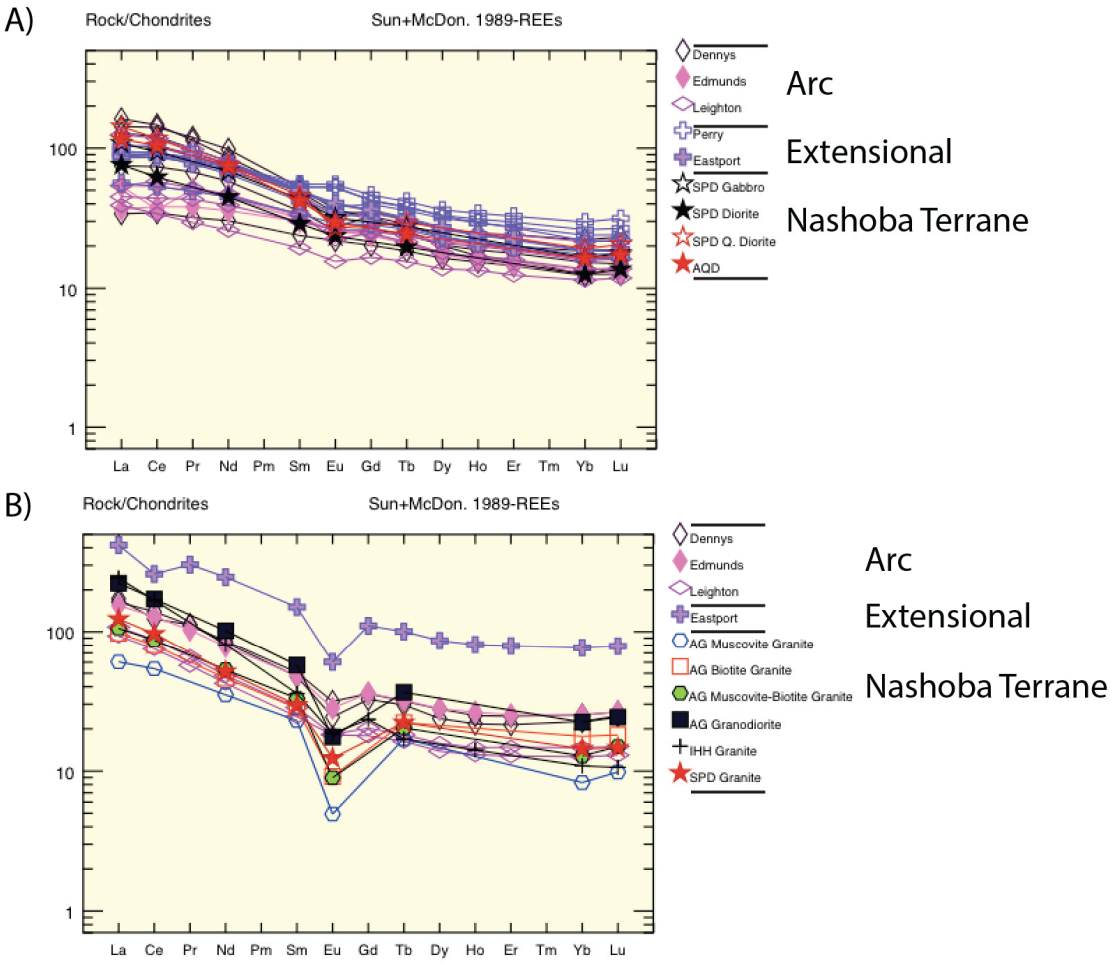

Figure 6.2 – REE multielement spider diagrams for the mafic and intermediate rocks (A) and felsic rocks (B) of the Coastal Volcanic Belt (CVB) and the plutons of the Nashoba terrane. AG – Andover Granite, AQD – Assabet Quartz Diorite, IHH – Indian Head Hill, SPD – Sharpners Pond Diorite. Plots are normalized to a chondrite composition following Sun and McDonough (1989). CVB REE data from Piñán Llamas (2002). Andover Granite REE data from Collins (1987). Assabet River Quartz Diorite REE data from Kane (1996). Indian Head Hill REE data from Kay (2012). Sharpners Pond Diorite REE data from Loftenius (1988).

A) Comparison between the mafic and intermediate rocks of the CVB with an affinity for arc (Dennys, Edmunds, and Leighton Formations) and extensional (Eastport and Perry Formations) magmatism with the intermediate plutons of the Nashoba terrane. The overlap between the Nashoba terrane plutons and the CVB make it unclear to which group the Nashoba terrane correlates with. B) Comparison between the felsic rocks of the CVB with an affinity for arc (Dennys, Edmunds, and Leighton Formations) and extensional (Eastport Formation) magmatism with the felsic plutons of the Nashoba terrane. Note the overlap between the Nashoba terrane plutons and the volcanic deposits of the CVB with an arc affinity.

6.3 Regional Implications

The volcanic arc affinity of the plutons in the Nashoba terrane suggest that the geodynamic shift from arc to extensional magmatism seen in Maine did not occur in eastern Massachusetts until at least the Early Devonian. While it can take upwards of 5 m.y. after slab break off before granitic melts start to show an extensional affinity (Whalen et al., 2006), the lack of any plutons in the Nashoba terrane with a non-arc affinity indicates that extensional magmatism did not occur in the terrane in the Silurian. Thus, the lack of extensional magmatism in the Nashoba terrane suggests that by the Late Silurian – Early Devonian, Avalonia was still outboard of Laurentia in the vicinity of southern New England.

6.4 Tectonic Model for Granite Formation and Silurio-Devonian Orogenesis

In the Early Silurian (440 Ma – 423 Ma), the passive margin of Ganderia, on which the Nashoba terrane currently resides, converged and collided with Laurentia during the Salinic orogeny (Dunning et al., 1990; van Staal, 1994; van Staal et al., 2009; 2011a; 2011b). Following this, to accommodate for the convergence of Avalonia towards Laurentia, the ocean basin separating Avalonia and Laurentia moved beneath the eastern Ganderian passive margin leading to the construction of a subduction zone (Figure 6.3A). By the Late Silurian, this subduction zone generated mafic and intermediate composition magmas that under-plated and heated the overriding Ganderian crust (van Staal et al., 2009). Some of these magmas proceeded to either erupt as continental arc volcanic deposits (i.e. the Newbury Volcanic Complex and the Dennys, Edmunds, and Leighton

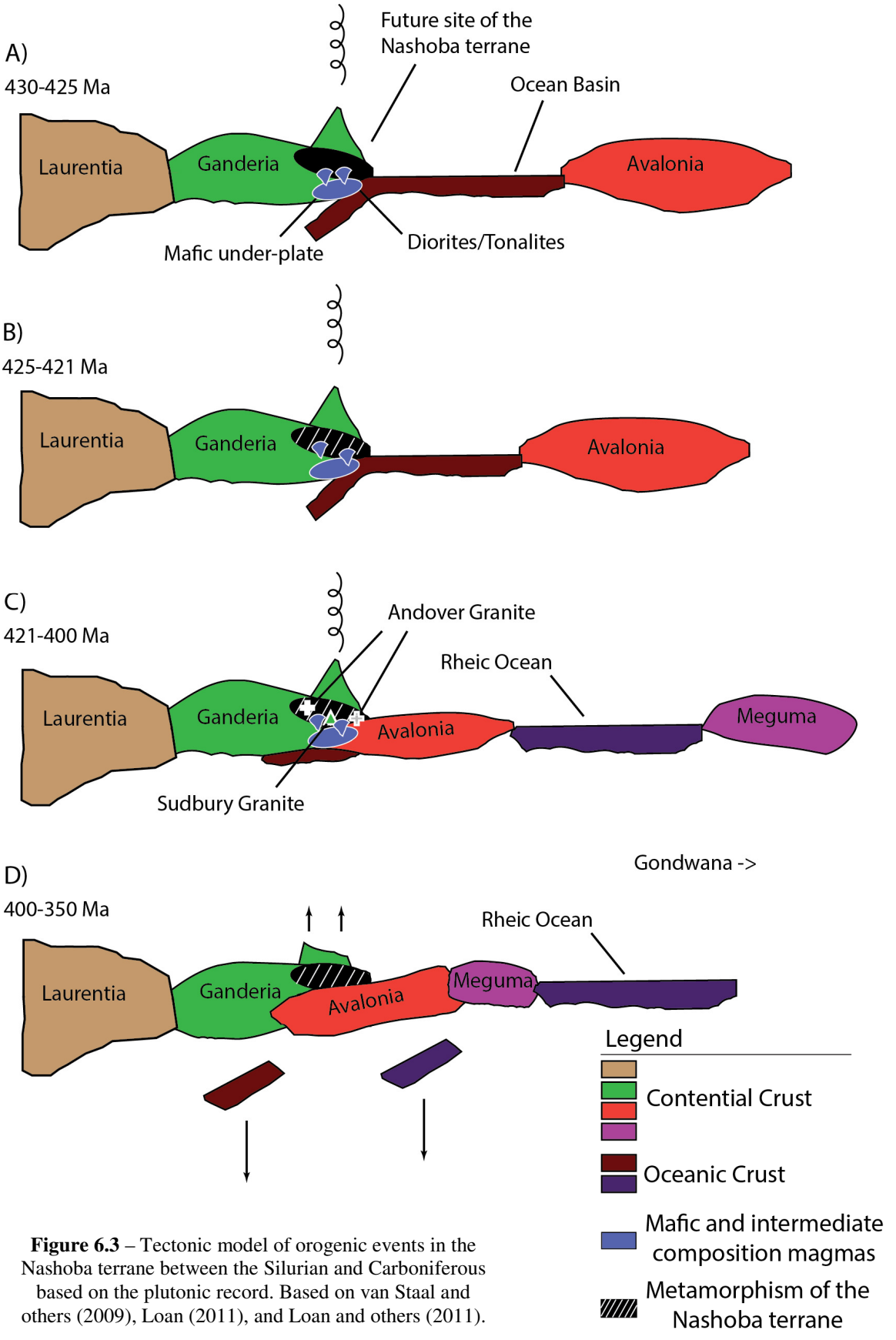

Figure 6.3 – Tectonic model of orogenic events in the Nashoba terrane between the Silurian and Carboniferous based on the plutonic record. Based on van Staal and others (2009), Loan (2011), and Loan and others (2011).

Formations of the Coastal Volcanic Belt) or to be emplaced within the crust as calc-alkaline plutons (i.e. the Sharpners Pond Diorite in the Nashoba terrane) along the eastern Ganderian margin (Hepburn et al., 1995; van Staal et al., 2009; Kay, 2012; Piñán Llamas & Hepburn, 2013; Figure 6.3A).

When the intermediate composition magmas intruded into the warm Ganderian crust (already warm due to heat from the mafic under-plate and crustal thickening), the additional heat provided by these plutons increased the temperature of the surrounding crustal rocks and triggered the Late Silurian – Early Devonian amphibolite facies metamorphism in the Nashoba terrane (Hepburn et al., 1995; Stroud et al., 2009) (Figure 6.3B). Local to these intruding plutons the temperatures of the surrounding country rocks would have reached anatectic conditions, thereby promoting the formation of granitic melts (i.e. the Andover Granite and the Sgr Group of granites) (Figure 6.3C).

The Acadian orogeny began in the Late Silurian – Early Devonian, when the collision between Avalonia and composite-Laurentia started (van Staal et al., 2009; Hatcher, 2010). As the Acadian orogeny progressed, Avalonia was thrust beneath Ganderia (Figure 6.3D) contributing to the widespread Acadian deformation (Stroud et al., 2009; van Staal et al., 2009; Hatcher, 2010). During this time Avalonia may have also contributed some material to Ganderian magmatism. The zircons found in the Carboniferous Indian Head Hill granite, for example, show Avalonian inheritance (Hepburn et al., 1995). This indicates that by the Carboniferous, Avalonia was either beneath Ganderia or close enough to contribute material.

With the collision of Avalonia, the subduction zone along the eastern margin of Ganderia shut down and a shift in magmatism from an arc to a non-arc magmatic regime occurred. This led to the eruption of bimodal alkaline volcanic rocks (i.e. the Silurio-Devonian Eastport Formation of the Coastal Volcanic Belt) and the intrusion of alkaline diorite, tonalites, and granites (i.e. the Coastal Maine Magmatic Province) (Hogan & Sinha, 1989; Piñán Llamas & Hepburn, 2013). If slab breakoff occurred, the under-plating of alkaline mafic and intermediate composition magmas would also bring additional heat into the crust and contribute to the widespread Acadian metamorphism and non-arc magmatism (van Staal et al., 2009; Piñán Llamas & Hepburn, 2013). By the Late Devonian, the micro-continent Meguma converged and collided with composite-Laurentia (van Staal et al., 2009; Hatcher, 2010). This initiated the Neo-Acadian orogeny, further extending the east coast of what would become North America.

Chapter 7: Conclusions

Based on CA-TIMS U-Pb zircon geochronology, XRF geochemistry, and petrography of the foliated Andover Granite and the Sgr Group, the following can be concluded:

- The foliated Andover Granite is a high-K calc-alkaline, peraluminous, S-type granite that crystallized at the Silurian-Devonian boundary (419.43 ± 0.52 Ma and 419.65 ± 0.51 Ma).
- The Sgr Group is composed of multiple granites.
    - The southernmost body of this group, the Sudbury Granite, is a high-K calc-alkaline, metaluminous to slightly peraluminous, I-type biotite granite that crystallized 420.49 ± 0.52 Ma.
    - The central and northern Sgr granites are composed of multiple slightly metaluminous to slightly peraluminous, high-K calc-alkaline to calc-alkaline, I-type biotite granites thought to be coeval with the Silurian Sharpners Pond diorite based on contact relationships and the presence of magmatic pillows.
- The Bloody Bluff fault type locality is composed of Sudbury Granite, indicating the Bloody Bluff fault is younger than Late Silurian.
- These granites are coeval with Silurian orogenesis and are interpreted to form as the result of heat influx associated with the intrusion of diorite/tonalite magmas into the Nashoba terrane during arc magmatism.
- The plutonic record in southeastern New England shows that by the earliest Devonian, Avalonia had yet to collide with Laurentia.

Chapter 8: References

Abu-moustafa, A., and Skehan, J. W., 1976, Petrography and geochemistry of the Nashoba Formation east-central Massachusetts, *in* Lyons, P. C., and Brownlow, A. H., eds., *Studies in New England Geology*, Geological Society of America Memoir 146, Geological Society of America, p. 31-70.

Acaster, M., and Bickford, M. E., 1993, U-Pb geochronology of metavolcanic and metavolcanogenic sedimentary rocks; Nashoba Block, eastern Massachusetts, *Geological Society of America – Abstracts with Programs*, vol. 25, p. A484.

Barbarin, B., 1990, Granitoids: Main petrogenetic classifications in relation to origin and tectonic setting, *Geological Journal*, vol. 25, p. 227-238.

Barbarin, B., 1999, A review of the relationships between granitoid types, their origins and their geodynamic environments, *Lithos*, vol. 46, p. 605-626.

Barr, S. M., 1990, Granitoid rocks and terrane characterization: An example from the northern Appalachian orogen, *Geological Journal*, vol. 25, p. 295-304.

Bell, K. G., and Alvord, D. C., 1976, Pre-Silurian stratigraphy of northeastern Massachusetts, *in* Page, L. R., ed., *Contributions to the stratigraphy of New England*, Geological Society of America Memoir 148, Geological Society of America, p. 179-216.

Bober, R., 1989, Metamorphism of the Nashoba Block and the Tadmuck Brook Schist, East Central Massachusetts, M.S. Thesis, Boston College, Chestnut Hill, MA, 194 p.

Bowring, J. F., McLean, N. M., and Bowring, S. A., 2011, Engineering cyber infrastructure for U-Pb geochronology: Tripoli and U-Pb_Redux, *Geochemistry, Geophysics, Geosystems*, vol. 12, p. Q0AA19.

Brown, M., 2013, Granite: From genesis to emplacement, *Geological Society of America Bulletin*, vol. 125, p. 1079-1113, doi: 10.1130/B30877.1.

Buchanan, J. W., II, Kuiper, Y. D., and Buchwaldt, R., 2014, Constraining the timing of deformation in the Nashoba Formation, Eastern Massachusetts, *Geological Society of America – Abstracts with Programs*, vol. 46, no. 2, p. 122.

Cameron, B., and Naylor, R. S., 1976, General geology of southeastern New England, *in* Cameron, B., ed., *Geology of southeastern New England,* New England Intercollegiate Geological Conference, 68th Annual Meeting, Science Press, Princeton, NJ, p. 13-27.

Castle, R. O., 1964, Geology of the Andover Granite and surrounding rocks, Massachusetts, *USGS Open File Report #64-33*, U. S. Geological Survey, 550 p.

Castle, R. O., and Theodore, T. G., 1972, Some genetic implications of the phase composition of a simple New England Pegmatite, *USGS Professional Paper 800-B*, U. S. Geological Survey, p. B105-B117.

Chappell, B. W., and White, A. J. R., 1974, Two contrasting granite types, *Pacific Geology*, vol. 8, p. 173-174.

Chappell, B. W., and Stephens, W. E., 1988, Origin of infracrustal (I-Type) granite magmas, *Transactions of the Royal Society of Edinburgh: Earth Sciences*, vol. 79, p. 71-86.

Chappell, B. W., White, A. J. R., Williams, I. S., and Wyborn, D., 2004, Low- and high-temperature granites, *Transactions of the Royal Society of Edinburgh: Earth Sciences*, vol. 95, p. 125-140.

Chappell, B. W., Bryant, C. J., and Wyborn, D., 2012, Peraluminous I-Type Granites, *Lithos*, vol. 153, p. 143-153.

Clapp, C. H., 1921, Geology of the igneous rocks of Essex County, Massachusetts, *USGS Bulletin 704*, U. S. Geological Survey, 132 p.

Clemens, J. D., and Wall, V. J., 1981, Origin and crystallization of some peraluminous (S-Type) granitic magmas, *Canadian Mineralogist*, vol. 19, p. 111-131.

Clemens, J. D., and Vielzeuf, D., 1987, Constraints on melting and magma production in the crust, *Earth and Planetary Science Letters*, vol. 86, p. 287-306.

Clemens, J. D., Stevens, G., and Farina, F., 2011, The enigmatic sources of I-type granites; The peritectic connection, *Lithos*, vol. 123, p. 174-181.

Collins, R.D., 1987, Geology and Geochemistry of the Andover Granite: An Anatectic Granite in the Nashoba Zone of Eastern Massachusetts, M.S. Thesis, Boston College, Chestnut Hill, MA, 293 p.

Corfu, F., Hanchar, J. M., Hoskin, P. W. O., and Kinny, P. D., 2003, Atlas of zircon Textures, *in* Hanchar, J. M., and Hoskin, P. W. O., eds., *Zircon*, Reviews in Mineralogy and Geochemistry, Mineralogical Society of America, vol. 53, p. 469-500.

Dunning, G. R., Barr, S. M., Raeside, R. P., and Jamieson, R. A., 1990, U-Pb zircon, titanite, and monazite ages in the Bras d'Or and Aspy terranes of Cape Breton Island, Nova Scotia: Implications for igneous and metamorphic history, *Geological Society of America Bulletin*, vol. 102, p. 322-330.

Emerson, B. K., 1917, Geology of Massachusetts and Rhode Island, *USGS Bulletin 597*, U. S. Geological Survey, 289 p.

Gibson, D., and Lux, D. R., 2009, Geochemical signatures of Early to Late Devonian plutons of the Piscataquis Magmatic Belt, Central Maine, *Geological Society of America – Abstracts with Programs*, vol. 41, no. 3, p. 80.

Gladney, E. S., Jones, E. A., Nickell, E. J., and Roelandts, I., 1992, 1988 Compilation of elemental concentration data for USGS AGV-1, GSP-1, and G-2, *Geostandards Newsletter*, vol. 16, p. 111-300.

Goldsmith, R., 1991a, Stratigraphy of the Nashoba Zone, eastern Massachusetts; an enigmatic terrane, *in* Hatch, N. L., Jr., ed., *The bedrock geology of Massachusetts*, U. S. Geological Survey Professional Paper 1366-E-J, United States (USA), U. S. Geological Survey, Reston, VA, United States (USA), p. F1-F22.

Goldsmith, R., 1991b, Structural and metamorphic history of eastern Massachusetts, *in* Hatch, N. L., Jr., ed., *The bedrock geology of Massachusetts*, U. S. Geological Survey Professional Paper 1366-E-J, United States (USA), U. S. Geological Survey, Reston, VA, United States (USA), p. H1-H63.

Goldsmith, R., 1991c, Stratigraphy of the Milford-Dedham Zone, Eastern Massachusetts: An Avalonian Terrane, *in* Hatch, N. L., Jr., ed., *The bedrock geology of Massachusetts*, U. S. Geological Survey Professional Paper 1366-E-J, United States (USA), U. S. Geological Survey, Reston, VA, United States (USA), p. E1-H62.

Govindaraju, K., 1989, 1989 Compilation of working values and sample description of 272 geostandards, *Geostandards Newsletter*, vol. 13, p. 1-113.

Govindaraju, K., 1994, 1994 Compilation of working values and description for 383 geostandards, *Geostandards Newsletter*, vol. 18, p. 1-158.

Handford, L. S., Fairbairn, H. W., Pinson, W. A., and Hurley, P. M., 1965, Rb-Sr whole rock age study of the Andover and Chelmsford Granites, Massachusetts, *in* Hurley, P. M., ed., *13th Annual Progress Report*, United States Atomic Energy Commission, No. 1381-12, Massachusetts Institute of Technology, Cambridge, Massachusetts, p. 11-14.

Hansen, W. R., 1956, Geology and mineral resources of the Hudson and Maynard quadrangles, Massachusetts, *USGS Bulletin 1038*, U. S. Geological Survey, 104 p.

Harris, N. B. W., Pearce, J. A., and Tindle, A. G., 1986, Geochemical characteristics of collision-zone magmatism, *in* Coward, M. P., and Ries, A. C., eds., *Collision Tectonics*, Geological Society Special Publication 19, The Geological Society, p. 67-81.

Hatcher, R. D., Jr., 2010, The Appalachian orogen: A brief summary, *in* Tollo, R. P., Bartholomew, M. J., Hibbard, J. P., and Karabinos, P. M., eds., *From Rodinia to Pangea: The Lithotectonic Record of the Appalachian Region*, Geological Society of America Memoir 206, Geological Society of America, p. 1–19, doi: 10.1130/2010.1206(01).

Hepburn, J. C., and Munn, B., 1984, A geologic traverse across the Nashoba block, eastern Massachusetts, *in* Hanson, L. S., ed., *Geology of the Coastal lowlands: Boston, MA to Kennebunk, ME*, New England Intercollegiate Geological Conference, 76th Annual Meeting, Salem State College, Salem, Massachusetts, p. 103-114.

Hepburn, J. C., Hon, R., Dunning, G. R., Bailey, R. H., and Galli, K., 1993, The Avalon and Nashoba terranes (eastern margin of the Appalachian orogen in southeastern New England), *in* Cheney, J. T., and Hepburn, J. C., eds., Field Trip Guidebook for the Northeastern United States, 1993 Geological Society of America Annual Meeting, Department of Geology and Geography, University of Massachusetts, Amherst, Massachusetts, v. 2, p. X1-X31.

Hepburn, J. C., Dunning, G. R., and Hon, R., 1995, Geochronology and regional tectonic implications of Silurian deformation in the Nashoba terrane, southeastern New England, U.S.A., *in* Hibbard, J. P., van Staal, C. R., and Cawood, P. A., eds., *Current Perspectives in the Appalachian-Caledonian Orogen*, Geological Society of Canada Special Paper 41, Geological Society of Canada, p. 349-366.

Hepburn, J. C., and Bailey, R. H., 1999, The Avalon and Nashoba terranes in eastern Massachusetts, *in* Wright, S. F., ed., *Guidebook to Field Trips in Vermont and Adjacent Regions of New Hampshire and New York*, New England Intercollegiate Geologic Conference, 91st Annual Meeting, University of Vermont, Burlington, Vermont, p. C-3.

Hibbard, J. P., van Staal, C. R., and Miller, B. V., 2007a, Links among Carolinia, Avalonia, and Ganderia in the Appalachian peri-Gondwanan realm, *in* Sears, J. W., Harms, T. A., and Evenchick, C. A., eds., *Whence the Mountains? Inquiries into the Evolution of Orogenic Systems: A Volume in Honor of Raymond A. Price*, Geological Society of America Special Paper 433, Geological Society of America, p. 291-311.

Hibbard, J. P., van Staal, C. R., and Rankin, D. W., 2007b, A comparative analysis of pre-Silurian crustal building blocks of the Northern and Southern Appalachian orogen, *American Journal of Science*, vol. 307, p. 23-45.

Hibbard, J., and Waldron, J. W. F., 2009, Truncation and translation of Appalachian promontories: Mid-Paleozoic strike-slip tectonics and basin initiation, *Geology*, vol. 37, p. 487-490, doi:10.1130/G25614A.1.

Hitchcock, E., 1833, *Report on the geology, mineralogy, botany, and zoology of* Massachusetts, Amherst, MA: Press of J. S. and C. Adams, 700 p. and 19 plates.

Hiess, J., Condon, D. J., McLean, N., and Nobel, S. R., 2012, $^{238}U/^{235}U$ Systematic in Terrestrial Uranium-Bearing Minerals, *Science*, vol. 335, p. 1610-1614, doi: 10.1126/science.1215507.

Hill, M. D., Hepburn, J. C., Collins, R. D., and Hon, R., 1984, Igneous rocks of the Nashoba Zone, eastern Massachusetts, *in* Hanson, L., ed., *Geology of the Coastal Lowlands: Boston, MA to Keenebunk, ME,* New England Intercollegiate Geological Conference, 76th Annual Meeting, Salem State College, Salem, Massachusetts, p. 61-80.

Hogan, J. P., and Sinha, A. K., 1989, Compositional variation of plutonism in the Coastal Maine Magmatic Province: Mode of Origin and Tectonic Setting, *Studies in Maine Geology*, Maine Geological Survey, vol. 4, p. 1-33.

Hoskin, P. W. O., and Schaltegger, U., 2003, The composition of zircon and igneous and metamorphic petrogenesis, *in* Hanchar, J. M., and Hoskin, P. W. O., eds., *Zircon*, Reviews in Mineralogy and Geochemistry, Mineralogical Society of America, vol. 53, p. 27–62.

Hyndman, D. W., 1981, Controls on source and depth of emplacement of granitic magmas, *Geology*, vol. 9, p. 244-249.

Huppert, H. E., and Sparks, R. S. J., 1988, The generation of granitic magmas by intrusion of basalt into continental crust, *Journal of Petrology*, vol. 29, p. 599-624, doi: 10.1093/petrology/29.3.599.

Jaffey, A. H., Flynn, K. F., Glendenin, L. E., Bentley, W. C., and Esslin, A. M., 1971, Precision measurements of half-lives and specific activities of ^{235}U and ^{238}U, *Physical Reviews*, vol. C4, p. 1,889-1,906.

Jerden, J. L., Jr., 1997, Polyphase metamorphism and structure of the Tadmuck Brook Schist, eastern Massachusetts, M.S. Thesis, Boston College, Chestnut Hill, MA, 323 p.

Kane, R. W., Jr., 1996, The Comparative Geochemistry of Ordovician-Devonian Dioritic to Gabbroic Plutons of the Nashoba and Avalon Terranes of Eastern Massachusetts, M. S. Thesis, Boston College, Chestnut Hill, MA, 47 p.

Karabinos, P., Samson, S. B., Hepburn, J. C., and Stoll, H. M., 1998, Taconian orogeny in the New England Appalachians: Collision between Laurentia and the Shelburne Falls arc, *Geology*, vol. 26, p. 215-218.

Kay, A., Hepburn, J. C., and Kuiper, Y., 2011, Trace element and isotopic geochemical characteristics of the Nashoba terrane, eastern Massachusetts, *Geological Society of America – Abstracts with Programs*, vol. 43, no. 1, p. 150.

Kay, A., 2012, Sm-Nd Isotope, major element, and trace element geochemistry of the Nashoba terrane, eastern Massachusetts, M.S. Thesis, Boston College, Chestnut Hill, MA, 143 p.

Kohut, E. J., 1999, The bedrock geology of the Weston-Lexington Area, southeastern New England Avalon and Nashoba terranes, M.S. Thesis, Boston College, Chestnut Hill, MA, 159 p.

Langford, C. D., 2007, Preliminary bedrock geologic map of the Concord Quadrangle, Massachusetts, Boston College with cooperation with the office of the Massachusetts State Geologist, 1:24,000.

LeBas, M. J., Lemaitre, R. W., Streckeisen, A., and Zanettin, B., 1986, A chemical classification of volcanic rocks based on the Total Alkali Silica Diagram, *Journal of Petrology*, vol. 27, no. 3, p. 745-750.

Loftenius, C. J., 1988, The geochemistry and the petrogenesis of the Sharpners Pond plutonic suite, NE Massachusetts, M.S. Thesis, Boston College, Chestnut Hill, MA, 284 p.

Loan, M. L., 2011, New Constraints on the Age and Deposition of the Metasedimentary Rocks in the Nashoba terrane, SE New England, M.S. Thesis, Boston College, Chestnut Hill, MA, 125 p.

Loan, M. L., Hepburn, J. C., Kuiper, Y., and Tubrett, M. N., 2011, Age constraints on the deposition and provenance of meta-sedimentary units of the Nashoba terrane, *Geological Society of America – Abstracts with Programs*, vol. 43, no. 1, p. 160.

Markwort, R. J., 2007, Geology of the Shrewsbury Quadrangle, East-Central Massachusetts, M. S. Thesis, Boston College, Chestnut Hill, MA, 193 p.

Maniar, P. D., and Piccoli, P. M., 1989, Tectonic discrimination of granitoids, *Geological Society of America Bulletin*, vol. 101, p. 635-643.

Mattinson, J. M., 2005, Zircon U-Pb chemical abrasion ("CA-TIMS") method: Combined annealing and multi-step partial dissolution analysis for improved precision and accuracy of zircon ages, *Chemical Geology*, vol. 220, p. 47-66.

McLean, N. M., Bowring, J. F., and Bowring, S. A., 2011, An algorithm for U-Pb isotope dilution data reduction and uncertainty propagation, *Geochemistry, Geophysics, Geosystems*, vol. 12, p. Q0AA18.

Miller, C. F., 1981, Comment on "Controls on Source and Depth of Emplacement of Granitic Magmas", *Geology*, vol. 9, p. 509.

Miller, C. F., Stoddard, E. F., Bradfish, L. J., and Dollase, W. A., 1981, Composition of plutonic muscovite: Genetic implications, *Canadian Mineralogist*, vol. 19, p. 25-34.

Munn, B. J., 1987, Bedrock geology at the western margin of the Nashoba Block, East-Central, Massachusetts, M.S. Thesis, Boston College, Chestnut Hill, MA, 323 p.

O'Brien, S. J., Wardle, R. J., and King, A. F., 1983, The Avalon Zone: A Pan-African terrane in the Appalachian orogen of Canada, *Geological Journal*, vol. 18, p. 195-222.

O'Brien, S. J., O'Brien, B. H., Dunning, G. R., and Tucker, R. D., 1996, Late Neoproterozoic Avalonian and related peri-Gondwanan rocks of the Newfoundland Appalachians, *in* Nance, R. D., and Thompson, M. D., eds., *Avalonian and related Peri-Gondwanan terranes in the Circum-North Atlantic*, Geological Society of America Special Paper 304, Geological Society of America, p. 9-28.

Pearce, J. A., 1983, The role of sub-continental Lithosphere in magma genesis at destructive plate boundaries, *in* Hawkesworth, C. J., and Norry, M. J., eds., *Continental Basalts and Mantles Xenoliths*, Shiva, Nantwich, p. 230-249.

Pearce, J. A., Harris, B. W., and Tindle, A. G., 1984, Trace element discrimination diagrams for the tectonic interpretation of granitic rocks, *Journal of Petrology*, v.25, p. 956-983.

Piñián Llamas, A., 2002, The origin of the Coastal Volcanic Belt, Easternmost Maine: A petrological and geochemical study, M. S. Thesis, Boston College, Chestnut Hill, MA, 223 p.

Piñián Llamas, A., and Hepburn, J. C., 2013, Geochemistry of Silurian-Devonian volcanic rocks in the Coastal Volcanic belt, Machias-Eastport area, Maine: Evidence for a pre-Acadian arc, *Geological Society of America Bulletin*, vol. 125, p. 1930-1942.

Ramezani, J., Schmitz, M., Davydov, V., Bowring, S., Snyder, W., and Northrup, C., 2007, High-precision U-Pb zircon age constraints on the Carboniferous-Permian boundary in the southern Urals stratotype, *Earth and Planetary Science Letters*, vol. 256, no. 1-2, p. 244-257.

Rast, N., and Skehan, J. W., 1993, Mid-Paleozoic orogenesis in the North Atlantic: The Acadian Orogeny, *in* Roy, D. C., and Skehan, J. W., eds., *The Acadian Orogeny: Recent Studies in New England, Maritime Canada and the Autochthonous Foreland*, Geological Society of America Special Paper 275, Geological Society of America, p. 1-25.

Reynolds, E., Kuiper, Y. D., Hepburn, J. C., and Olszewski, W. J., 2010, New $^{40}Ar/^{39}Ar$ age constraints on the timing of metamorphism and deformation in the western Nashoba terrane, Eastern Massachusetts, *Geological Society of America – Abstracts with Programs,* vol. 42, no. 1, p. 85.

Rhodes, J. M., and Vollinger, M. J., 2004, Composition of basaltic lavas sampled by phase-2 of the Hawaii Scientific Drilling Project: Geochemical stratigraphy and magma types, *Geochemistry, Geophysics, Geosystems*, vol. 5, p. 1-38, doi: 10.1029/2002GC000434.

Rhodes, J. M., and Vollinger, M. J., 2005, Ferric/ferrous ratios in 1984 Mauna Loa lavas: a contribution to understanding the oxidation state of Hawaiian magmas, *Contributions to Mineralogy and Petrology*, vol. 149, p. 666-674, doi: 10.1007/s00410-005-0662-y.

Roberts, M. P., and Clemens, J. D., 1993, Origin of high-potassium, calc-alkaline, I-type granitoids, *Geology*, vol. 21, p. 825-828.

Rosenberg, C. L., and Handy, M. R., 2005, Experimental deformation of partially melted granite revisit: Implications for the continental crust, *Journal of Metamorphic Geology*, vol. 23, p. 19-28, doi: 10.1111/j.1525-1314.2005.00555.x.

Schofield, D. I., and D'Lemos, R. S., 2000, Granite petrogenesis in the Gander Zone, NE Newfoundland: Mixing of melts from multiple sources and the role of lithospheric delamination, *Canadian Journal of Earth Science*, vol. 37, p. 535-547.

Shride, A. F., 1971, Igneous rocks of the Seabrook, New Hampshire – Newbury, Massachusetts area, *in* Stewart, G. W., and Lyons, J. B. eds., New England Intercollegiate Geological Conference, 63rd Annual Meeting, University of New Hampshire, Concord, New Hampshire, p. 105-117.

Shride, A. F., 1976a, Preliminary map of bedrock geology in the Newburyport East and West quadrangles, Massachusetts-New Hampshire, *USGS Open File Report #76-488*, U. S. Geological Survey, 1 p.

Shride, A. F., 1976b, Stratigraphy and correlation of the Newbury Volcanic Complex, northeastern Massachusetts, *in* Page, L. R., ed., *Contributions to the stratigraphy of New England*, Geological Society of America Memoir 148, Geological Society of America, p. 147-179.

Skehan, J. W., and Abu-Moustafa, A. A., 1976, Stratigraphic analysis of rocks exposed in the Wachusett-Marlborough Tunnel, East-central Massachusetts, *in* Lyons, P. C., and Brownlow, A. H., eds., *Studies in New England Geology*, Geological Society of America Memoir 146, Geological Society of America, p. 217-240.

Skehan, J. W., and Rast, N., 1983, Relationship between Precambrian and Lower Paleozoic rocks of southeastern New England and other North Atlantic Avalonian terranes, *in* Schenk, P. E., ed., *Regional Trends in the Geology of the Appalachian-Caledonian-Hercynian-Mauritanide Orogen*, NATO Advanced Science Institutes Series, D. Reidel Publishing Co., Dordrecht, p. 131-162.

Sorota, K., Hepburn, J. C., Kuiper, Y. D., and Tubrett, M. N., 2011, Detrital zircon study of the Merrimack terrane, MA and NH, *Geological Society of America – Abstracts with Programs*, vol. 43, no. 5, p. 42.

Sorota, K., 2013, Age and origin of the Merrimack Terrane, southeast New England: A detrital zircon U-Pb geochronology study, M.S. Thesis, Boston College, Chestnut Hill, MA, 217 p.

Spear, F. S., Kohn, M. J., and Cheney, J. T., 1999, P-T paths from anatectic pelites, *Contributions to Mineralogy and Petrology*, vol. 134, p. 17-32.

Stroud, M. M., Markwort, R. J., and Hepburn, J. C., 2009, Refining temporal constraints on metamorphism in the Nashoba Terrane, southeastern New England, through monazite dating, *Lithosphere,* vol. 1, no. 6, p. 337-342.

Sun S., and McDonough, W. F., 1989, Chemical and isotopic systematics of oceanic basalts: implications for mantle composition and processes, *in* Saunders, A. D., and Norry, M. J., eds., *Magmatism in the Ocean Basins*, Geological Society Special Publication 42, The Geological Society, p. 313-345.

Thompson, M. D., Grunow, A. M., and Ramezani, J., 2003, New paleomagnetic pole from the Late Cambrian Nahant Gabbro, Nahant, Massachusetts: Implications for drift history of the Southeastern New England Avalon Zone, *Geological Society of America – Abstracts with Programs*, vol. 35, no. 3, p. 18.

Tucker, R. D., Osberg, P. H., and Berry, H. N., IV, 2001, The geology of a part of Acadia and the nature of the Acadian Orogeny across Central and Eastern Maine, *American Journal of Science*, vol. 301, p. 205-260.

van Staal, C. R., 1994, Brunswick subduction complex in the Canadian Appalachians: Record of the Late Ordovician to Late Silurian collision between Laurentia and the Gander margin of Avalon, *Tectonics*, vol. 13, p. 946-962.

van Staal, C. R., Sullivan, R. W., and Whalen, J. B., 1996, Provenance and tectonic history of the Gander Zone in the Caledonian/Appalachian orogeny: Implications for the origin and assembly of Avalon, *in* Nance, R. D., and Thompson, M. D., eds., *Avalonian and related Peri-Gondwanan terranes in the Circum-North Atlantic*, Geological Society of America Special Paper 304, Geological Society of America, p. 347-367.

van Staal, C. R., Dewey, J. F., Niocaill, and C. M., Mckerrow, 1998, The Cambrian-Silurian tectonic evolution of the northern Appalachians and British Caledonides: History of a complex, west and southwest Pacific-type segment of Iapetus, *in* Blundell, D. J., and Scott, A. C. eds., *Lyell: the Past is the Key to the Present*, Geological Society Special Publication 143, The Geological Society, p. 199-242.

van Staal, C. R., Whalen, J. B., McNicoll, V. J., Pehrsson, S., Lissenberg, C. J., Zagorevski, A., van Breemen, O., and Jenner, G. A., 2007, The Notre Dame arc and the Taconic orogeny in Newfoundland, *in* Hatcher, R. D. Jr., Carlson, M. P., McBride, J. H., and Martinez Catalan, J. R., eds., *4-D Framework of Continental Crust*, Geological Society of America Memoir 200, p. 511-552, doi: 10.1130/2007.1200(26).

van Staal, C. R., Whalen, J. B., Valverde-Vaquero, P., Zagorevski, A., and Rogers, N., 2009, Pre-Carboniferous, episodic accretion-related, orogenesis along the Laurentian margin of the Northern Appalachians, *in* Murphy, J. B., Keppie, J. D., and Hynes, A. J., eds., *Ancient orogens and modern analogues*, Geological Society Special Publication 327, The Geological Society, p. 271-316.

van Staal, C. R., Barr, S. M., Whalen, J. B., and White, C. E., 2011a, Constraints on the tectonic setting of Devonian magmatism and orogenesis, *Geological Society of America – Abstracts with Programs*, vol. 43, no. 1, p. 158.

van Staal, C. R., Barr, S., Fyffe, L. R., Johnson, S. C., Park, A. F., White, C. E., and Wilson, R. A., 2011b, The Defining Tectonic Elements of Ganderia in New Brunswick, Geological Association of Canada – Mineralogical Association of Canada – Society of Economic Geologists – Society for Geology Applied to Mineral Deposits Joint Annual Meeting, Ottawa 2011, Guidebook to Field Trip 1B, 30 p.

Waldron, J. W. F., White, C. E., Barr, S. M., Simonetti, A., and Heaman, L. M., 2009, Provenance of the Meguma terrane, Nova Scotia: Rifted margin of early Paleozoic Gondwana, *Canadian Journal of Earth Science*, vol. 46, p. 1-8, doi: 10.1139/E09-004.

Walker, J. D., Geissman, J. W., Bowring, S. A., and Babcock, L. E., 2012, The Geological Society of America Geologic Time Scale, *Geological Society of America*, version 4.0.

Walsh, G. J., Aleinkoff, J. N., Wintsch, R. P., and Ayuso, A., 2011, Origin of the Quinebaug-Marlboro Belt in southeastern New England, *Geological Society of America – Abstracts with Programs*, vol. 43, no. 1, p. 158.

Whalen, J. B., 1993, *Geology, Petrography, and Geochemistry of Appalachian Granites in New Brunswick and Gaspésie, Quebec*, Geological Survey of Canada Bulletin 436, Canada, Geological Survey of Canada, Ottawa, Ontario, Canada, p. 124.

Whalen, J. B., McNicoll, V. J., van Staal, C. R., Lissenberg, C. J., Longstaffe, F. J., Jenner, G. A., van Breeman, O., 2006, Spatial, temporal and geochemical characteristics of Silurian collision-zone magmatism, Newfoundland Appalachians: An example of a rapidly evolving magmatic system related to slab break-off, *Lithos*, vol. 89, p. 377-404, doi: 10.1016/j.lithos.2005.12.011.

Williams, H., and Hatcher, R. D., Jr., 1983, Appalachian suspect terranes, *in* Hatcher Jr., R. D., Williams, H., and Zietz, I., eds., *Contributions to the Tectonics and Geophysics of Mountain Chains*, Geological Society of America Memoir 158, Geological Society of America, p. 33-53.

Wilson, M., 1989, Igneous Petrogenesis: A Global Tectonic Approach, Chapman & Hall, London, England, 466 p.

Winkler, H. G. F., 1979; Petrogenesis of Metamorphic Rocks, Springer Verlag, New York, New York, U. S. A., 349 p.

Winter, J. D., 2001, An Introduction to Igneous and Metamorphic Petrology, Prentice-Hall Inc., Upper Saddle River, New Jersey, U.S.A., 697 p.

Wintsch, R. P., and Aleinkoff, J. N., 1987, U-Pb Isotopic and Geologic Evidence for a Late Paleozoic Anatexis, Deformation, and Accretion of the Late Proterozoic Avalon Terrane in Southcentral Connecticut, *American Journal of Science*, vol. 287, no. 2, p. 107-126.

Wintsch, R. P., Aleinikoff, J. N., Walsh, G. J., Bothner, W. A., and Hussey, A. M., II., 2007, Provenance and metamorphic implications of zircon and monazite U-Pb ages of rocks of the Merrimack and Putnam-Nashoba terranes, eastern New England, *American Journal of Science*, v. 207, p. 63-118.

Wones, D. R., and Goldsmith, R., 1991, *Intrusive rocks of eastern Massachusetts, in* Hatch, N. L., Jr., ed., *The bedrock geology of Massachusetts*, U. S. Geological Survey Professional Paper 1366-E-J, United States (USA), U. S. Geological Survey, Reston, VA, United States (USA), p. I1-I61.

Yang, X., Lentz, D. R., Chi, G., and Thorne, K. G., 2008, Geochemical characteristics of gold-related granitoids in southwestern New Brunswick, Canada, *Lithos*, vol. 104, p. 355-377, doi: 10.1016/j.lithos.2008.01.002.

Zartman, R. E., and Gallego, M. D., 1979, Radiometric ages: Compilation B, USGS, *in* Marvin, R. F., and Dobson, S. W., eds., *Isochron West*, The Bulletin of Isotopic Geochronology, no. 26, p. 18-19.

Zartman, R. E., and Naylor, R. S., 1984, Structural implications of some radiometric ages of igneous rocks in southeastern New England, *Geological Society of America Bulletin*, vol. 95, no. 5, p. 522-539.

Zen, E., Goldsmith, R., Ratcliffe, N. M. Robinson, P., and Stanley, R. S., 1983, Bedrock geologic map of Massachusetts: United States Geological Survey, 1:250,000.

Appendix A: Sample Locations

Table A-1 - Sample Locations				
	Geographic		UTM – 19T	
Sample	Latitude (°N)	Longitude (°W)	Easting (m)	Northing (m)
Foliated Andover Granite				
A-4	42.67202	71.17990	0321374	4726698
A-5	42.37707	71.55521	0289631	4694806
Sgr Group				
Sudbury Granite				
SgrType	42.39016	71.34648	0306856	4695763
D311_5	42.38599	71.35407	0306219	4695318
S83	42.44155	71.26595	0313637	4701290
Sgrtypeenclave	42.39016	71.34648	0306856	4695763
SgrDark	42.41051	71.31660	0309377	4697956
S22	42.40997	71.31724	0309323	4697897
S96	42.44162	71.27046	0313267	4701308
BFFType	42.44758	71.26513	0313723	4701958
BFF-A	42.44759	71.26518	0313719	4701959
BSC-1	42.39948	71.27880	0312455	4696647
Central Sgr Granite				
M3a	42.58671	71.0614	0330853	4716980
M6	42.59436	71.04952	0331849	4717806
M7	42.59398	71.03123	0333348	4717728
M18	42.61906	71.05056	0331830	4720551
M19	42.63015	70.99007	0336820	4721664
M20	42.67106	70.98872	0337037	4726204
Northern Sgr Granite				
M9/N1	42.75546	70.92496	0342476	4735456
N2a	42.77578	70.87759	0346403	4737625
N3	42.76337	70.91542	0343277	4736316

Foliated Andover Granite:

A-4: Andover, MA, Northbound side of Interstate 495, 150 meters northeast of the Chandler Road overpass. Outcrop DC-25a/b of Collins (1987).

A-5: Hudson, MA, East of MA-85, 40 meters northeast of the intersection between Reed Road and Rotherham Way.

Sgr Group:

Sudbury Granite:

SgrType: Wayland, MA, East of MA-126, Intersection of Hazelbrook Lane and Lincoln Road. The location of the type locality defined by Kohut (1999)

D311_5: Wayland, MA, East of MA-126, 50 meters east of the intersection of Moore Road and Concord Road (MA-126).

S83: Lexington, MA, Southeast of Hanscom AFB, 650 meters south of the intersection of Old Massachusetts Avenue and MA-2A, along the western side of the high voltage power lines.

SgrTypeEnclave: Wayland, MA, East of MA-126, Intersection of Hazelbrook Lane and Lincoln Road.

SgrDark: Lincoln, MA, East of Todd Pond, 30 meters from the end of Todd Pond Road.

S22: Lincoln, MA, East of Todd Pond, 125 meters from the end of Todd Pond Road.

S96: Lincoln, MA, South of Hanscom AFB, 430 meters south of Minuteman Regional High School, 375 meters west of S83.

BBFType: Lexington, MA, Southeast of Hanscom AFB, 40 meters northwest of the intersection of Old Massachusetts Avenue and MA-2A.

BBF-A: Lexington, MA, Southeast of Hanscom AFB, 40 meters northwest of the intersection of Old Massachusetts Avenue and MA-2A.

BSC-1: Waltham, MA, Southwest of Cambridge Reservoir, Southeastern corner of the Boston Sports Club parking lot.

Central Sgr Granite:

M3a: North Reading, MA, Southwest of Swan Pond, 225 meters Northeast of the intersection between Pickard Lane and Shasta Drive.

M6: North Reading, MA, Just northeast of Swan Pond, End of Adam Street.

M7: Middleton, MA, North of Middleton Pond, 175 meters down (heading to the southwest) the fire access road that surrounds Middleton Pond starting from the intersection of the fire access road with Lake Street, 15 meters to the northwest off the road.

M18: Middleton, MA, MA-114, 260 meters southeast from the intersection of N Main Street (MA-114) with Rockaway Road, on the south side of the road.

M19: Boxford, MA, West of Interstate-95 near exit 51, 50 meters from the end of Burning Bush Drive, 40 meters north of Burning Bush Drive.

M20: Boxford, MA, South of Lowe Pond, 30 meters north of the intersection between Depot Road and Boren Lane.

Northern Sgr Granite:

M9/N1: Newbury, MA, East of Interstate-95 near exit 55, 190 meters northeast of the intersection between Orchard Street and Pearson Drive, 19 meters northwest of Orchard Street.

N2a: Newbury, MA, East of MA-1, 220 meters down Hay Street (traveling to the southeast) from the intersection between Hay Street and Boston Road, on south side of the road.

N3: Newbury, MA, South of the Martin H. Burns Wildlife Management Area, 315 meters north of the intersection between Orchard Street and the southern entrance to the Martin H. Burns Wildlife Management Area, on east side of the road.

Appendix B: Geochemical Laboratory Standard Data

Major Elements in wt. % USGS Granite Standard G-2						
	Measured Value				Accepted Value	Error (± wt %)
	Run Number:					
	MRS00576	MRS00577	MRS00578	MRS00579		
SiO_2	69.28	69.43	69.36	69.38	69.14	0.30
TiO_2	0.47	0.47	0.47	0.47	0.45	0.03
Al_2O_3	15.36	15.48	15.29	15.25	15.39	0.30
Fe_2O_3*	2.65	2.65	2.65	2.65	2.66	0.17
MnO	0.04	0.04	0.04	0.04	0.03	0.01
MgO	0.79	0.75	0.84	0.81	0.75	0.03
CaO	1.88	1.88	1.88	1.88	1.96	0.08
Na_2O	4.19	4.19	4.19	4.19	4.08	0.13
K_2O	4.49	4.51	4.50	4.49	4.48	0.13
P_2O_5	0.13	0.14	0.13	0.13	0.14	0.01
Total	99.18	99.31	99.48	99.21	99.08	-

Trace Elements in ppm USGS Granite Standard G-2			
	Measured Value	Accepted Value	Error (± ppm)
Ba	1850	1880	23
Rb	163.9	170	3
Sr	477	478	2
Y	9.8	11	2
Zr	316	309	35
Nb	12.1	12	-
Zn	91	86	8
Ga	21	23	2
Ni	3	-	-
V	33	36	4
La	101	89	8
Ce	185	160	10
Cr	10	-	-
Th	24	25	2
U	0	-	-
Pb	30	30	4

Table B.1 – Major and trace element data for the USGS G-2 Laboratory Granite standard. Accepted values and associated error for the USGS Granite G-2 standard are from Gladney and others (1992), Govindaraju (1989), and Govindaraju (1994). Note: Fe_2O_3* is TOTAL Fe and totals have not been recalculated using the LOI value.

Appendix C: Andover Granite Geochemical Data from Collins (1987)

Table C.1 – Muscovite Phase geochemical data

Table C.2 – Biotite Phase geochemical data

Table C.3 – Muscovite-Biotite Phase geochemical data

Table C.4 – Granodiorite Phase geochemical data

Table C.5 – Average values for each phase

Sample	WDC-2	RDC-5	RDC-9	RDC-10A	RDC-10E	RDC-24	RDC-36
SiO_2	74.88	74.07	74.25	74.96	73.88	73.25	74.08
TiO_2	0.06	0.05	0.08	0.07	0.14	0.1	0.07
Al_2O_3	14.7	14.91	14.97	14.66	14.4	14.45	15.01
Fe_2O_3*	0.94	1.08	0.92	0.76	1.23	1.03	0.88
MnO	0.12	0.1	0.04	0.06	0.04	0.03	0.07
MgO	0.57	0.28	0.58	0.27	0.39	0.36	0.64
CaO	0.49	0.56	0.53	0.52	0.75	0.74	0.44
Na_2O	3.66	3.89	3.77	3.55	3.19	3.28	3.85
K_2O	4.6	4.18	4.31	4.85	5.39	4.89	4.43
P_2O_5	0.16	0.26	0.2	0.24	0.17	0.3	0.27
Ba	59	100	82	142	292	212	79
Rb	210	236	266	274	245	295	318
Sr	27	22	31	25	66	45	27
Y	17	21	18	27	45	32	22
Zr	39	29	49	39	76	64	39
Nb	13	8	17	11	9	10	19
Cr	9	18	9	19	17	14	12
Cs	5.2	10.1	14.3	11	9.9	18.9	19.6
Sc	3.2	3.2	5.2	4.2	4.2	4.3	4.1
Co	0.4	0.4	0.4	0.4	1	0.6	0.4
Ta	2.7	2.2	2.5	1.9	1.9	2.1	3.6
U	9.2	40.6	4.9	3.6	12.5	13.7	4.3
Th	5.6	1.9	5.1	4.5	15	10.2	4
Hf	1.5	1.5	1.7	1.7	3	2.3	1.4
La	6	6.5	6.2	9.4	29.5	14.5	9.3
Ce	15.2	17.9	16	21	65.2	34.6	21.3
Nd	8.9	10.2	9	10.9	32.6	17.5	11.4
Sm	2	2.2	2.3	2.1	6.2	4.4	2.6
Eu	0.2	0.1	0.2	0.2	0.6	0.4	0.2
Tb	0.4	0.4	0.6	0.4	1.2	0.8	0.6
Yb	1.3	0.9	1.1	1.3	2	2.1	1.2
Lu	0.2	0.2	0.2	0.2	0.3	0.3	0.2

Table C.1 – Major element abundances (in wt. %) and trace element concentrations (in ppm) of the Muscovite Granite Phase of the Andover Granite. Note: Fe_2O_3* is TOTAL Fe.

Sample	SGDC-3	DC-5	DC-23	M-1	R-1	SG-1	WDC-10
SiO_2	74.35	74.55	74.55	74.21	75.13	74.56	72.98
TiO_2	0.06	0.1	0.17	0.09	0.13	0.02	0.21
Al_2O_3	15.49	14.64	14.1	14.85	14.59	14.93	14.45
Fe_2O_3*	0.58	1.06	1.38	1.32	0.87	0.92	1.43
MnO	0.04	0.05	0.04	0.12	0.07	0.34	0.04
MgO	0.51	0.29	0.7	0.17	0.1	0.06	0.32
CaO	0.6	0.56	0.43	0.54	0.52	0.39	1.01
Na_2O	3.81	3.58	3.1	3.9	3.49	4.91	3.04
K_2O	4.63	4.82	5.16	4.8	5.52	3.23	5.02
P_2O_5	0.22	0.25	0.1	0.17	0.21	0.22	0.11

Ba	70	189	298	96	118.4	-	393
Rb	180	288	262	193	39.4	6.5	226
Sr	59	42	49	26	47.7	-	80
Y	12	30	38	24	-	-	20
Zr	25	48	109	29	252	47.3	111
Nb	13	13	18	16	15.3	13	7
Cr	11	15	10	18	5.6	1.4	2
Cs	6.3	19	4.2	-	2	3.7	3.1
Sc	4.9	3.8	4.2	5.2	4.5	2.5	2.4
Co	0.3	0.7	1.1	0.7	0.6	0	1.2
Ta	2.6	2.7	1.8	-	2.6	1.2	1.1
U	7.5	12.1	7.7	-	-	-	4.6
Th	0.5	8.8	21.9	6.5	5.7	1	17.8
Hf	0.8	2.1	3.9	1.5	4.1	5.9	3.2
La	2.6	12.9	29.7	6.8	7.1	2.7	57.3
Ce	7	28.2	69.3	17.4	18.2	12.1	119.4
Nd	3.9	15.5	34	9.3	9.7	8.2	47.9
Sm	1.1	4.5	8.1	2.3	2.5	0.5	8.3
Eu	0.2	0.4	0.4	0.2	0.3	0	0.6
Tb	0.4	0.7	1	0.4	0.5	0.2	1.3
Yb	1.3	1.3	2.9	1.1	1.3	1.3	0.6
Lu	0.2	0.2	0.5	0.2	0.2	0.2	0.4

Table C.1 (Cont.) – Major element abundances (in wt. %) and trace element concentrations (in ppm) of the Muscovite Granite Phase of the Andover Granite. Note: Fe_2O_3* is TOTAL Fe.

Sample	WDC-6	W-2	W-2D	LDC-3	DC-5A	MDC-35	3DC-13
SiO_2	73.64	74.78	74.81	73.03	73.8	73.8	75.54
TiO_2	0.16	0.12	0.11	0.19	0.2	0.11	0.1
Al_2O_3	13.97	13.72	13.87	15.09	14.02	14.1	14.09
Fe_2O_3*	1.77	1.55	1.43	1.77	1.48	1.26	1.56
MnO	0.04	0.09	0.09	0.08	0.04	0.03	0.09
MgO	0.6	0.16	0.14	0.83	0.45	0.16	0.59
CaO	0.97	0.88	0.85	0.93	1.34	0.91	0.85
Na_2O	3.51	3.49	3.45	4.15	3.3	3.44	3.53
K_2O	4.11	4.82	4.79	3.68	4.72	5.36	4.66
P_2O_5	0.07	0.1	0.07	0.15	0.02	0.08	0.08

Ba	497	371	383	265	429	-	361
Rb	156	136	78	196	179	170	192
Sr	81	71	74	79	100	100	74
Y	33	-	-	30	24	50	27
Zr	111	-	79	122	151	70	74
Nb	13	6.9	6.3	21	10	20	8
Cr	5	-	1.6	7	18	10	7
Cs	4.1	-	-	13	4.2	3.9	7.8
Sc	5.5	5.1	3.9	5.7	3.5	4.9	4.1
Co	1.4	0.9	0.7	1.4	1.8	0.7	12.2
Ta	1.8	-	-	3.6	1.5	0.8	0.5
U	4.1	-	-	8.1	5.7	2.4	3.5
Th	20.7	10.6	9.3	10.5	36.9	10.6	10.5
Hf	3.8	2.5	2.4	3.9	5.3	2.9	2.7
La	38.5	21.1	16.7	25.6	34.9	15.3	20.1
Ce	77.1	47.2	38.4	56.5	64.9	33.2	42.7
Nd	34.3	19.3	16.9	27	28.3	16.4	18
Sm	6.5	4.1	3.7	5.5	4.7	3.3	4.1
Eu	0.7	0.5	0.5	0.6	0.6	0.4	0.5
Tb	0.9	0.7	0.6	1	0.9	1.1	0.7
Yb	2.5	2.8	2.6	3.2	3.3	4.2	2.9
Lu	0.4	0.5	0.5	0.4	0.4	0.6	0.4

Table C.2 – Major element abundances (in wt. %) and trace element concentrations (in ppm) of the Biotite Granite Phase of the Andover Granite. Note: Fe_2O_3* is TOTAL Fe.

Sample	3DC-16	W-1	MDC-33
SiO_2	74.16	76.67	73.08
TiO_2	0.12	0.1	0.27
Al_2O_3	14.51	12.69	14.08
Fe_2O_3*	1.53	1.45	2.12
MnO	0.08	0.1	0.4
MgO	0.67	0.16	0.58
CaO	1.24	0.78	1.57
Na_2O	3.67	3.18	3.34
K_2O	3.6	4.61	4.28
P_2O_5	0.08	0.11	0.09

Ba	277	379	-
Rb	105	121	-
Sr	80	76	-
Y	25	36	-
Zr	70	69	-
Nb	7	0	-
Cr	4	20	-
Cs	2.3	-	-
Sc	4.8	5.1	-
Co	1.3	0.9	-
Ta	0.4	0.2	-
U	4.1	-	-
Th	12.3	9.3	-
Hf	2.7	2.7	-
La	20.9	17.4	20.8
Ce	43.4	41	43.5
Nd	18.7	18.2	18.2
Sm	4	3.3	3.8
Eu	0.5	0.5	0.5
Tb	1	0.7	0.7
Yb	3.3	2.7	2.6
Lu	0.5	0.4	0.5

Table C.2 (Cont.) – Major element abundances (in wt. %) and trace element concentrations (in ppm) of the Biotite Granite Phase of the Andover Granite. Note: Fe_2O_3* is TOTAL Fe.

Sample	RDC-10D	DC-36	DC-37	DC-38	3DC-15
SiO_2	73.62	73.41	73.07	74.7	74.23
TiO_2	0.15	0.17	0.16	0.11	0.9
Al_2O_3	14.27	14.31	14.69	14.1	14.34
Fe_2O_3*	1.27	1.35	1.3	1.02	1.21
MnO	0.04	0.04	0.04	0.08	0.12
MgO	0.42	0.48	0.76	0.16	0.32
CaO	0.66	0.96	0.78	0.62	1.2
Na_2O	3.2	3.42	3.47	3.95	3.6
K_2O	5.22	4.77	4.66	4.48	4.04
P_2O_5	0.15	0.13	0.15	0.08	0.03

Ba	283	375	305	-	404
Rb	226	172	162	230	181
Sr	71	90	76	30	130
Y	42	36	24	40	39
Zr	71	99	91	70	88
Nb	7	3	10	20	9
Cr	49	15	12	10	17
Cs	7.9	2.8	1.2	4	3.5
Sc	4.1	3	5.7	4.4	4.3
Co	1.2	1.4	1.1	0.7	1.4
Ta	1.9	0.8	1.4	2.7	1.6
U	5.9	5.2	8.2	10.8	3.3
Th	17.1	20.4	17.3	16.7	13.2
Hf	3	3.6	3.2	3.3	3.6
La	30.2	30.1	22.9	19.6	22.7
Ce	70.5	59	47.8	44.8	44.2
Nd	35.6	26.2	21.5	22.8	17.8
Sm	6.9	5.5	4.5	5	3.4
Eu	0.6	0.6	0.4	0.4	0.6
Tb	1	0.6	0.6	0.8	0.8
Yb	1.9	1.7	1.7	3	2.6
Lu	0.3	0.3	0.3	0.6	0.4

Table C.3 – Major element abundances (in wt. %) and trace element concentrations (in ppm) of the Muscovite-Biotite Granite Phase of the Andover Granite. Note: Fe_2O_3* is TOTAL Fe.

Sample	LDC-8	DC-26A	DC-26B	DC-26C	DC-24	SGDC-4
SiO_2	70.55	70.59	72	71.36	69.86	70.9
TiO_2	0.37	0.4	0.32	0.39	0.41	0.46
Al_2O_3	14.88	14.73	14.72	14.88	14.9	15.09
Fe_2O_3*	2.74	3.11	2.51	3.04	3.36	3.05
MnO	0.07	0.07	0.06	0.07	0.08	0.07
MgO	0.97	0.75	0.61	0.76	1.12	0.83
CaO	1.65	2.01	1.68	1.98	1.47	2.18
Na_2O	3.62	3.57	3.59	3.65	3.52	3.75
K_2O	4.15	4.07	4.51	4.17	3.97	3.49
P_2O_5	0.13	0.11	0.12	0.17	0.17	0.14

Ba	495	530	464	551	414	-
Rb	179	167	177	175	185	-
Sr	126	140	123	140	112	-
Y	43	58	52	56	34	-
Zr	284	326	268	324	280	-
Nb	19	12	11	12	18	-
Cr	11	20	12	13	16	-
Cs	4.3	15.7	4.9	15.2	4.1	11
Sc	5.3	6.2	4.9	5.2	5.7	5.4
Co	3.6	4.4	2.9	3.6	3.8	4
Ta	2.7	2.2	2.5	2.3	1.6	2.6
U	6.7	5.1	3.1	6.1	2.7	6.1
Th	17.6	19.7	16.5	17.1	14.7	16.1
Hf	8.2	9.3	7.5	7.9	8	6.6
La	61.7	59.8	54.6	52.3	52.8	36.3
Ce	121.3	114.4	109.8	101.4	108.8	76.2
Nd	57.7	50.7	55.2	48.1	46	27.4
Sm	10.2	10.2	9.4	8.8	8.4	5.5
Eu	1.1	1.1	0.9	1.1	0.9	1
Tb	1.8	1.4	1	1.5	1.1	1.4
Yb	4.7	4.4	3.9	4.3	2.8	2.7
Lu	0.7	0.7	0.6	0.7	0.5	0.5

Table C.4 – Major element abundances (in wt. %) and trace element concentrations (in ppm) of the Granodiorite Phase of the Andover Granite. Note: Fe_2O_3* is TOTAL Fe.

Sample	Avg Musc	Avg Bio	Avg Musc-Bio	Avg Grano
SiO_2	74.26	74.33	73.81	70.88
TiO_2	0.10	0.15	0.30	0.39
Al_2O_3	14.73	14.01	14.34	14.87
Fe_2O_3*	1.03	1.59	1.23	2.97
MnO	0.08	0.10	0.06	0.07
MgO	0.37	0.43	0.43	0.84
CaO	0.58	1.03	0.84	1.83
Na_2O	3.64	3.51	3.53	3.62
K_2O	4.70	4.46	4.63	4.06
P_2O_5	0.21	0.09	0.11	0.14
Ba	163.9	370.3	341.8	490.8
Rb	217.1	148.1	194.2	176.6
Sr	42.1	81.7	79.4	128.2
Y	25.5	32.1	36.2	48.6
Zr	68.3	93.3	83.8	296.4
Nb	13.0	10.2	9.8	14.4
Cr	11.5	9.1	20.6	14.4
Cs	9.8	5.9	3.9	9.2
Sc	4.0	4.7	4.3	5.5
Co	0.6	2.4	1.2	3.7
Ta	2.2	1.3	1.7	2.3
U	11.0	4.7	6.7	5.0
Th	7.8	14.5	16.9	17.0
Hf	2.5	3.2	3.3	7.9
La	14.3	23.1	25.1	52.9
Ce	33.1	48.8	53.3	105.3
Nd	16.4	21.5	24.8	47.5
Sm	3.5	4.3	5.1	8.8
Eu	0.3	0.5	0.5	1.0
Tb	0.6	0.8	0.8	1.4
Yb	1.4	3.0	2.2	3.8
Lu	0.3	0.5	0.4	0.6

Table C.5 – Major element abundances (in wt. %) and trace element concentrations (in ppm) of the mean of each phase of the Andover Granite. Note: Fe_2O_3* is TOTAL Fe.